FEM ANALYSIS OF BULGING BETWEEN ROLLS IN CONTINUOUS CASTING

BY

LAN YU

B.E., Tsinghua University, 1996

THESIS

Submitted in partial fulfillment of the requirements
for the degree of Master of Science in Mechanical Engineering
in the Graduate College of the
University of Illinois at Urbana-Champaign, 2000

Urbana, Illinois

Abstract

Mathematical models have been developed to analyze the thermal and mechanical behavior of slab bulging during the continuous casting process. The thermal history of the slab has been predicted by a two-dimensional, transient, finite element, heat transfer model, which serves as input to the stress model. The stress model has been formulated for a two-dimensional longitudinal plane through the center of the wide face and is a transient, elastic-plastic, finite element analysis of the thermal stress field. Important features of the model include the incorporation of temperature history and temperature-dependent material properties, and the employment of a periodic boundary condition. A linear kinematic hardening model is used as the constitutive model based on tensile-test measurements from the literature. Mechanical properties of steel at high temperature play an important role on bulging prediction. The commercial package ABAQUS is used to conduct the numerical simulations. The model predictions demonstrate that the surface temperature fluctuation caused by the support rolls and the water spray has a small penetration depth, so it has relatively little effect on the bulging behavior. A multiple roll pitch model has been developed in order to predict the evolution of the bulging profile due to changes in the geometry of the support system. A sudden change in roll pitch or a misaligned roll may lead to a bigger bulge and tensile strain on the solidification front than those encountered for a uniform roll pitch model. The disturbances due to the changes in the geometry of the caster usually settle down after four to five roll pitches. Parametric studies of roll pitch and surface temperature demonstrate that the bulging displacement is very sensitive to roll pitch and surface temperature. Three empirical bulging prediction equations have been evaluated.

To my parents and my dear husband.

Acknowledgement

I would like to express my sincere appreciation and gratitude to my advisor, Professor Brian G. Thomas. I am very grateful for the opportunity to work with him. This work would not have been possible without his guidance, support and encouragement. I would like to thank members of the Continuous Casting Consortium at the University of Illinois: Allegheny Ludlum, Armco Inc., Columbus Stainless Steel, Inland Steel, LTV Steel, and Stollberg, for their continued support of our research. I would also like to thank the National Center for Supercomputing Application (NCSA) for its computing facilities.

Thanks also go to my friends and colleagues in the research group at the Metals Processing Simulation Laboratory, who have made my life at the University of Illinois very enjoyable.

Finally, I would like to thank my family for their endless love and encouragement.

Table of Contents

Page

List of Tables

Page

List of Figures

Page

Nomenclature

Symbol	Definition	Unit
A, j, k, l, m, n	Constants (Equation 2.1, Table 2.3)	
$[B]^e$	Element strain-displacement matrix	
$C(T_{surf})$	Constant dependent on temperature profile across solidified shell (Equation 2.3)	
C_p	Specific heat	J/kgK
$\{d\}$	Nodal displacement vector	
d_{max}	Maximum bulging deflection	mm
d_N	Negative bulging	mm
d_P	Positive bulging	mm
D	Solidified shell thickness	mm
$[E]$	Elasticity matrix for plane stress	
E	Elastic Modulus	MPa (N/mm^2)
$\{F_{\varepsilon_P}\}$	Thermal force vector	
$\{F_{\varepsilon_T}\}$	Plastic force vector	
F(W/L)	2-D shape factor, a function of aspect ratio of slab width to roll pitch (Equation 2.1, 2.2)	
g	Gravity acceleration (g=9.8)	m/s^2
h	Heat transfer coefficient	W/m^2K
H	Height from meniscus	m
k	Thermal conductivity	W/mK
$[K_\sigma]$	Global stiffness vector	
L	Roll pitch	mm
NE	Number of elements in mesh	
P	Ferrostatic pressure ($P=10^{-6}\rho gH$)	MPa (N/mm^2)
R	Caster radius	m
t_c	Loading / creep time (Equation 2.3)	s
t	Time	s

Δt	Time increment	s
T	Temperature	°C (K-273)
T_{surf}	Surface temperature	°C (K-273)
u, v	Displacements in X and Y directions	mm
v_{max}	Maximum displacement in Y direction	mm
V_c	Casting speed	M/min
W	Slab width	mm
x, y	Coordinates in X and Y directions	mm
X, Y	Coordinate directions	
α	Thermal expansion coefficient	$°C^{-1}$
$\{\varepsilon\}$	Total strain vector	
$\{\Delta\varepsilon\}$	Incremental total strain vector	
$\{\Delta\varepsilon_e\}$	Incremental elastic strain vector	
$\{\Delta\varepsilon_P\}$	Incremental plastic strain vector	
$\{\Delta\varepsilon_T\}$	Incremental thermal strain vector	
ε_b	Bulging strain	
$\dot{\varepsilon}_P$	Scalar plastic strain rate	1/s
ν	Poisson’s ratio	
ρ	Liquid steel density	kg/m^3
$\{\Delta\sigma\}$	Incremental stress vector	MPa (N/mm^2)
$\{\sigma\}$	Total stress vector	MPa (N/mm^2)
$\{\sigma_b\}$	Back stress vector	
σ_0	Yield stress at zero plastic strain	
σ_x, σ_y	Normal tress	MPa (N/mm^2)
τ_{xy}	Shear stress	MPa (N/mm^2)

1 Introduction

Continuous casting is the predominant way by which steel is produced in the world. It is now used to cast over 80% of the western world's steel production [1]. Despite the fact that the continuous casting process is generally superior to the ingot casting process, some serious production problems still remain.

A schematic of the continuous casting process is illustrated in Figure 1.1 [2]. Molten steel is poured from the ladle into the tundish. Through a ceramic submerged entry nozzle, it flows into the mold. Once in the mold, the steel freezes against the water-cooled copper mold walls to form a solid shell, which is continuously withdrawn from the bottom of the mold. After the shell exits the mold and moves between successive rolls in the spray zones, it is subject to large surface temperature fluctuations. The strand can also be deformed during solidification by thermal stresses, ferrostatic pressure, and mechanical interaction with rolls.

The formation of cracks in continuously cast products mainly depends on the amount of deformations induced in the solidifying shell, which are due to thermal or mechanical stresses imposed on the strand. In continuous casting of slabs, one of the main phenomena responsible for the deformation of the product is the bulging between rolls (see Figure 1.2), which is caused by internal ferrostatic pressure acting on the solidifying strand shell due to the weight of liquid steel and the height from the meniscus.

It is widely believed that bulging plays a major role in the formation of centerline segregation and internal cracks [3] [4] [5], which lead to poor quality of the continuously cast products. The bulging of slabs can also cause an increase of the load transmitted to the containment rolls and enhance their rate of wear.

In practice, a quantitative characterization of the strand bulging behavior is essential in continuous caster design and set-up of secondary cooling conditions so as to restrain bulging, especially in high-speed casting. Various process parameters contribute to the bulging, which may include mechanical properties of steel at high temperature, strand shell thickness, roll spacing, height from meniscus, slab width, casting speed and surface temperature.

In this work, mathematical models are developed and utilized to shed light on understanding of the bulging phenomenon in a quantitative manner. The objectives of this work are the following:

- Develop FEM thermal stress models of slab bulging (both single roll pitch model and multiple roll pitch model) to predict stress and strain distribution, and shape of strand throughout caster. Validate the model by investigating:
    - Numerical accuracy
    - Comparison with experimental measurements
- Use the model to identify the relative importance of phenomena such as:
    - Bulging due to hydrostatic pressure from the molten steel
    - Effect of surface temperature fluctuations on bulging (by incorporating the temperature history calculated by a heat transfer model into the stress model)
    - Influence of upstream rolls on bulging due to changes in the geometry of the continuous caster supporting system such as sudden roll pitch changes and defects like roll misalignments or eccentricities
- Determine quantitatively the effects of various casting process parameters on variables related to steel quality (stress, strain on the solidification front and bulge deflection) by conducting parametric studies.
- Use the model to evaluate existing bulge prediction models, which appear in the literature.

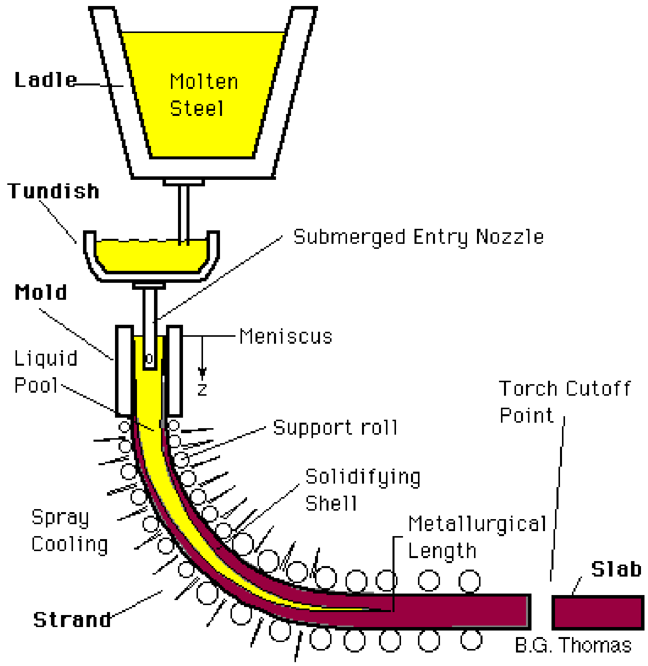

Figure 1.1. Schematic of the steel continuous casting process

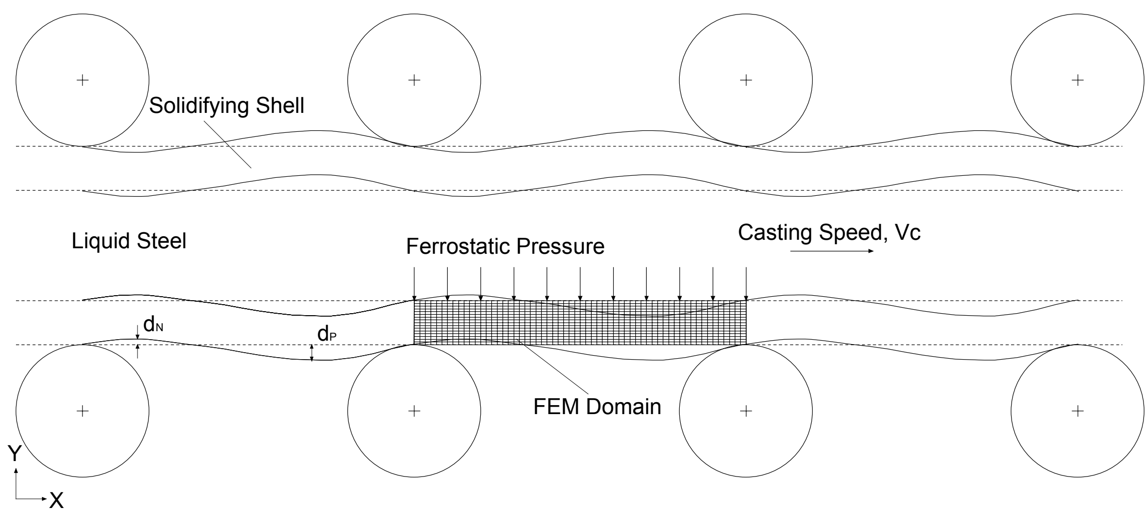

Figure 1.2. Bulging between rolls during continuous casting

2 Literature Review

In order to quantify and better understand the bulging phenomenon, both theoretical and experimental approaches have been reported in the literature. However, measuring bulging is very difficult during the actual casting process. Therefore, many mathematical models for slab bulging have been developed to calculate bulging and its dependence on various process parameters. In bulging analysis, appropriate mechanical properties of steel at high temperature are crucial for accurate results.

2.1 Experimental Studies

Only a few experimental measurements of bulging have appeared in the literature [6] [7] [8] [9]. It should be noted that two experimental studies quantitatively measured bulging in pilot casters [6] [7] and bulging measurements of strand and bloom were made on operating BHP casters [8] [9]. The following phenomena have been reported:

- The bulging profile is non-symmetric with the maximum deflection located beyond the mid point between rolls in the direction of withdrawal. The maximum deflection of 6.5 mm is located at 75% of the roll pitch from the upstream roll for measurements on the BS pilot slab caster [6] under the casting conditions listed in Table 2.1. The maximum deflection is at about 60~65% of the roll pitch for measurements on the pilot caster at Sumitomo Metals in Japan [10] [11] under the casting conditions listed in Table 2.2.

- "Negative bulging" takes place at the vicinity of the support rolls, even for those casting conditions of the pilot caster at Sumitomo Metals, where the ferrostatic pressure is rather low. As shown in Figure 1.2, bulging that makes the strand thicker due to expansion towards rolls is called positive bulging, $d_{P,}$ and bulging away from rolls into the strand is called negative bulging, d_N. The ratio between negative bulging and positive bulging is around 0.4 [10].

Table 2.1. Casting conditions for BS pilot slab caster (Wunnenberg)

Steel grade	X60 (C: 0.26%, Mn: 1.35%, P: 0.040%, Nb: 0.05%, V: 0.02%, Ti: 0.03%)
Caster Radius (R)	3.9 m
Slab width (W)	>1300 mm (1350 mm)
Roll pitch (L)	860 mm
Shell thickness (D)	79 mm
Surface Temperature (T_{surf})	1030 °C *
Casting speed (V_c)	0.85 m/min = 14.2 mm/s
Liquid steel density (ρ)	7000 kg/m^3
Height from meniscus (H)	3.9 m
Ferrostatic pressure (P)	0.26 MPa

* Due to lack of the surface temperature measurements (a single value of 1030°C), a constant surface temperature of 1000°C is assumed for the rest of this work.

- A sudden change in roll pitch leads to large downstream disturbances of the bulging profile, which stabilizes after a few rolls. Measurements of bulging were carried out for 310mm roll pitch, just after a succession of at least 3 roll pitches of 250mm at Sumitomo Metals [11]. The maximum deflection in the first roll pitch of 310mm was 4.5mm which compares to the deflection for uniform 310mm roll pitches, 3.2mm.

- Large supporting roller spacing, high strand surface temperature, and high casting speed with small shell thickness each cause increasingly large bulging [6]. On BS pilot slab caster under casting conditions listed in Table 2.1, for roll pitch at 430mm, 860mm and 1290mm, the bulging measurements are 0.5~2mm, 5~7mm and 35~42mm respectively. For surface temperature at 900 °C, 1000 °C and 1050°C, the measurements are 3mm, 5mm and 7mm. For slab width at 550mm and shell thickness at 68mm, 65mm, 63mm and 58mm, the measurements are 1.5mm, 2mm, 2.3mm and 4mm respectively.

- Stopping the casting process completely causes the strand to experience a larger bulging due to the creeping caused by ferrostatic pressure than during operation [6]. P. Woodberry, et al. [9] also observed large oscillation in bulging after the restart of casting. This oscillation disappears as the strand regains its equilibrium during casting.

Table 2.2. Casting conditions for pilot caster at Sumitomo Metals

Steel grade	AISI 1518 Steel (C: 0.18%)
Caster Radius (R)	3 m
Slab width (W)	400 mm (400 x 100 mm^2 slab)
Roll pitch (L)	310 mm
Shell thickness (D)	23.17 mm
Surface Temperature (T_{surf})	1220 °C
Casting speed (V_c)	1.65 m/min = 27.5 mm/s
Liquid steel density (ρ)	7000 kg/m^3
Height from meniscus (H)	2.65 m
Ferrostatic pressure (P)	0.18 MPa

A schematic of the pilot caster at Sumitomo Metals is shown in Figure 2.1. Assuming Mold Length = 0.7 m for the pilot caster, # of rolls $= \frac{3.25 - 0.7}{0.31} \approx 8$. So the point of measurement is about 8-9 rolls down the mold.

2.2 Mathematical Modeling

Many authors use mathematical modeling to study bulging phenomena. Both analytical and numerical methods are found among the investigations, which may be generally classified as using beam bending theory and Finite Element Method (FEM). Several empirical equations for maximum bulge deflection are available.

2.2.1 Beam Bending Theory

Beam bending theory can be applied to the rectangular longitudinal slice at the mid-width of the slab to calculate the deflection of the strand shell under uniform transverse loading. If elastic, elasto-plastic and visco-plastic creep deformation and slab movement are taken into account, beam theory can be a very good approximation and has the advantage of efficiency.

All of the beam bending models [4] [10] [12] [13] have essentially the same features and governing equations. The boundary conditions under the rolls, however, are not the same for all the models. A fixed-end condition, i.e. no deflection and no rotation at the ends, is employed with [4] [10] or without [13] an additional condition that the curvature at the upstream roll is zero. In other models [10] [12], cyclic boundary conditions are used, which imply no deflection and equal rotation and curvature at the ends. This leads to bulging profiles with negative bulging. Other differences lie in the choice of material laws and strand dynamics, i.e. stationary vs. moving strand. Miyazawa and Schwerdtfeger [4] have concluded that creep is the dominant mode of deformation and incorporated it into beam theory.

The continuous beam bending model over several successive rolls was developed by J. Gancarz et al. [11] in order to describe the effects of variations in geometry of the supporting system. It also provides an idea of the bulging profile over the entire slab strand rather than a single roll pitch.

The limitations of beam bending theory are obvious: it can only provide a good approximation of maximum bulging without being able to evaluate true bulging profile, and the strain and stress distributions on the entire strand shell. Furthermore, the effect of property variations through the thickness cannot be included into the model.

2.2.2 Finite Element Analysis

Analysis using the finite element method (FEM) in two or three dimensions can give a complete bulging profile and distributions of other field variable (strains, stresses, etc.), which may expose the relationship between bulging deformation and internal cracks as well as other quality problems. The disadvantages of this method are the overwhelming mesh refinement and associated computational cost required for stability and accuracy and difficulties in choosing boundary conditions to handle slab movement.

Two-dimensional FEM models [5] [14] [15] [16] [17] have been applied to a longitudinal slice at the mid-width of the slab. The plane stress state is usually assumed though in reality the strand shell is in a state closer to generalized plane strain for a sufficiently large slab width. It is important to note that for narrow slabs and blooms, shell deflection at the center will also be governed by additional factors such as the width of the slab and the shell thickness at the corner. Consequently, employment of a 2-D model for narrow slabs/blooms is expected to predict the upper limit of the bulging. It is only accurate for large slab width to roll pitch aspect ratio. However, due to extensive computation and complexity associated with a 3-D model, attempts have been made to account for the corner effects by incorporating a "shape factor" into a 2-D model [15]. 3-D models [15] [16] [17], which include the effect of slab width on bulging, have been applied to a quarter of the solidified strand shell between two adjacent rolls.

2.2.3 Empirical Equations for Maximum Bulge

Many authors have summarized the effects of various process parameters on maximum bulging with a simple algebraic relationship. Okamura, et al. [15] gave the following regression equation for maximum bulging deflection and bulging strain as a function of process parameters (based on FEM simulations).

$$d_{\max}, \varepsilon_b = AF(W/L)D^j P^k L^l T_{surf}^m V_c^{\,n} \tag{2.1}$$

Where the coefficient A and the exponents j, k, l, m, n are listed in Table 2.3. The 2-D shape factor F(W/L) is defined to be the ratio of the 3-D result to the 2-D result, which depends on the ratio of slab width to roll pitch, W/L. If the ratio W/L is large enough, the 2-D shape factor reaches unity and the bulging deflection is not affected by the slab width. However, it decreases drastically with the reduction of W/L. This tendency is approximated by the following equation:

$$F(W/L) = 1 - \{(\pi W/2L)\tanh(\pi W/2L) + 2\}/2\cosh(\pi W/2L) \tag{2.2}$$

Table 2.3. Constants in Okamura Equation 2.1

	A	j	k	l	m	n
d_{max}	$10^{0.102D-20.3}$	-4.23	2.75	6.34	$-3.58\times10^{-2}D+4.94$	$-6.5\times10^{-4}D-0.065$
ε_b	$10^{0.163D-22.7}$	-4.23	2.9	5.01	$-5.52\times10^{-2}D+6.78$	$-6.5\times10^{-4}D-0.065$

Palmaers, et al. [13] gave the following equation (based on beam bending analysis)

$$d_{max} = C(T_{surf})\frac{P^{1.5}L^{4.9}t_c^{\ 0.22}}{D^{3.8}} \tag{2.3}$$

Where $C(T_{surf})$ is a constant depending mainly on temperature profile across the solidified shell, given in Equation 2.5, and t_c loading/creep time is defined as $t_c = 0.5L/V_c$. We then have

$$d_{max} = 0.4623C(T_{surf})\frac{P^{1.5}L^{5.12}}{V_c^{\ 0.22}D^{3.8}} \tag{2.4}$$

$$C(T_{surf}) = \begin{cases} 0.609\times10^{-4} & T_{surf} = 900°\text{C} \\ 0.725\times10^{-4} & T_{surf} = 1000°\text{C} \\ 0.929\times10^{-4} & T_{surf} = 1100°\text{C} \end{cases} \tag{2.5}$$

Lamant, et al. [10] gave another formula based on beam-analysis. The maximum bulging is expressed in terms of H (height from meniscus) instead of P (ferrostatic pressure):

$$d_{\max} = 7.4088 \times 10^{-14} \exp(0.003866(T_{surf} + 273)) \frac{L^{7.16} H^{2.18}}{V_c^{0.4} D^{5.47}} \tag{2.6}$$

In conclusion, many processing parameters influence bulging of the continuously cast strand shell. All of the three Equations 2.1, 2.4 and 2.6 listed above reveal the fact that larger roll spacing and smaller shell thickness contribute more than other parameters to the maximum bulging amount. The exponent on roll spacing (L) ranges from 5.12 to 7.16 and that on shell thickness (D) from -3.8 to -5.47. The roles of ferrostatic pressure and surface temperature are obvious: larger bulging is caused by larger pressure and higher temperature. The effect of casting speed is complex, however. On one hand, increasing casting speed while maintaining constant strand shell thickness reduces creeping time, which in turn reduces bulging. On the other hand, the shell thickness decreases as casting speed increases. The combined effect will increase bulging.

2.2.4 Comments

The bulging of continuously cast strand shells is a three dimensional dynamic problem involving heat transfer, elastic, elasto-plastic and visco-plastic creep deformation. The finite element model is preferred in order to get a complete bulging profile and distributions of stress, strain etc. It is also important to consider creep deformation, strand movement and appropriate boundary conditions in the model. It appears that a combination of a 2-D model with an appropriate shape factor can be utilized to predict bulging behavior of narrow slabs/blooms.

2.3 Mechanical Properties of Steel at High Temperatures

With the increase of computational speed, the finite element stress analysis of continuous casting process has become more feasible and desirable. However it is critical to use simple constitutive equations that adequately describe the complex stress-strain relationship under conditions typically encountered during the continuous casting process:

1) Temperature range of austenite (900°C to 1500°C)
2) Small strains (usually below 4%)
3) Low strain rate (from 10^{-3} to 10^{-6} s^{-1})
4) Varying carbon contents (0.005 to 1.54% wt. C)
5) Complex loading histories

An important part of the constitutive model is the elastic modulus (E) in the temperature range of 900°C to 1500°C, which is typical for the continuous casting process. However, at elevated temperatures, all metals are subject to plastic deformation and/or creep upon application of load. The inelastic deformation should not be included in the strain measurement of the elastic modulus test. Uncertainty exists concerning the true value of E at high temperatures. This is partly because some experimental methods allow time for some creep to occur during the test, which leads to smaller estimates of elastic modulus. For temperatures above 900°C, few measurements are available.

Based on experimental data (relaxed value) from Mizukami [18] under continuous casting conditions for plain carbon steel, the following two equations were used to calculate E. The Mizukami data for elastic modulus are much lower than data obtained with no creep relaxation, such as those surveyed by Wray [19] and Hub [20].

1) P.F. Kozlowski, B.G. Thomas, J.A. Azzi and H.Wang [21]:

$$E[GPa] = 968 - 2.33(T-273) + 1.90\times10^{-3}(T-273)^2 - 5.18\times10^{-7}(T-273)^3 \qquad (2.7)$$

Where T is the temperature of interest in Kelvin. This relation applies to temperature between 900°C and the liquidus.

2) T. Matsumiya and Y. Nakamura [12]:

$$E[kgf/cm^2] = \begin{cases} 2\times10^5 - 187.5(T-1000) & (1000°C \le T \le 1400°C) \\ 1.25\times10^5(1475-T)/75 & (1400°C \le T \le 1475°C) \\ 0 & (T > 1475°C) \end{cases} \qquad (2.8)$$

$$\text{i.e. } E[GPa] = \begin{cases} 19.6 - 1.84\times10^{-2}(T-1000) & (1000°C \le T \le 1400°C) \\ 0.163(1475-T) & (1400°C \le T \le 1475°C) \\ 0 & (T > 1475°C) \end{cases} \tag{2.9}$$

Elastic modulus (E) controls the initial slope of the stress-strain curve. However, its influence diminishes with increasing strain and it has little effect beyond about 0.2 % total strain. It was also found that numerical difficulties were fewer with a smaller elastic modulus, since the resulting size of the elastic strains, relative to the inelastic strains, is larger.

Kozlowski, et al. [21] developed and compared the abilities of four different forms of elsto-viscoplastic constitutive relations: constant structure, time-hardening, strain-hardening, and simultaneous time and strain-hardening models, to quantify the mechanical behavior of plain carbon steel at elevated temperature. Wray [22] and Suzuki, et al. [23] give us several sets of temperature dependent stress-strain curves obtained for plain carbon steel experimentally.

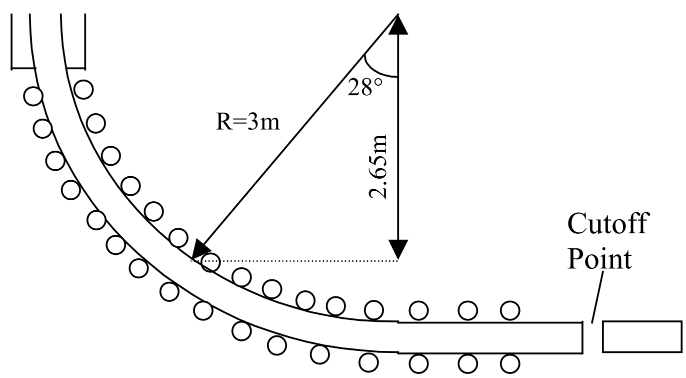

Figure 2.1. Pilot caster at Sumitomo Metals in Japan

3 Model Formulation

Two dimensional finite element heat transfer and thermal stress models, which are applied to a longitudinal plane through the center of the wide face, have been developed to understand the thermal and mechanical behavior of slab bulging. Due to extensive computation and complexity associated with 3-D models and the time limitation of this work, we cannot make a 3-D model to accommodate for the corner effects on bulging. However the empirical 2-D shape factor (Equation 2.2) from the literature can be used to take the aspect ratio of slab width to roll pitch into account.

3.1 Stress Analysis Model

The 2-D simulation domain is shown in Figure 1.2. The Lagrangian reference frame is attached to the slab and the rolls move past the domain to simulate the transient elastic-plastic thermal stress problem.

3.1.1 Governing Equations

Regardless of the nature of loading, the stress components acting on an elementary volume of an elastic continuum must satisfy certain equilibrium conditions, and the strain components must satisfy the compatibility relations. Those equations are well known in classical elasticity theory, and directly applicable to the thermal stress problem. [24]

A state of plane stress was assumed and only small strains were considered. Thus, the stress distribution within the two-dimensional domain is governed by the equilibrium equations:

$$\begin{bmatrix} \frac{\partial}{\partial x} & 0 & \frac{\partial}{\partial y} \\ 0 & \frac{\partial}{\partial y} & \frac{\partial}{\partial x} \end{bmatrix} \begin{Bmatrix} \sigma_x \\ \sigma_y \\ \tau_{xy} \end{Bmatrix} + \begin{Bmatrix} F_x \\ F_y \end{Bmatrix} = \begin{Bmatrix} 0 \\ 0 \end{Bmatrix} \tag{3.1}$$

Assuming stress is caused solely by elastic strain, the standard displacement formulation was used to relate stress increments, $\{\Delta\sigma\}$, to displacement increments, $\{u,v\}^{-1}$, through the kinematic relations:

$$\{\Delta\varepsilon\} = \begin{bmatrix} \frac{\partial}{\partial x} & 0 \\ 0 & \frac{\partial}{\partial y} \\ \frac{\partial}{\partial y} & \frac{\partial}{\partial x} \end{bmatrix} \begin{Bmatrix} u \\ v \end{Bmatrix} \tag{3.2}$$

and the constitutive equations for an elastic, plane-stress, isotropic condition:

$$\{\Delta\sigma\} = [E]\{\Delta\varepsilon_e\} \tag{3.3}$$

where

$$[E] = \frac{E}{1-\nu^2} \begin{bmatrix} 1 & \nu & 0 \\ \nu & 1 & 0 \\ 0 & 0 & \frac{1-\nu}{2} \end{bmatrix} \tag{3.4}$$

and E is temperature dependent and ν is temperature independent. The incremental total strain vector, $\{\Delta\varepsilon\}$, was divided into three parts in order to relate it to the elastic strain increments, $\{\Delta\varepsilon_e\}$:

$$\{\Delta\varepsilon\} = \{\Delta\varepsilon_e\} + \{\Delta\varepsilon_T\} + \{\Delta\varepsilon_P\} \tag{3.5}$$

$\{\Delta\varepsilon_T\}$ and $\{\Delta\varepsilon_P\}$ contain the incremental thermal strain components and plastic strain components respectively.

The volume changes that accompany changing temperature gradients are accounted for in thermal stress models through a constant thermal expansion coefficient. This results in an incremental thermal strain vector.

$$\{\Delta\varepsilon_T\} = \begin{Bmatrix} \alpha\Delta T \\ \alpha\Delta T \\ 0 \end{Bmatrix} \tag{3.6}$$

where ΔT defines the change in temperature over a time interval.

A linear kinematic hardening model is used as the constitutive model in this work. This model is appropriate for inelastic behavior of materials that are subjected to cyclic loading and is a pressure-independent plasticity model. The pressure-independent yield surface is defined by the function

$$F = f(\{\sigma\} - \{\sigma_b\}) - \sigma_0 = 0 \tag{3.7}$$

where σ_0 is the yield stress at zero plastic strain and $f(\{\sigma\} - \{\sigma_b\})$ is the equivalent Mises stress with respect to the back stress, $\{\sigma_b\}$.

In a kinematic hardening model, the center of the yield surface moves in stress space. It allows modeling the Bauschinger effect induced by work hardening, which is characterized by a reduced yield stress upon load reversal after plastic deformation has occurred during the initial loading. Isotropic and kinematic hardening models are the same if there is no reverse loading. The linear kinematic hardening model approximates the hardening behavior with a constant rate of hardening. This hardening rate should be matched to the average hardening rate measured in stabilized cycles over a strain range corresponding to that expected in the application. The linear kinematic hardening modulus is defined by sets of two data pairs as a function of temperature. Note that this model gives physically reasonable results for only relatively small strains (less than 5%). [25]

A linear kinematic hardening model describes the translation of the yield surface in stress space through the back stress.

$$\{\dot{\sigma}_b\} = C\frac{1}{\sigma_0}(\{\sigma\} - \{\sigma_b\})\dot{\varepsilon}_P \tag{3.8}$$

where C is the kinematic hardening modulus.

Unknowns are u and v, displacements in X and Y directions. These equations are solved incrementally, as described in Section 3.4.

The following assumptions have been used to simplify the complex problem to a manageable size.

- The 2-D assumption of plane stress state is applied:

$$\begin{aligned} \varepsilon_z &= \frac{-\nu}{1-\nu}\left(\varepsilon_x + \varepsilon_y\right) \\ \sigma_z &= \tau_{yz} = \tau_{zx} = \gamma_{yz} = \gamma_{zx} = 0 \end{aligned} \tag{3.9}$$

- Constant solidified shell thickness.
- Uniform loading due to ferrostatic pressure.
- Constant temperature gradient across the shell thickness with uniform temperature profile along X direction is assumed, except when temperature field from heat transfer analysis shown in Section 3.2 is incorporated into the thermal stress model.

3.1.2 Single Roll Pitch Model

The single roll pitch FEM domain is shown in Figure 1.2. A periodic boundary condition (i.e. coupled X & Y displacement) is applied on the two ends of the domain. This is a dynamic model with more rolls moving in from the right in order to simulate the slab movement. The boundary condition accounting for the roll is a fixed Y displacement on the contact point, which must be changed each time step.

3.1.3 Multiple Roll Pitch Model

A multiple roll pitch model is developed in order to study the influences from the upstream rolls, the bulging profile of the entire strand and its evolution. It is the same as the single roll pitch model except for that, as shown in Figure 3.1, the domain of interest includes at least 4 successive roll pitches, which are not necessarily uniform.

The periodic boundary condition is used for the multiple roll pitch model with uniform roll pitch. However, for non-uniform roll pitches, the two ends should not always act the same, so this periodic boundary condition may not be the appropriate one. A more detailed study of the boundary conditions on the two ends in the multiple roll pitch model will be discussed in Chapter 6.

3.2 Heat Transfer Model

To investigate the relative importance of variations in thermal strain on bulging and related properties, the temperature distribution in the solidifying shell can be obtained by developing a 2-D transient heat transfer model. As shown in Figure 3.2, the domain and mesh are the same as those used in the stress analysis in order to incorporate the temperature profile into the thermal stress model. The prescribed boundary conditions as described later in this section are moved along the X direction with time.

3.2.1 Governing Equations

The following energy balance equation for this 2-D problem was solved:

$$\rho C_p \frac{\partial T}{\partial t} = \frac{\partial}{\partial x} k \frac{\partial T}{\partial x} + \frac{\partial}{\partial y} k \frac{\partial T}{\partial y} \tag{3.10}$$

The material properties are given in Section 3.3, and include temperature dependent thermal conductivity. Note that the effect of latent heat of solidification was ignored. The importance of this assumption was evaluated by comparison with a solidification model.

3.2.2 Prescribed Boundary Conditions

The boundary conditions for the heat transfer model are shown in Figure 3.2. The hot surface (top) is subjected to a fixed temperature of 1500°C to represent the solid/liquid interface. Due to symmetry, an insulated boundary condition is applied on the two ends. On the bottom surface, a heat convection boundary condition with heat transfer coefficient h(x), as shown in Figure 3.3, and ambient temperature of 130°C is employed. Slab movement is simulated as the same prescribed boundary condition moving in the X direction with time. The heat transfer coefficient is then a function of time and x. The heat transfer coefficient of 332 W/m^2K beneath the sprays corresponds to a water flow rate of 1.17 l/m^2s using Nozaki's equation [26]. In order to account for random slow-moving water droplets, the value of 92 W/m^2K between the direct spray and the rolls represents an average effect for radiation and natural convection alone and the spray zone. Note that the average heat transfer coefficient is 218 W/m^2K for this profile.

3.3 Thermal and Mechanical Properties

Density, specific heat, thermal expansion and Poisson's ratio for plain carbon steel are listed in Table 3.1. They are independent of temperature in these ABAQUS models. Temperature dependent thermal conductivity, elastic modulus and stress-strain relations are listed in Table 3.2.

Table 3.1. Thermal and mechanical properties for plain carbon steel

	Density (ρ)	Specific heat (C_p)	Thermal expansion (k)	Poisson's ratio (ν)
Plain carbon steel	7000 kg/m^3	460 J/kgK	1.77e-5	0.3

As shown in Figure 3.5, the constitutive model is chosen to match the Wray data [22] for plain carbon steel with a strain rate of about 10^{-3} s^{-1} at 950°C, 1100°C and 1200°C. Note that the model roughly matches the Suzuki data [23] if all temperatures are shifted by 100°C.

Table 3.2. Temperature-dependent material properties

Temperature (T)	Thermal conductivity (k)	Elastic modulus (E)	Yield stress σ (ε_p=0)	Stress at 5% plastic strain (ε_p=0.05)
900°C		32.09 GPa		
950°C			20 MPa	50 MPa
1000°C	28.5 W/mK	19.60 GPa		
1100°C		14.01 GPa	12.7 MPa	27.7 MPa
1200°C		12.20 GPa	10 MPa	17.5 MPa
1300°C		11.08 GPa		
1400°C		7.51 GPa	3 MPa	13 MPa
1500°C	34 W/mK	3.75 GPa	0.5 MPa	1 MPa

3.4 Solution Methodology

A stress analysis consists of 30 to 60 simple explicit time steps (fixed size of 1.01 seconds), which incorporates the changes in boundary conditions that accompany the rolls moving past each element along the axial casting direction. Each of these large time steps is then divided into multiple increments, using an automatic time incrementation scheme. The scheme uses a "half-step residual" control to ensure an accurate solution [25], which increases the time step size from the first initial size small enough to satisfy the input tolerance for accuracy. Further iteration within each sub time step is needed to solve the nonlinear equations discussed next.

Using standard finite-element techniques to reformulate and solve the elasto-plastic thermal stress problem described mathematically by Equation 3.1 through 3.6 and 3.8 results in a set of simultaneous equation, for the unknown displacements, $\{d\}$, which contain the X an Y displacements, u and v, for each node in the mesh.

$$[K_\sigma]\{d\} = \{F_{\varepsilon_T}\} + \{F_{\varepsilon_P}\} \tag{3.11}$$

The global stiffness matrix, $[K_\sigma]$, global thermal force vector, $\{F_{\varepsilon_T}\}$, and global plastic strain force vector, $\{F_{\varepsilon_P}\}$, are found by summing the contributions from individual elements:

$$[K_\sigma] = \sum_{i=1}^{NE} [K_\sigma]_i^e = \sum_{i=1}^{NE} \int_A\int [B]_i^{e^T} [E]_i [B]_i^e \, dA \tag{3.12}$$

$$\{F_{\varepsilon_T}\} = \sum_{i=1}^{NE} \{F_{\varepsilon_T}\}_i^e = \sum_{i=1}^{NE} \int_A\int [B]_i^{e^T} [E]_i \{\Delta\varepsilon_T\} dA \tag{3.13}$$

$$\{F_{\varepsilon_P}\} = \sum_{i=1}^{NE} \{F_{\varepsilon_P}\}_i^e = \sum_{i=1}^{NE} \int_A\int [B]_i^{e^T} [E]_i \{\Delta\varepsilon_P\} dA \tag{3.14}$$

where, $[B]^e$ is the matrix containing the displacement gradients.

Plastic strain rate values, $\dot{\varepsilon}_P$, were calculated based on current stress state, as shown in Equation 3.8, which depends on strain calculation. This creates non-linearity in Equation 3.11. Plastic strains for the time interval were then evaluated from:

$$\Delta\varepsilon_P = \Delta t \dot{\varepsilon}_P \tag{3.15}$$

Incremental thermal loads for the time increment, $\{\Delta\varepsilon_T\}$, were calculated using Equation 3.6. Within each time increment, the nonlinear equilibrium Equations 3.11 are assembled and solved for the unknown nodal displacements using the standard Newton's method [27] for fast convergence rate. Total strain increments, $\{\Delta\varepsilon\}$, were then calculated from the displacements using Equation 3.2 and stress increments were evaluated from the strains with the expression:

$$\{\Delta\sigma\} = [E](\{\Delta\varepsilon\} - \{\Delta\varepsilon_P\} - \{\Delta\varepsilon_T\}) \tag{3.16}$$

Finally, the total state variables were updated prior to the next time increment:

$$\begin{aligned}
\{\sigma\}_{t+\Delta t} &= \{\sigma\}_t + \{\Delta\sigma\} \\
\{\varepsilon\}_{t+\Delta t} &= \{\varepsilon\}_t + \{\Delta\varepsilon\} \\
\{\varepsilon_P\}_{t+\Delta t} &= \{\varepsilon_P\}_t + \{\Delta\varepsilon_P\}
\end{aligned} \tag{3.17}$$

The commercial finite element package ABAQUS is used to perform both thermal and stress analysis. For the Wunnenberg case (860mm roll pitch) listed in Table 2.1, the standard 60x16 mesh for the single roll pitch model contains 960 8-node rectangular elements and 3033 nodes as presented in Figure 1.2 and Figure 3.2. The "CPS8R", 8-node rectangular continuum plane-stress element with reduced integration is used for stress analysis and the "DC2D8", 8-node quadratic diffusive heat transfer element is used for heat transfer analysis.

For stress analysis, it is important to apply the ferrostatic load incrementally to avoid large and permanent deformation by applying the load at once. The following scheme is used: 1/20 of the load is applied in the first cycle, 1/2 of the load in the second cycle and the full load in the third cycle. It is called a cycle when the rolls move past the domain of one roll pitch and a new roll enters the downstream boundary. The transient (Lagrangian) method is applied to solve the steady state problem. It may take up to 5 cycles to reach steady state.

The transient heat transfer analysis begins from the initial temperature field with constant temperature gradient across the shell thickness and constant temperature profile along the X direction.

In simulations where heat transfer is modeled, a sequentially coupled thermal stress analysis is adopted in which the temperature solution does not depend on the stress solution. This method includes two steps: First, the temperature field is calculated with the heat transfer model solely (without consideration of stress simulation). Second, the temperature field is read into the stress analysis at nodes as a predefined thermal load. For fast convergence, the coupled thermal stress analysis starts from an initial condition which is the solution to the stress analysis with constant surface temperature.

All simulations were run on a single-processor NCSA Origin 2000 workstation using ABAQUS (5.8-1). The following table lists the computational cost per cycle for some typical runs of stress analysis.

Table 3.3. Computational cost per cycle for typical runs

Typical runs	CPU time	Memory	Storage
Single roll pitch model (860mm)	30 min	16 M	200 M
8*430mm with one roll missing	300 min	25 M	800 M
5*250mm + 5*310mm	90 min	20 M	300 M

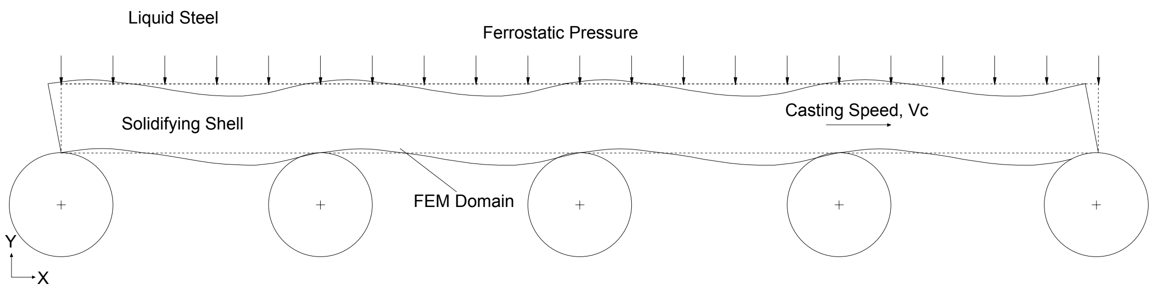

Figure 3.1. Multiple roll pitch bulging model (with at least 4 roll pitches)

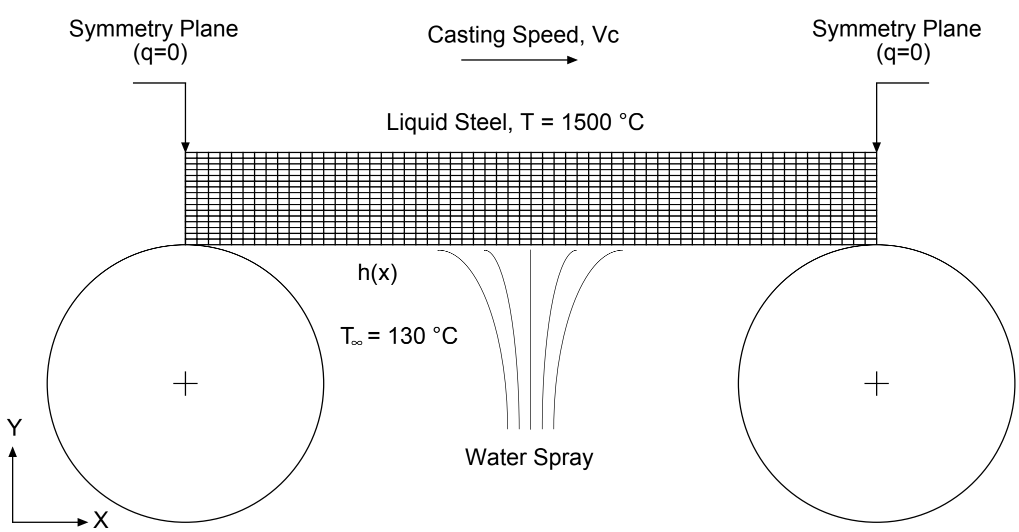

Figure 3.2. Heat transfer model for a single roll pitch - domain, mesh and B.C.

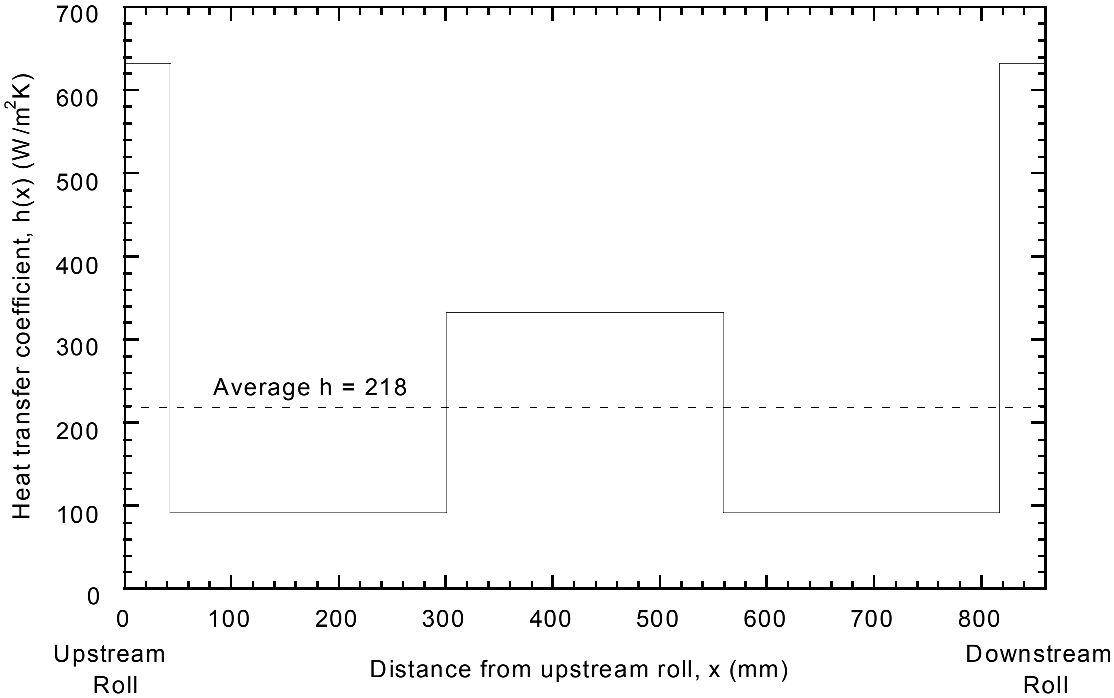

Figure 3.3. Heat transfer coefficient as a function of distance along strand

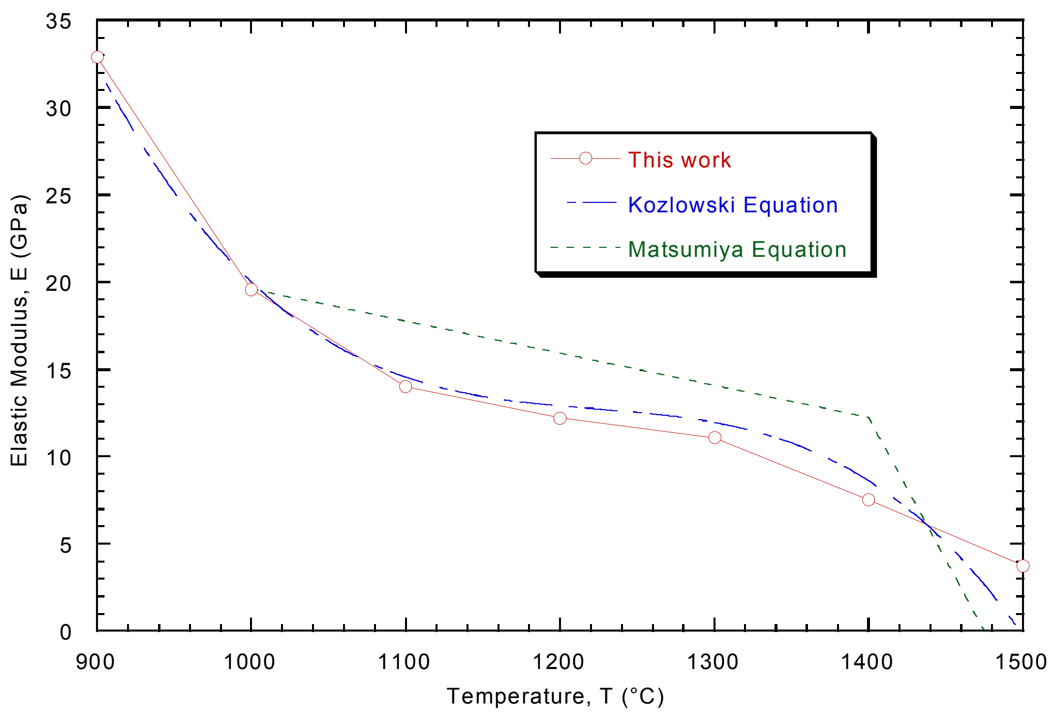

Figure 3.4. Temperature dependent elastic modulus

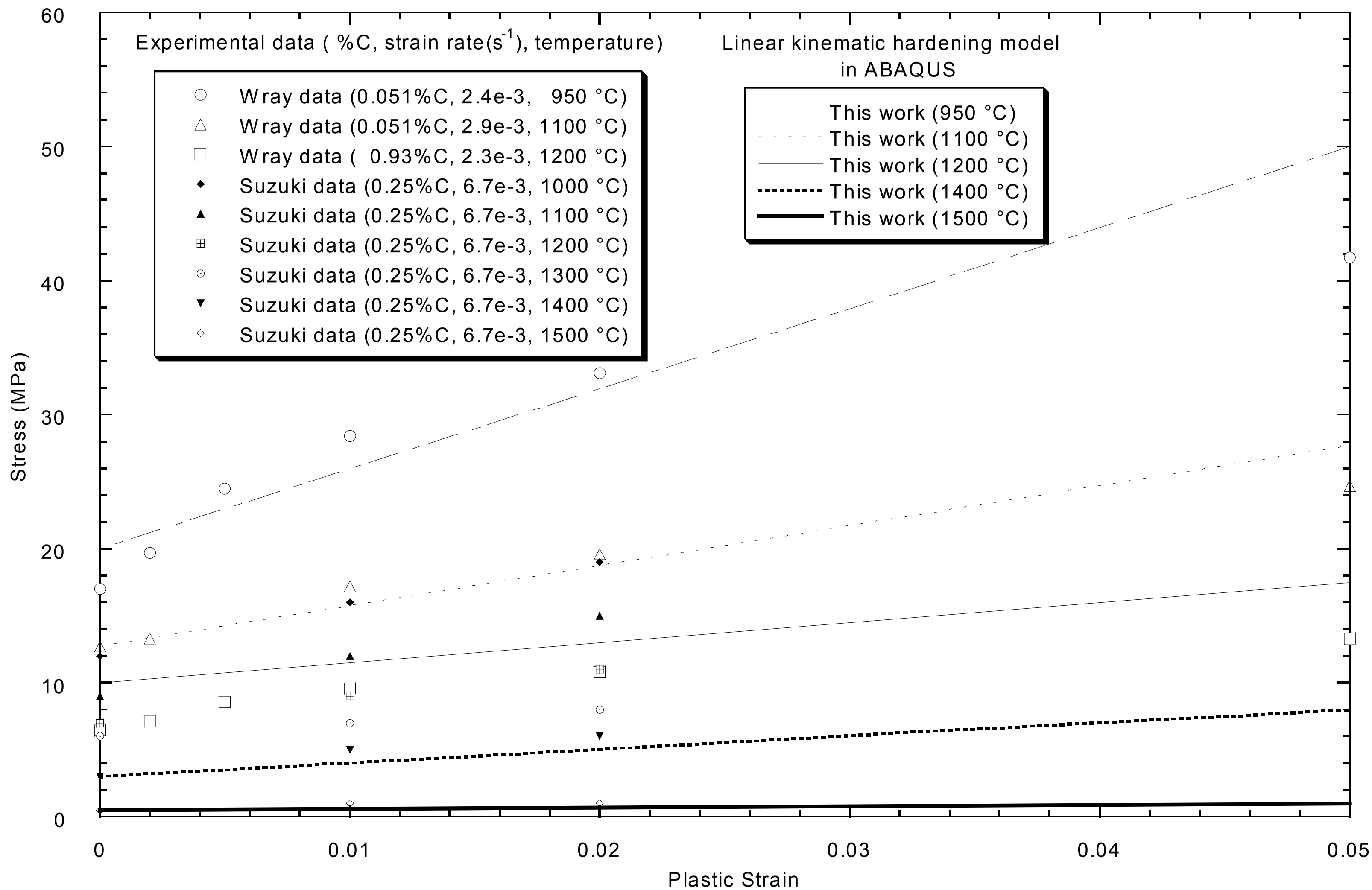

Figure 3.5. Temperature dependent stress strain relations

4 Model Verification

To verify that the stress model had been formulated and programmed correctly, it was first employed to a simple test problem that has an analytical solution. The numerical consistency of the model was demonstrated by convergence to a steady state and a mesh refinement study. The modeling approach was then verified by comparing numerical results with experimental measurements.

4.1 Test Problem

An elasto-static beam problem is illustrated in Figure 4.1. The beam is an over-simplified version of the slab bulging problem and has a length of L and a thickness of D. The beam is assumed unconstrained in the width direction, so the width does not matter. It is loaded with uniform steady pressure P with the two ends fixed, i.e. no deflection in X and Y directions and no rotation at the two ends. A constant elastic modulus E is assumed.

The general differential equation of the elastic beam is:

$$EI\frac{d^2v}{dx^2} = M(x) \tag{4.1}$$

Where, v is displacement in Y direction. The bending moment M(x) for a simply supported beam with constant pressure is given by the following equation:

$$M(x) = -\frac{1}{12}PL^2 + \frac{1}{2}PLx - \frac{1}{2}Px^2 \tag{4.2}$$

By applying the boundary conditions of fixed displacements and rotations at the ends, Equation 4.1 was integrated twice to get the displacement profile and the maximum displacement.

$$v = \frac{PL^4}{ED^4}\left(-\frac{1}{2}(x/L)^2 + (x/L)^3 - \frac{1}{2}(x/L)^4\right)$$
$$v_{\max} = v(x = L/2) = -\frac{1}{32}\frac{PL^4}{ED^3} \tag{4.3}$$

This result reveals an important insight into the effect of roll pitch (L) and shell thickness (D). The maximum bulging displacement is proportional to the 4^{th} power of the roll pitch and is inversely proportional to the 3^{rd} power of the shell thickness. It increases linearly with increasing pressure and decreasing elastic modulus.

4.2 Comparison with Test Problem

To help validate the model, a 2-D elastic steady state stress analysis was performed to solve the test problem in Section 4.1 using a simplified version of the ABAQUS model. Five different cases were studied with test parameters listed in Table 4.1. A uniform mesh with 8-node rectangular elements was used for each test problem.

Table 4.1. Test Problems for program validation

Test No.	1	2	3	4	5
Length, L(mm)	310	860	430	860	860
Thickness, D(mm)	23.17	79	79	30	20
Pressure, P(MPa)	0.18	0.26	0.26	0.26	0.26
Elastic modulus, E(GPa)	10	12	12	12	12
L/D	13.4	10.9	5.4	28.7	43
Mesh (X*Y)	16*8	60*16	60*16	16*8	16*8
Exact Solution (mm)	0.4176	0.7512	0.0470	13.72	46.30
ABAQUS Results (mm)	0.4433	0.8223	0.0648	13.89	46.53
Error (%)	6	9	38	1	0.5

The FEM solution by ABAQUS is in good accordance with the analytical solution within some extent of error. The reason for the big error (up to 38%) with the small L/D ratio is that the analytical solution is not valid for an L/D ratio less than 24 for rectangular beams [28]. For an L/D ratio as high as 29 in Test 4 and 43 in Test 5, the FEM approximation gives an excellent result (1% and 0.5% of error) even with a coarse mesh.

4.3 Numerical Consistency

The numerical consistency of the stress model was demonstrated by solving test problems to show that the results reach a steady state, and by a mesh refinement study. The single roll pitch model described in Chapter 3 was used in this section with Wunnenberg conditions (see Table 2.1).

4.3.1 Steady State Problem

The transient method used in this model was discussed in Section 3.4. In this method, recall that the ferrostatic pressure is applied incrementally in the first three cycles and continued for two further cycles. The simulation should continue until the results reach a steady state. To test this method, it was applied to solve a problem (Table 2.1 conditions). The surface bulging histories at different distances downstream are expected to reach a steady state. Figure 4.2 demonstrates that the bulging displacement converges to 10.61mm after five cycles (including the loading cycles).

4.3.2 Mesh Refinement Study

In this mesh refinement study, the modeled shell thickness was 83mm instead of 79mm (Table 2.1 conditions). Besides the standard uniform 60x16 mesh, several other meshes are studied to demonstrate the grid independence of the solution method. The simulation results and computational costs for the different mesh designs are compared in Table 4.2. The number of elements in the Y direction does not have much effect on results, but that in the X direction is more influential on bulging. The bulging displacement converges to 7.5 mm when mesh is refined from 120x16 to 120x20. There is a tradeoff between accuracy and computation costs. Finer mesh produces better results, but requires much more computational resources. In general, the best compromise is the 60x16 mesh, which is adopted as the standard mesh for the rest of this work. However, to guarantee accuracy needed for the variable surface temperature case, the 120x16 mesh with finer mesh outside should be adopted for analyses in which heat transfer is also computed.

Table 4.2. Mesh refinement study

Mesh (X×Y)	Number of element	CPU time/cycle (hour:minute)	Storage	Calculated Bulging (mm)
60×8	480	0:12	140 M	5.7
60×16	960	0:30	200 M	6.2
60×16*	960	1:00	200 M	6.3
120×16	1920	3:00	2 G	7.5
120×16*	1920	5:00	2 G	7.5
120×20	2400	8:00	2.5 G	7.5

* Finer mesh outside (cold face surface), uniform mesh size otherwise.

4.4 Comparison with Experimental Measurements

The 2-D elastic-plastic stress model described in Chapter 3 is used to simulate a single roll pitch with Wunnenberg conditions (see Table 2.1) and Sumitomo conditions (see Table 2.2) to compare with the corresponding experimental measurements. Constant surface temperature was assumed.

4.4.1 Sumitomo Case (uniform 310mm roll pitch)

Due to uncertainties about constitutive equations and lack of surface temperature measurements (a single value of 1220°C), a constant surface temperature of 1000°C was used with the Wray constitutive relations in Figure 3.5 for calibration. The simulation results are compared with the Sumitomo measurements in Table 4.3.

Table 4.3. Comparison with the Sumitomo measurements

	Maximum bulge	Position of Max bulge	Negative bulge	Ratio of Neg bulge to Max bulge
ABAQUS simulation	3.67 mm	63%	0.93 mm	0.25
Measurement	3.2 mm	60~65%	1.28 mm	0.4

Having been calibrated, the model reveals the same trends as the measurements regarding the value and position of the maximum bulge, the negative bulge and the ratio of the negative bulge to the maximum bulge. It confirms the existence of negative bulging. The position of the maximum bulge is at 60~65% of the roll pitch from the upstream roll. There is an error of 15% on the maximum bulge. The results simply indicate the error in material properties.

4.4.2 Wunnenberg Case (uniform 860mm roll pitch)

A constant surface temperature of 1000°C was assumed with the constitutive relations in Figure 3.5. The simulation results are compared with the Wunnenberg measurements in Table 4.4.

Table 4.4. Comparison with the Wunnenberg measurements

	Maximum bulge	Position of Max bulge	Negative bulge	Ratio of Neg bulge to Max bulge
ABAQUS simulation	10.61 mm	64.2%	2.9 mm	0.27
Measurement	6.7 mm	75%	N/A	N/A

The ABAQUS simulation again predicts the existence of negative bulging. The position of the maximum bulge is at 60~65% of the roll pitch from the upstream roll.

The difference between the simulation results and the measurements is due to the uncertainties of the data measurements. After multiplying the 2-D shape factor (Equation

2.2) to account for the constraining effect of the slab width, the maximum bulging becomes 6.64 mm, which matches the measurement very well.

4.5 Conclusions

The ABAQUS stress model is validated and can be used to simulate more realistic problems, which include the slab bulging with surface temperature variation, and the evolution of the bulging profile due to the changes in the geometry of the support system, such as sudden roll pitch changes and roll misalignment. These will be discussed in Chapter 5 and 6.

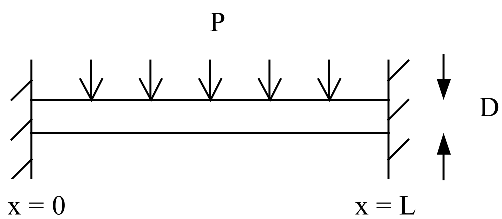

Figure 4.1. Elasto-static beam with uniform loading

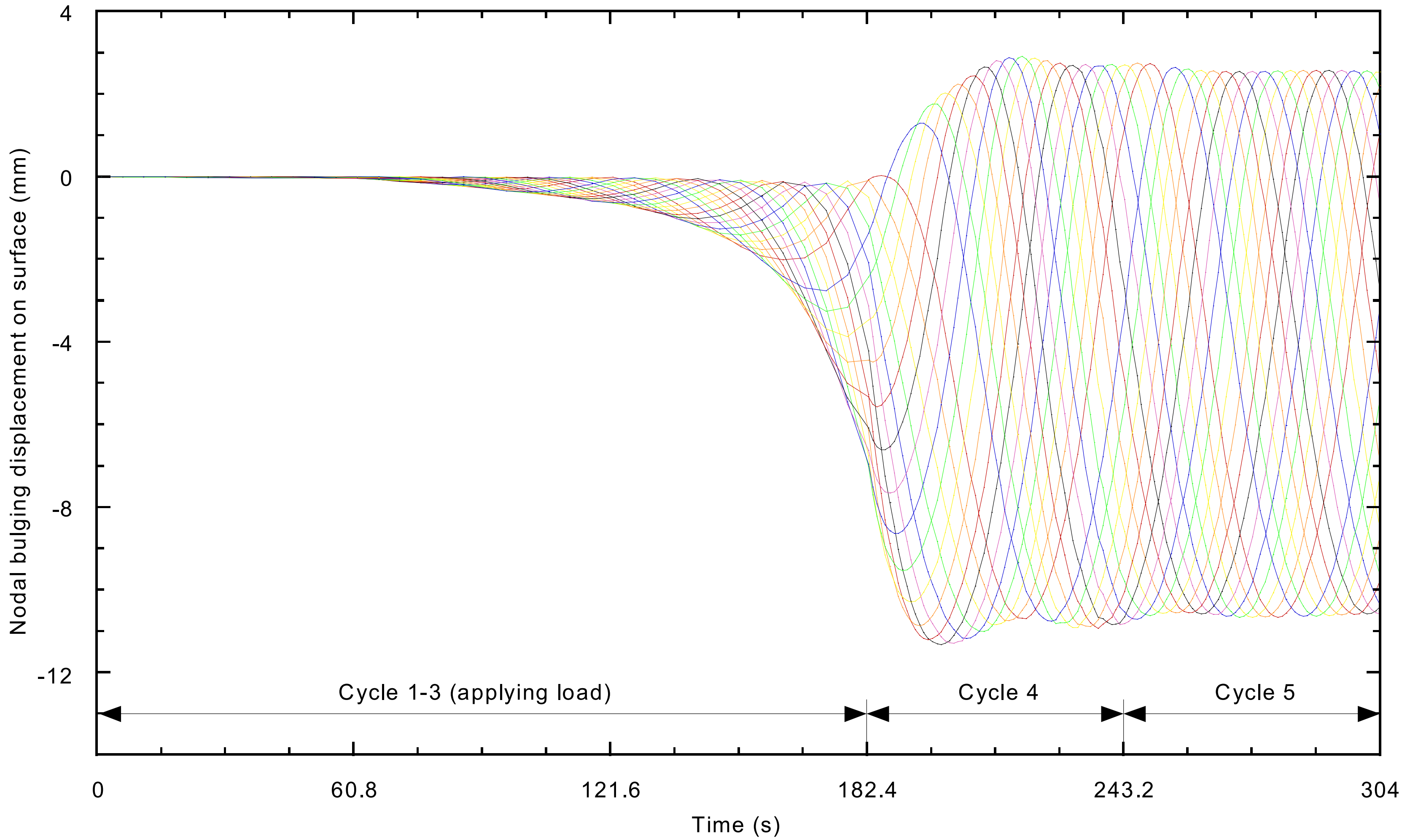

Figure 4.2. Surface bulging histories at different distances downstream showing convergence to steady state

5 Effect of Surface Temperature Variation

A typical stress analysis was simulated with a constant surface temperature of 1000°C with Wunnenberg conditions (see Table 2.1). In real casters, the surface temperature fluctuates because of roller contact and water spray. As mentioned in Section 3.4, a sequentially coupled thermal stress analysis is adopted in simulations where heat transfer is modeled. The temperature field was calculated with the heat transfer model. Stress analysis results both with and without the surface temperature variation are compared with respect to bulging displacement and surface stress.

5.1 Typical Stress Analysis with Constant Surface Temperature

A constant surface temperature of 1000°C was assumed for the typical stress analysis with Wunnenberg conditions (see Table 2.1). The temperature increases linearly up to 1500°C at the solidification front. The material properties were presented in Chapter 3 with the constitutive relations shown in Figure 3.5. As discussed in Section 4.4.2, the bulging profile is asymmetric with the maximum bulge found at 64% of the roll pitch from the upstream roll due to the existence of the negative bulging. The ratio of the negative bulge to the maximum bulge is 0.27.

Figure 5.1-4 present the typical results of strain, plastic strain, strain-rate and stress (in X direction) contour plots with a displacement magnification factor of 8. The total strains range from –1.33% to 2.32%, which consists mainly of plastic strain. The maximum tensile strain is located at the solidification front just past the top of the upstream roll as shown in Figure 5.1. For this case, the maximum tensile strain is about 2.3% which is in the range of concern for crack formation [29]. The strain rates in most of the domain are small, ranging from 10^{-3} to 10^{-5} s^{-1} and from -10^{-5} to -10^{-3} s^{-1}, except in the vicinity of the rolls and where the bulging displacement is changing from negative to positive. Figure 5.4 shows that the greatest stresses are compressive and are found at the cold surface in the vicinity of the rolls. The maximum tensile stresses are located at the cold surface in the middle between the two rolls, just upstream of the point of the maximum bulging.

The maximum stress of 18MPa corresponds to the stress at low plastic strain assumed in the constitutive model in Figure 3.5 for this temperature range (1000°C to 1100°C). Stresses near the solidification front are small because of the high temperatures which produce lower elastic modulus values.

5.2 Heat Transfer Analysis

The material properties and boundary conditions for the heat transfer analysis were presented in Chapter 3.

A temperature contour plot of the simulation is presented in Figure 5.5. The surface temperature profile is shown in Figure 5.6. The surface temperature fluctuates from the lowest temperature of 937°C, beneath the roll, to the highest temperature of 1045°C, located between the rolls and the water spray. This variation of 100°C is typical of the variations measured in practice. The temperature beneath the water spray is about 980°C. Note that the average heat transfer coefficient of 218 W/m^2K and the ambient temperature of 130°C keep the surface temperature about 1000°C.

Temperature distributions through the shell thickness are shown in Figure 5.7. Away from the cold surface, the temperature depends linearly on the distance into the shell. It should be noted that the surface temperature variations caused by the roller contact and the water spray have a small penetration depth, only about 20% of the shell thickness. Deep into the shell from the cold surface, the temperature remains almost constant along the axial casting direction.

5.3 Coupled Thermal Stress Analysis

The time-dependent temperature field is input into the stress analysis model to study the effect of the surface temperature variation on bulging and stress solutions. Figure 5.7-11 present the simulation results of strain, plastic strain, strain-rate and stress contour plots with a displacement magnification factor of 8. For this case, the maximum tensile strain of 2.7% at the solidification front is 16% bigger than that of the case with uniform surface temperature and the maximum stress of 19MPa at the surface is 6% larger.

The bulging profiles with and without the surface temperature variation are compared in Figure 5.12. Both bulging profiles have the same asymmetric shape with negative bulging and maximum bulging located at 64% from the upstream roll. However, the maximum bulging displacement increases by 15%, from 10.61mm (with constant surface temperature of 1000°C) to 12.21mm (with surface temperature variation).

The effect of the surface temperature variation on surface stress is illustrated in Figure 5.13. There is a local stress concentration in compression beneath the rolls due to compression by the rolls. The higher temperature between the rolls and the centered water spray region causes an extra compression stress on the surface for the case with surface temperature variation. This extra compression occurs in two places: from 50mm to 200mm and from 560mm to 780mm. This is balanced by a little extra tension directly under the spray. These variations in both temperature and stress likely are worse for surface cracking problems than the case with uniform surface temperature, which is not feasible in practice.

5.4 Conclusions

The surface temperature variation appears to be worse for cracking problem than the case with uniform surface temperature. It produces a 6% bigger tensile stress at the cold surface, which is important for surface cracks, and a 16% larger tensile strain at the solidification front, which is responsible for internal hot tear cracks. It also increases the magnitude of bulging displacement by only 15%. Moreover, it does not change the bulging behavior of the strand. For simplicity, a constant surface temperature is assumed for the further study of the bulging phenomena.

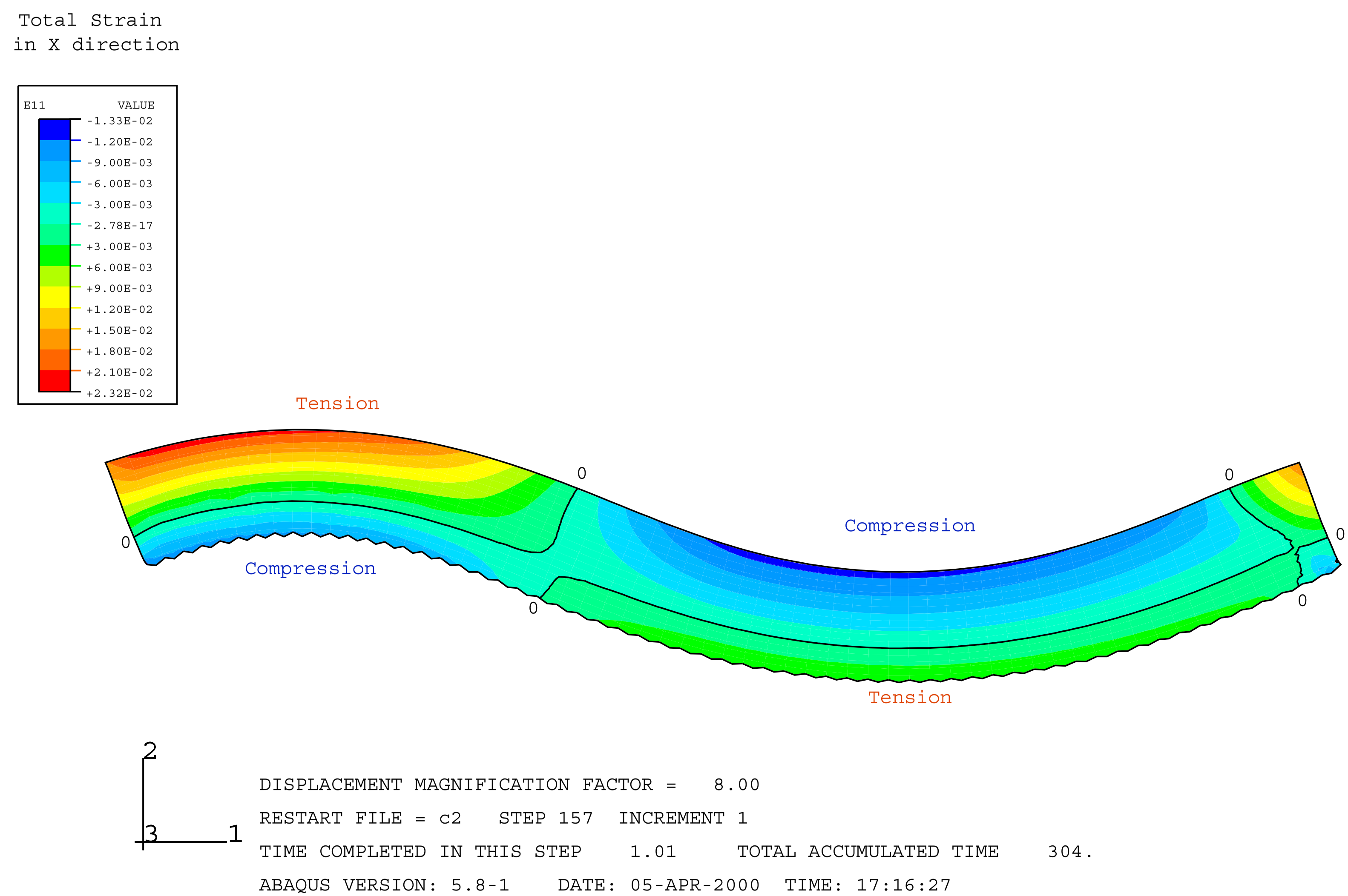

Figure 5.1. Strain contour plot for a typical run with constant surface temperature of 1000°C

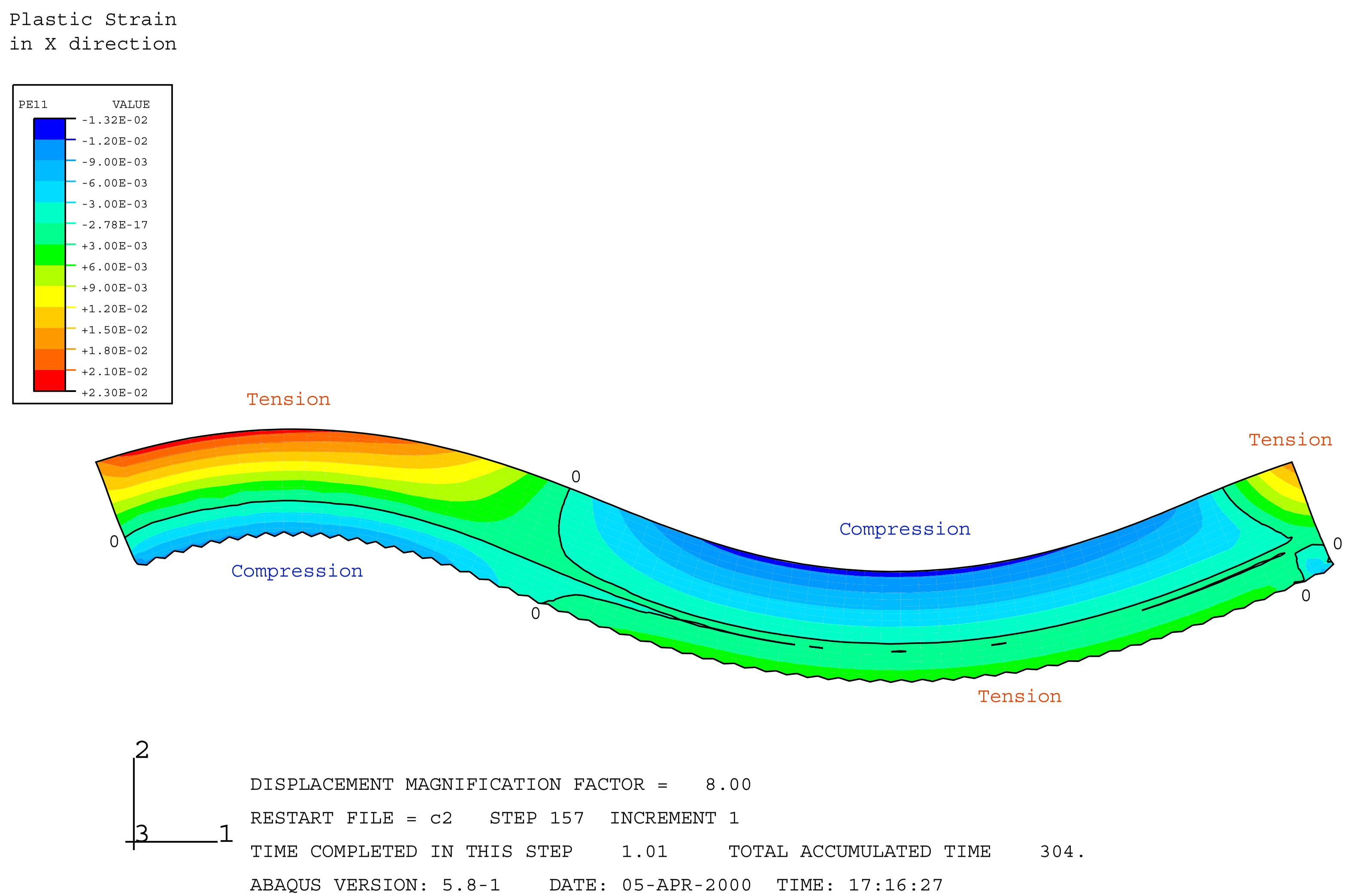

Figure 5.2. Plastic strain contour plot for a typical run with constant surface temperature of 1000°C

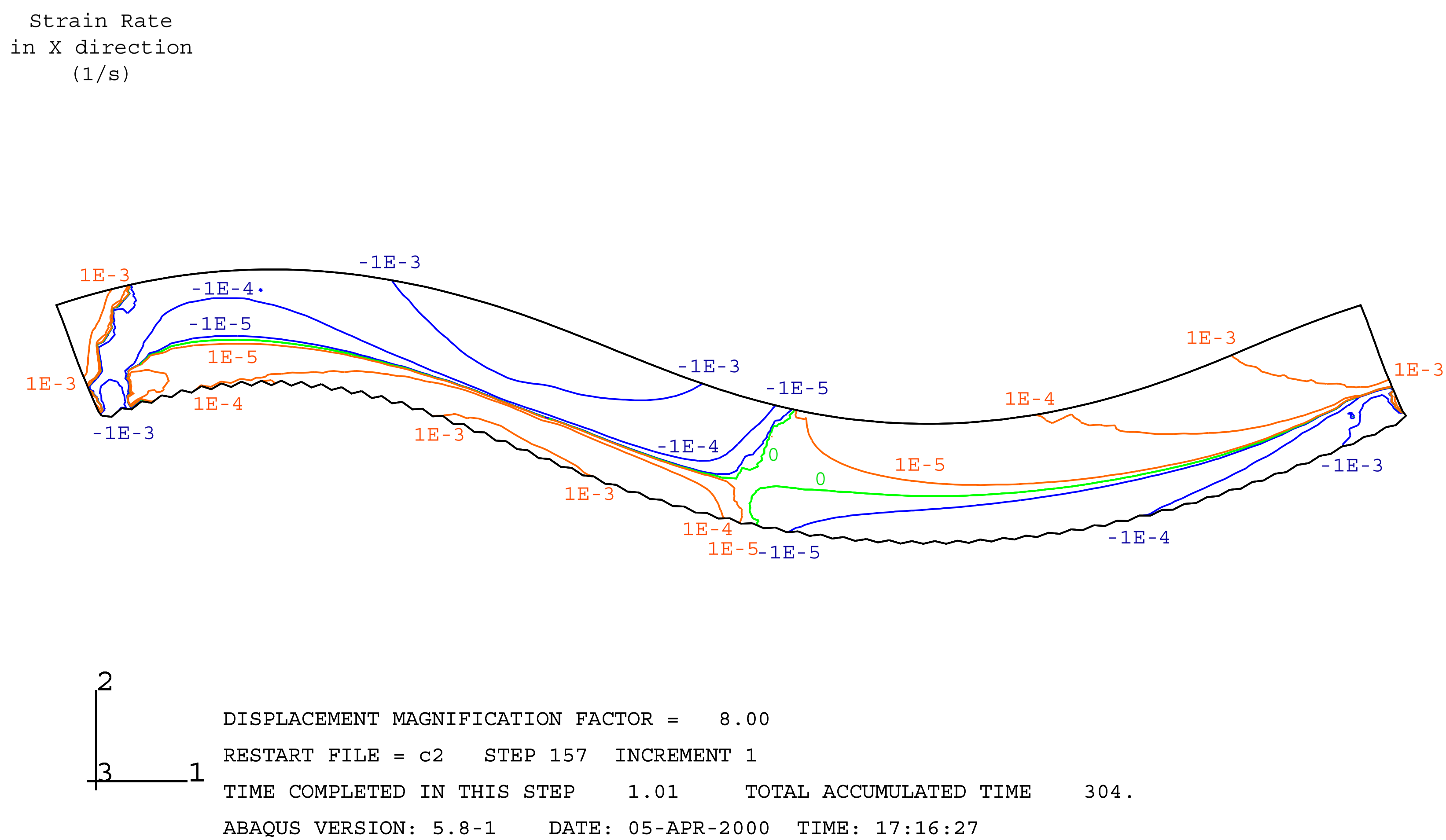

Figure 5.3. Strain rate contour plot for a typical run with constant surface temperature of 1000°C

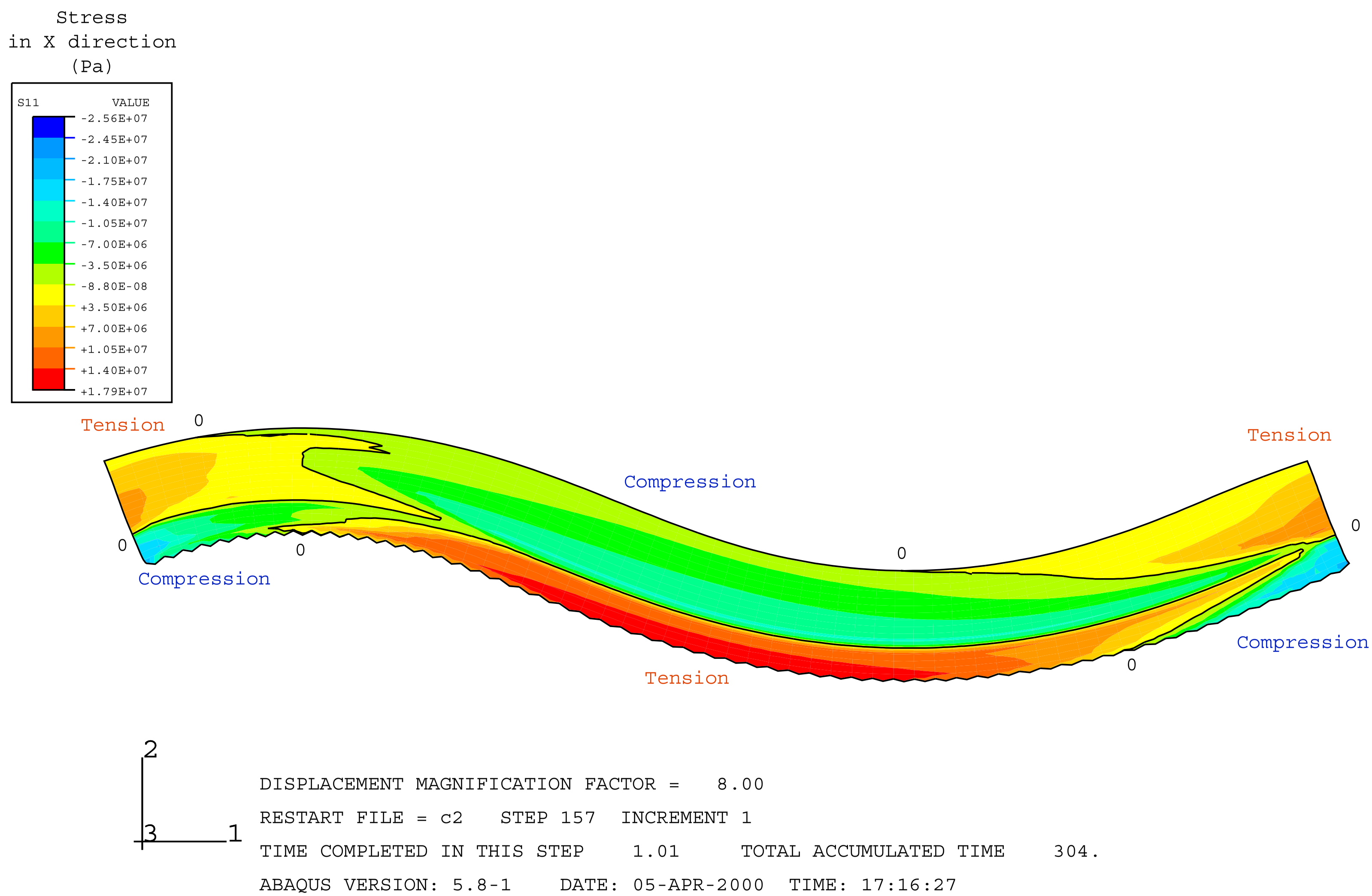

Figure 5.4. Stress contour plot for a typical run with constant surface temperature of 1000°C

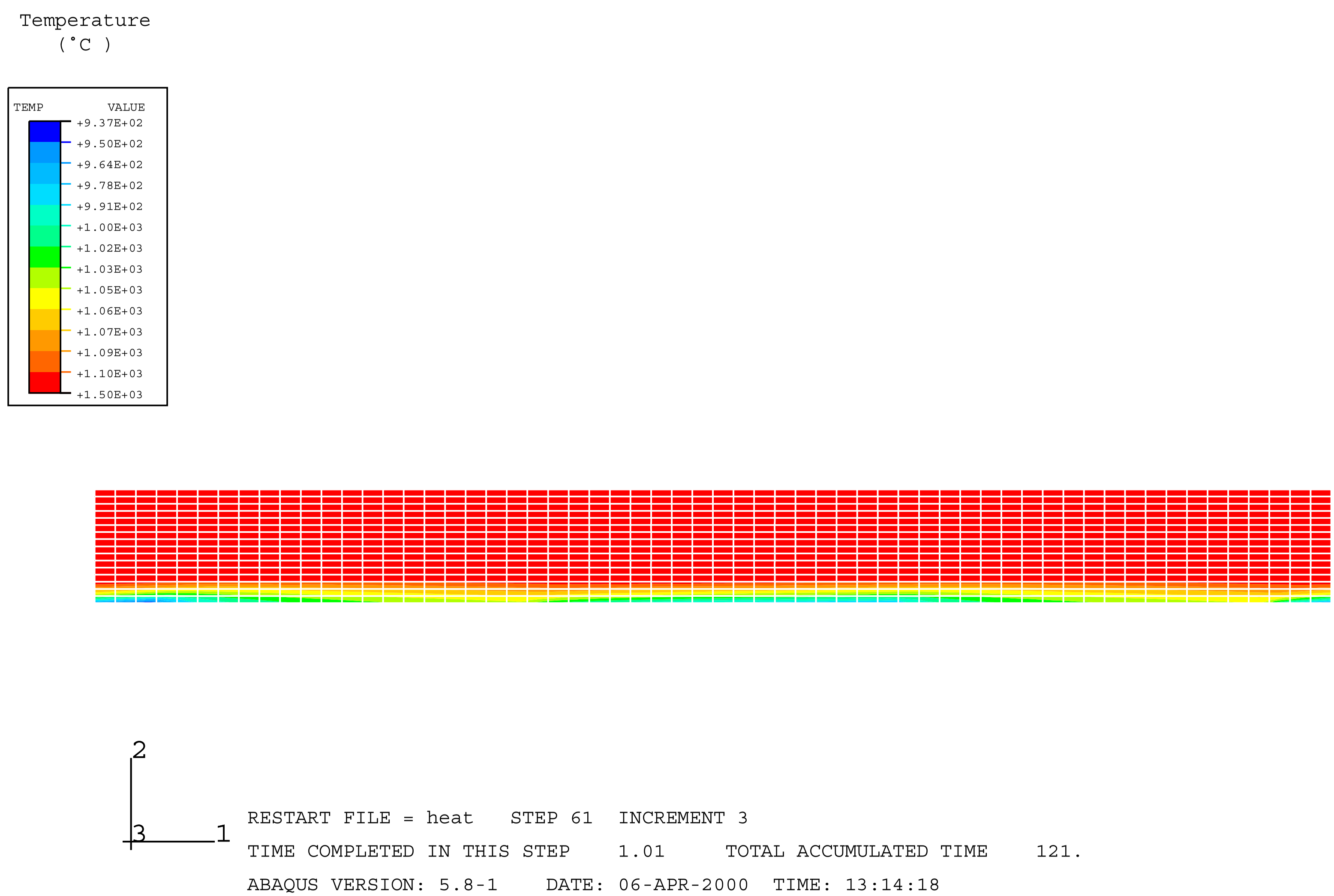

Figure 5.5. Temperature contour plot

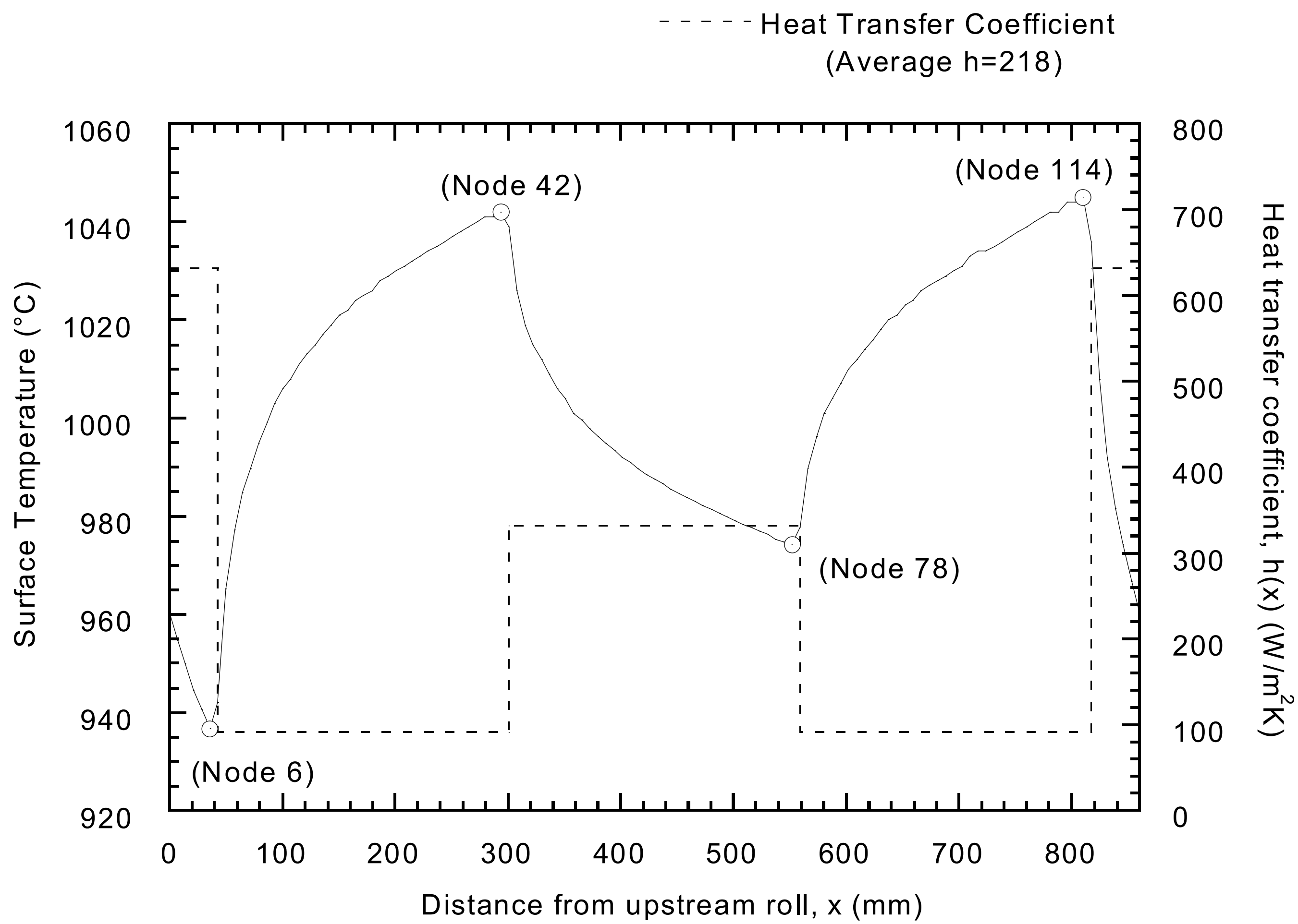

Figure 5.6. Surface temperature profile

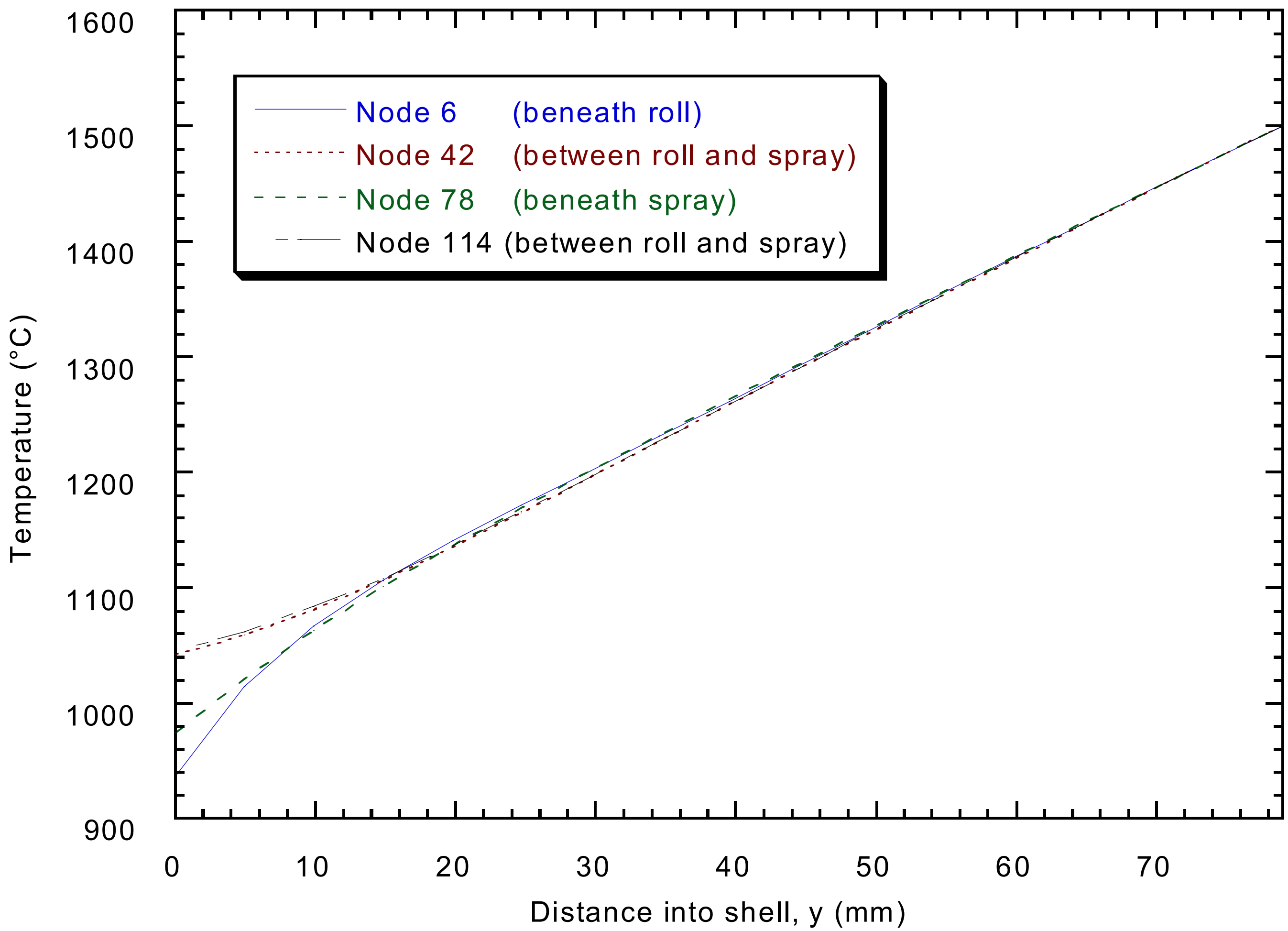

Figure 5.7. Temperature distributions through shell thickness

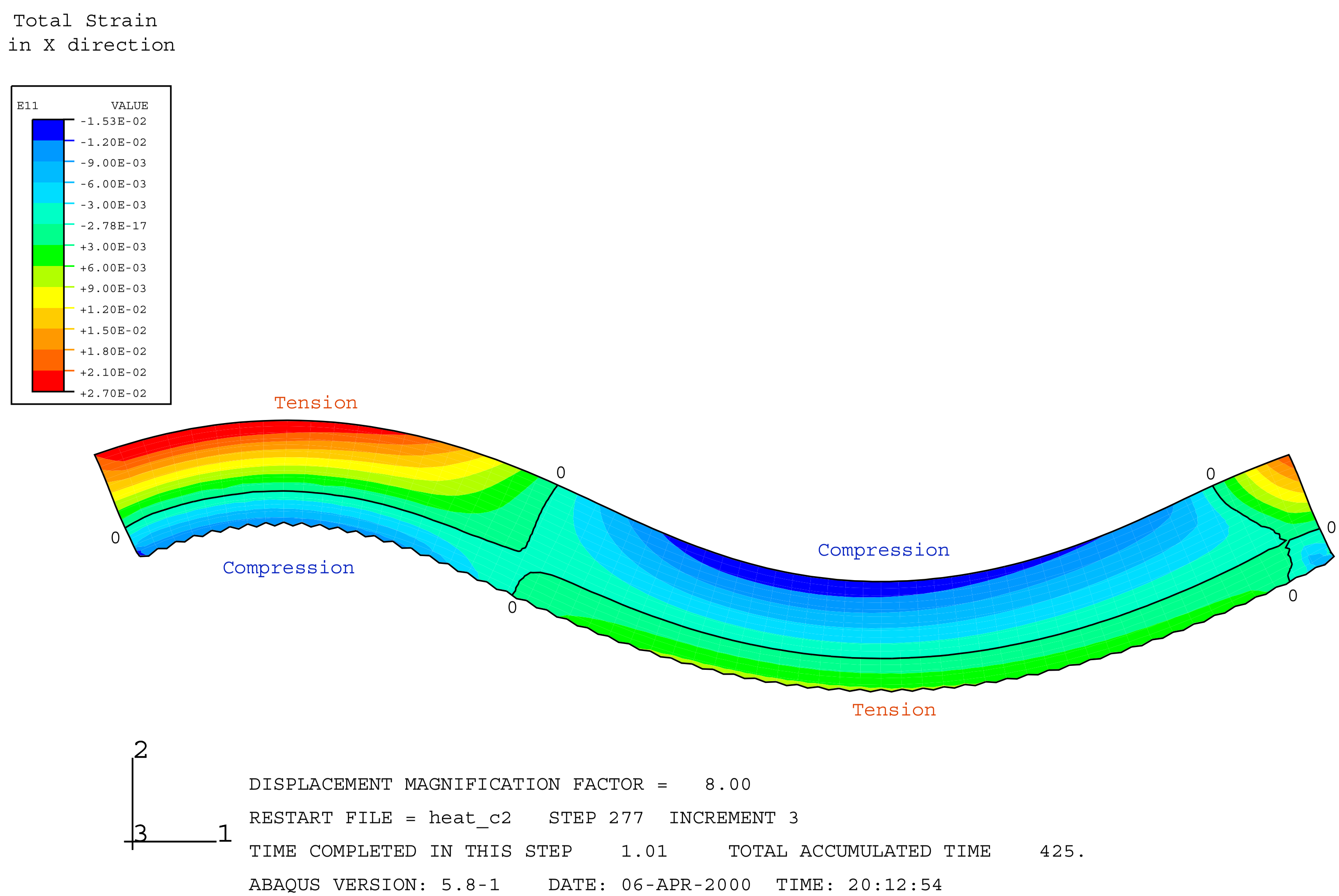

Figure 5.8. Strain contour plot for stress analysis with surface temperature variation

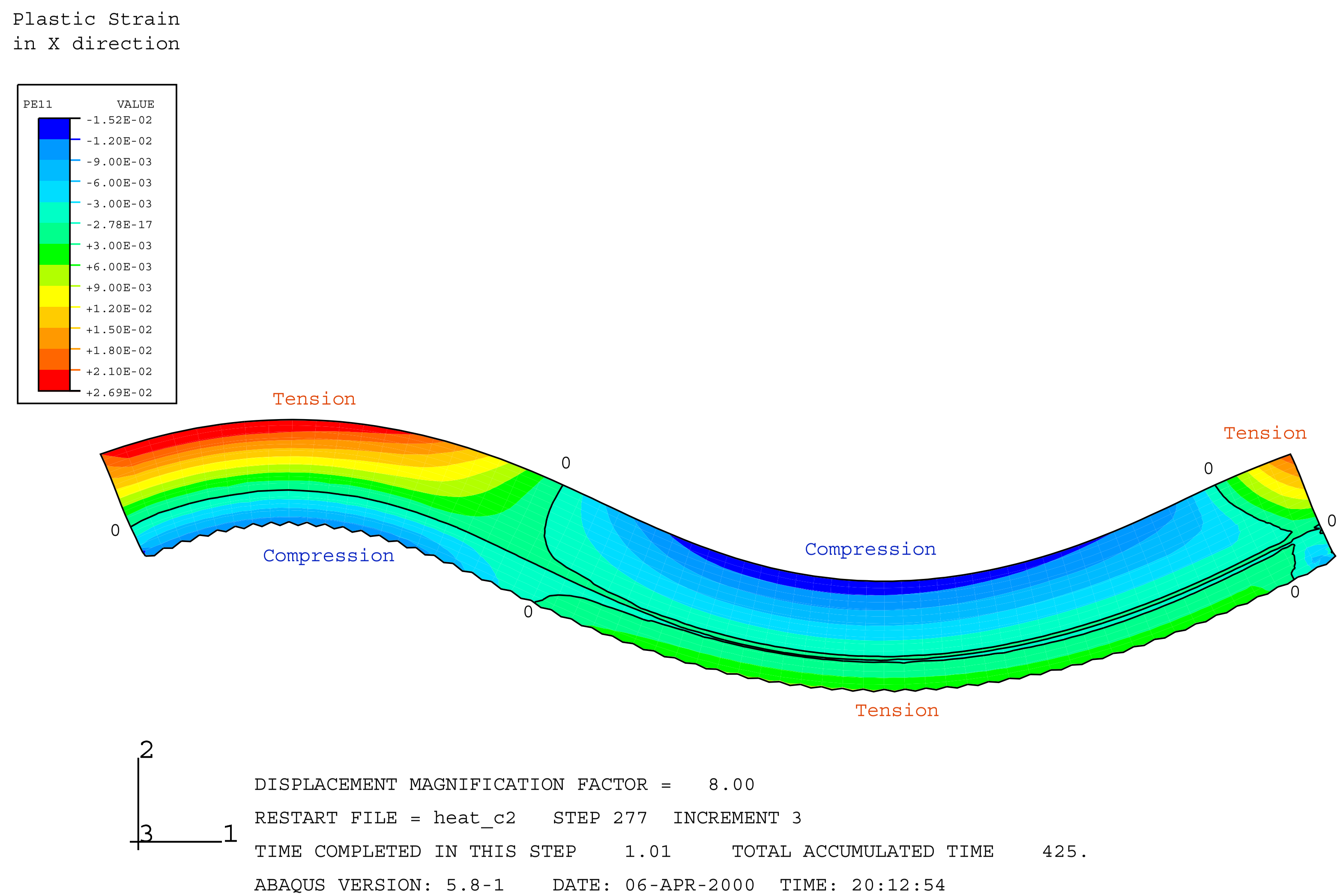

Figure 5.9. Plastic strain contour plot for stress analysis with surface temperature variation

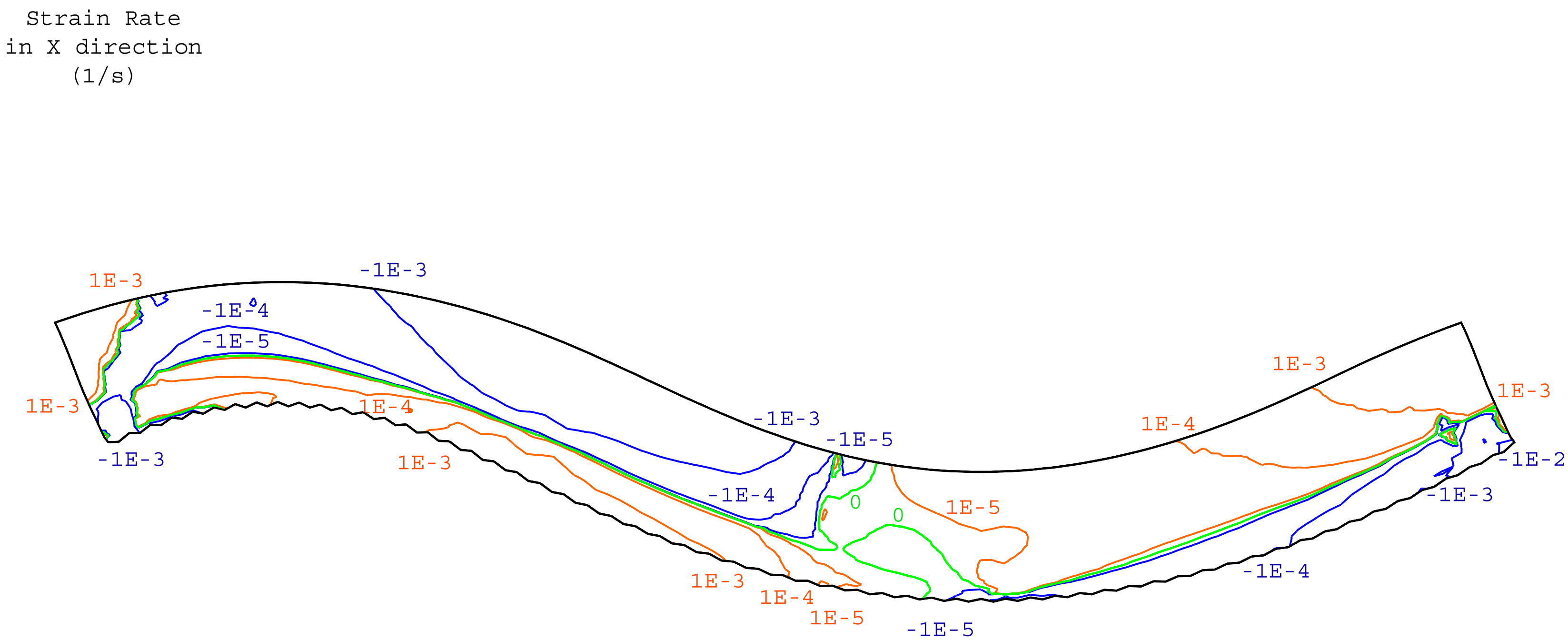

2
3 1

DISPLACEMENT MAGNIFICATION FACTOR = 8.00
RESTART FILE = heat_c2 STEP 277 INCREMENT 3
TIME COMPLETED IN THIS STEP 1.01 TOTAL ACCUMULATED TIME 425.
ABAQUS VERSION: 5.8-1 DATE: 06-APR-2000 TIME: 20:12:54

Figure 5.10. Strain rate contour plot for stress analysis with surface temperature variation

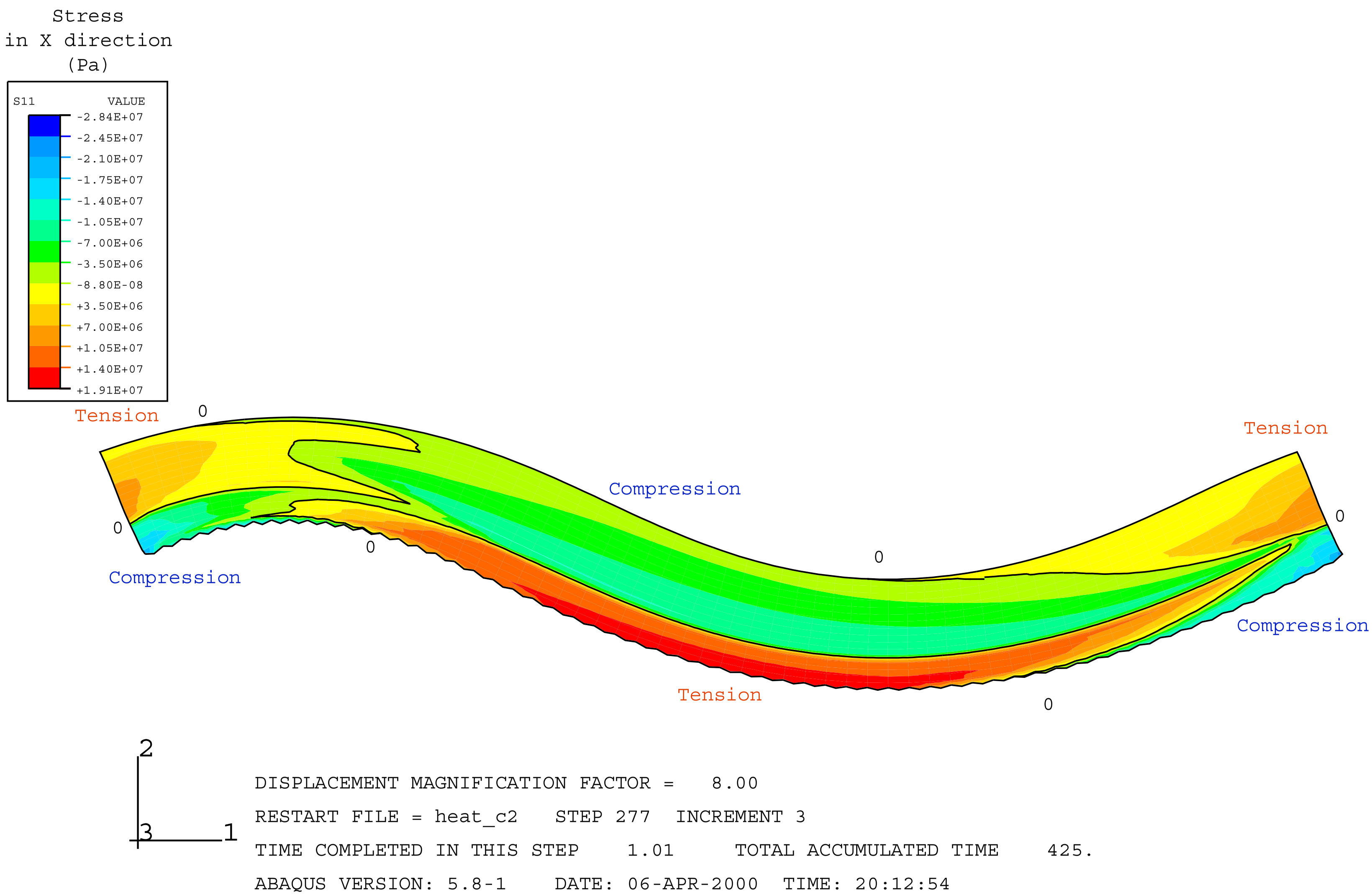

Figure 5.11. Stress contour plot for stress analysis with surface temperature variation

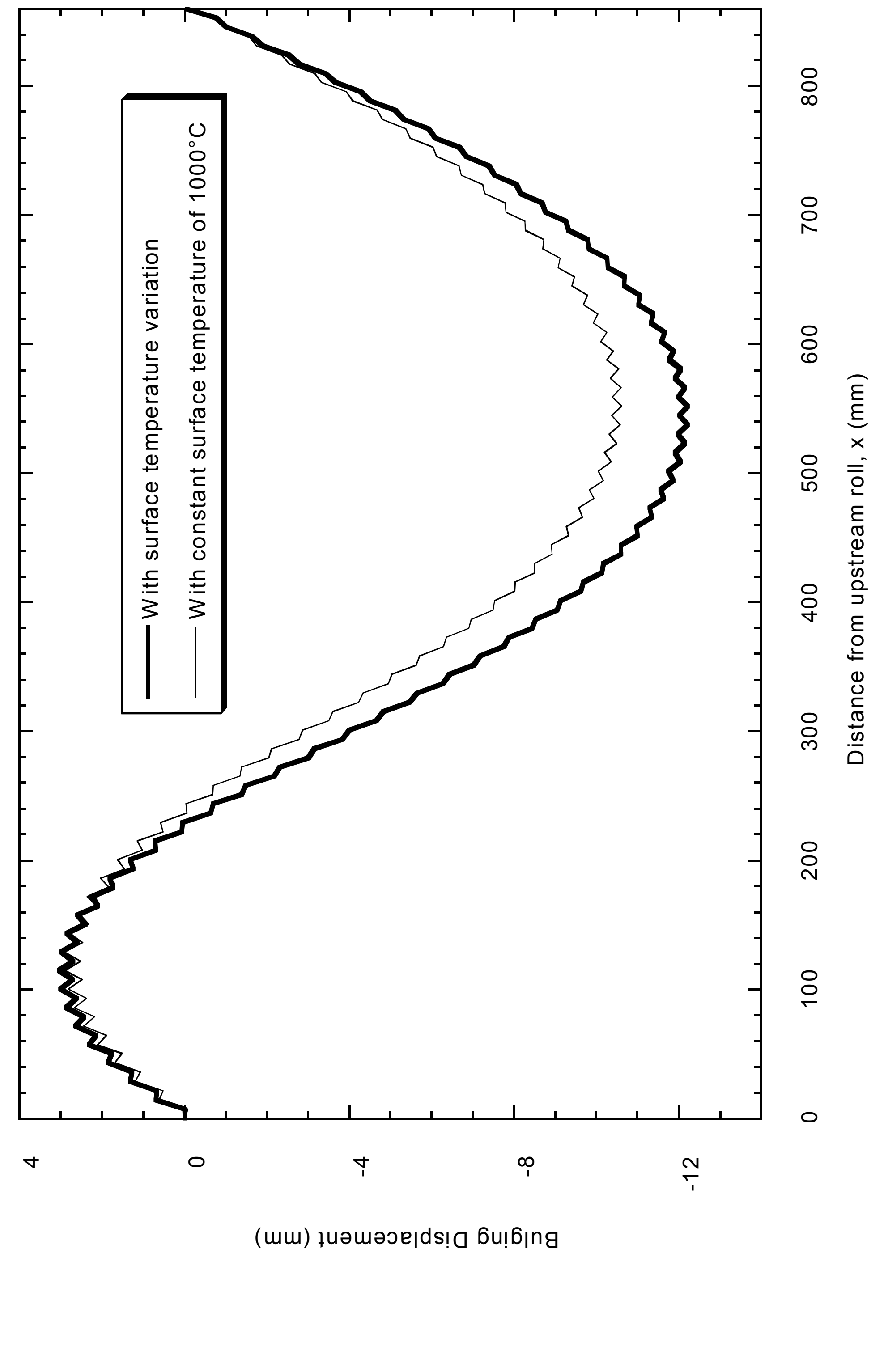

Figure 5.12. Comparison of bulging profiles

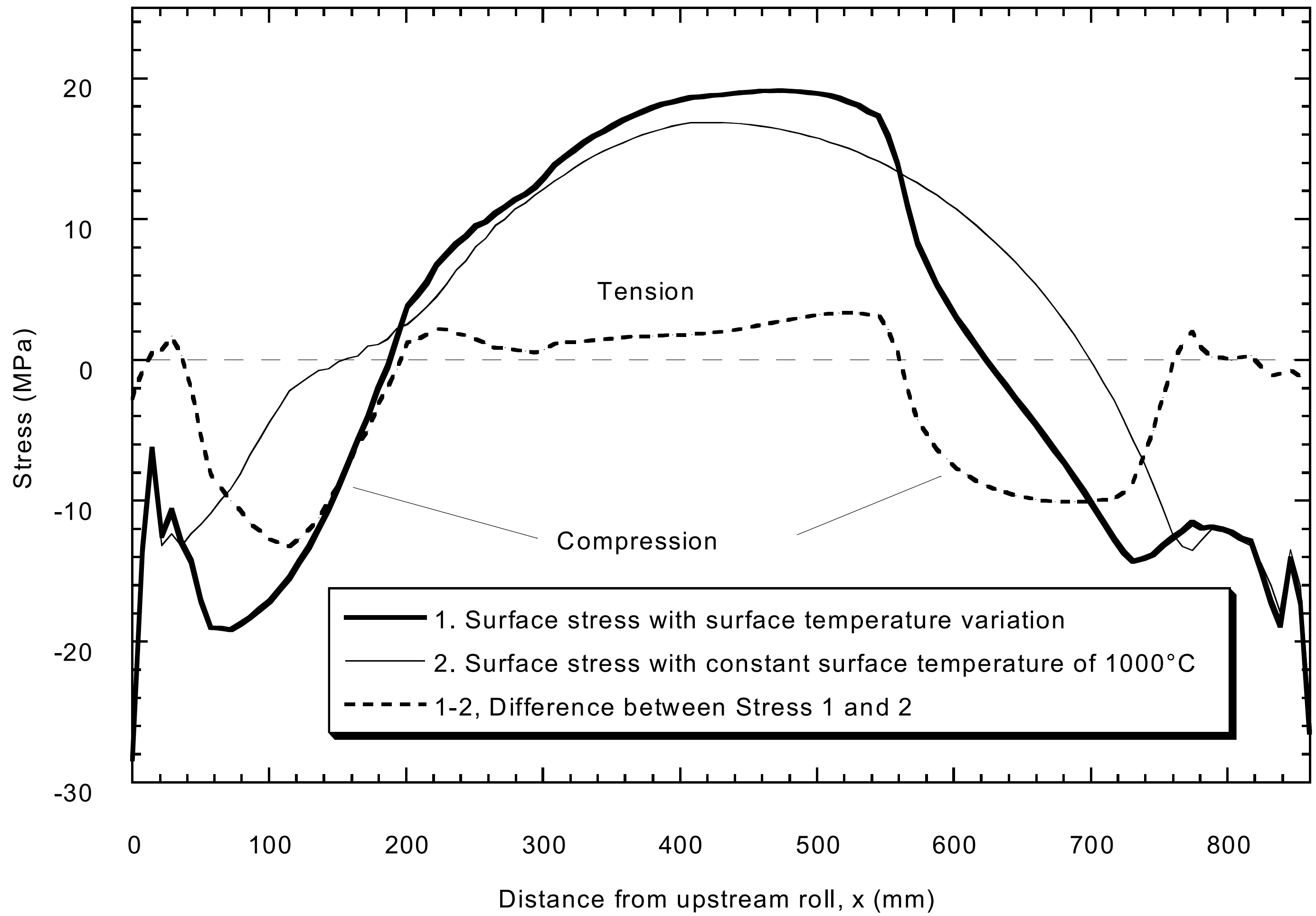

Figure 5.13. Effect of surface temperature variation on surface stress

6 Influence of Upstream Rolls

In real casters, changes in the geometry of the support system, such as sudden changes in the roll pitch between segments, roll misalignments or eccentricities, missing rolls or similar single large gap between segments, all lead to large downstream disturbances of the bulging profile[11]. To simulate this behavior of the strand, the single roll pitch model is insufficient. Thus, the multiple roll pitch model, which considers several roll intervals and is described in Section 3.1.3, was applied to perform this stress analysis of the influence of the upstream rolls. To validate the model, the first section shows a study of three types of boundary conditions on the two ends of the domain. The effects of a sudden roll pitch change and of a misaligned roll are discussed in the following two sections.

6.1 Study of Boundary Conditions

To obtain an accurate simulation, it is important to apply an appropriate boundary condition on the two ends of the multiple roll pitch model. Three types of boundary conditions are investigated for an 8-roll model with uniform 310mm pitch with Sumitomo conditions (see Table 2.1). The periodic boundary condition, described in Section 3.1.2, has coupled X and Y displacements on the two ends. Two other boundary conditions are defined as B.C. 1 which has coupled Y displacement on the two ends with zero displacement in the X direction and B.C. 2 which has two ends free except forcing the two points on bottom of the model ends fixed (zero X and Y displacements), i.e. there always are two rolls on the two ends.

Table 6.1 presents the simulation results with different boundary conditions. The bulging profiles are compared in Figure 6.1. If the roll pitch is uniform, the periodic boundary condition naturally reproduces the results of the single roll pitch model. The other two boundary conditions have a large influence on the bulging profile even three roll pitches downstream and two to three roll pitches upstream. Neglecting the end effects due to boundary condition, the bulging profile in the middle of the domain still matches the results of the single roll pitch model very well (see Figure 6.1).

Table 6.1. Results for an 8-roll 310mm pitch model with different boundary conditions

	Periodic B.C.	B.C. 1)	B.C. 2)
Maximum bulge	3.67 mm	5.62 mm	15.34 mm
Negative bulge	-0.93 mm	-1.59 mm	-3.11 mm
Influence downstream	No	3 roll pitches	3 roll pitches
Influence upstream	No	2 roll pitches	3 roll pitches

In general, the periodic boundary condition is best if appropriate, which would mean that a roll enters the downstream boundary at exactly the same time it leaves from the upstream boundary. It is exactly appropriate for the uniform roll pitch model. Even for some special cases with non-uniform roll pitches in the following two sections, it is still exact. Otherwise B.C. 2 is more feasible. It eliminates the difficulties encountered when new rolls move into the downstream boundary and force the displacement of the contact point to be zero in the Y direction, since there always are rolls on the ends. Because B.C. 1 prevents negative bulging near the ends and also has the same disadvantages as the periodic boundary condition for the Y displacement, it is not good for any case.

When none of the boundary conditions is truly appropriate, several roll pitches are needed on the ends for the error to dissipate. It is important to include at least 3 more roll pitches at each end in the model to account for the end effects due to the inappropriate boundary conditions.

6.2 Effect of Sudden Roll Pitch Change

The sudden change in roll pitch (for example, when moving between segments) is one cause of the downstream disturbances of the strand bulging. A multiple roll pitch model with 10-310mm and 10-250mm roll pitches was studied. The domain of interest alternates from 10-310mm to 10-250mm roll pitches. The periodic boundary condition is exactly appropriate for this special case since rolls always appear on the two ends at the same time. Two different roll pitch transitions were captured in this model: 1) roll pitch changes from 310mm to 250mm and 2) from 250mm to 310mm. In order to prevent interaction, it was important to separate these events by employing enough roll pitches (10 each) in this model. However, practically the change from smaller roll pitches to larger ones is more relevant.

Table 6.2 shows that this model qualitatively matches the Sumitomo measurements and the simulation results by J. Gancarz, et al [11]. A sudden change in roll pitch from 250mm to 310mm leads to a larger bulge and a bigger tensile strain on the solidification front in the first roll pitch immediately downstream of the transition. The results are compared with the results from the uniform roll pitch model, as shown in Table 6.3. The strain contour plot with a displacement magnification factor of 70 is shown in Figure 6.2.

Table 6.2. Bulging displacement for roll pitch changing from 250mm to 310mm

	Sudden change in roll pitch from 250mm to 310mm	Uniform 310mm roll pitch	Increase
Sumitomo measurements	4.6 mm	3.2 mm	44 %
J. Gancarz et al. model	3.6 mm	2.0 mm	80 %
This model	5.96 mm	3.67 mm	62 %

Table 6.3. Results for roll pitch changing from 250mm to 310mm

	Uniform 250mm roll pitch	Sudden change from 250mm to 310mm	Uniform 310mm roll pitch	Increase (Sudden change /uniform 310mm)
Maximum bulge	0.34 mm	5.96 mm	3.67 mm	62 %
Negative bulge	0 mm	-1.78 mm	-0.93 mm	91 %
Maximum strain on solidification front	0.2 %	2.1 %	1.75 %	20 %

There is a 62% increase in the maximum bulge in the first 310mm roll pitch, relative to the subsequent rolls. It increased because the strand does not need to overcome any large negative bulging displacement induced from the previous roll pitch. Elsewhere, this negative bulge acts to significantly reduce the size of the maximum bulge.

There is also a 20% increase in the maximum tensile strain, which is located at the solidification front just past the top of the first roll downstream from the roll pitch change, as shown in Figure 6.4.

The disturbance of the upstream rolls settles down (within 2%) after four roll pitches and also influences on one roll pitch upstream, shown in Figure 6.3. After the disturbance settles, the 310mm roll pitch generates the steady 3.67mm bulge, which is 108 times the 0.34mm bulge found for the 250mm roll pitch. This prediction is more sensitive to roll pitch than the 4th power relationship suggested by the measurements.

When the roll pitch is changing from 310mm to 250mm, the large bulging displacement for the 310mm pitch leads to a negative bulging on the following roll pitch. It takes six downstream roll pitches for the strand to settle down and it also has an influence on two roll pitches upstream.

6.3 Effect of Roll Misalignment

The mathematical model of slab bulging over multiple roll pitches was applied to analyze the effects of the misalignment of rolls in the caster. An 8-roll model with a uniform 430mm pitch for Wunnenberg conditions (see Table 2.1) is studied with misalignment of one roll.

An 8-roll pitch model with one roll missing represents an extreme case of roll misalignment. Table 6.4 presents the results with this infinite misalignment. The strain contour plot with a displacement magnification factor of 20 is shown in Figure 6.5. The bulging profile is compared with the uniform roll pitch model in Figure 6.6, and the strain on the solidification front is shown in Figure 6.7.

This single large gap leads to a 75% increase in the maximum bulge and a 152% increase in the negative bulge relative to the same uniform roll pitch. The bulging profile is asymmetric with the maximum bulge located at about 60% of the roll pitch from the upstream roll.

There is also a 12.9% increase in the maximum tensile strain on the solidification front, which is less significant than that of the bulging displacement. The maximum tensile strain is located on the solidification front just past the roll, which is between the maximum bulge and the negative bulge, as shown in Figure 6.7.

Table 6.4. Results for 8-roll 430mm pitch model with one roll missing

	430mm roll pitch with one roll missing	Uniform 860mm roll pitch	Increase
Maximum bulge	18.57 mm	10.61 mm	75 %
Negative bulge	-7.30 mm	-2.90 mm	152 %
Maximum strain on solidification front	2.62 %	2.32 %	12.9 %

A parametric study with misalignments of 1mm, 2mm, 3mm, 5mm, 10mm and 15mm was performed. Bulging profiles with different misalignments are compared in Figure 6.8. The large bulging displacement is found right at the place of the misalignment. It decays as it propagates downstream for at least four roll pitches, as shown in Figure 6.8.

The effect of roll misalignment on bulging is illustrated in Figure 6.9 and Table 6.5. The maximum bulge, the negative bulge and the maximum strain on the solidification front are almost linear functions of the misalignment till the effective maximum misalignment, which is 17.43 mm as shown in Figure 6.9. When the actual misalignment is larger than the effective maximum misalignment, it is the same as the case with one roll missing.

The misalignment of the support rolls has a significant effect on bulging and strain on the solidification front. The same thing should hold for negative misalignment and roll eccentricity where misalignment alternates from positive to negative. This study demonstrates the importance of caster maintenance.

6.4 Conclusions

In reality, the influence of the upstream rolls is very important. A sudden change in roll pitch may lead to bigger bulge and tensile strain on the solidification front than those encountered for the uniform roll pitch model. It is important to avoid big jumps between segments, which directly lead to extreme extra bulging and strain in the first downstream roll pitch relative to the subsequent similar roll pitches. A faulty geometry of the support system such as roll misalignment and eccentricity will also give rise to a bulging and strain problem at the exact location of the misaligned roll. Thus, it is recommended to tightly control parameters such as roll misalignment and eccentricity during operation of the caster. The disturbances due to the changes in the geometry of the caster and inappropriate boundary conditions are calculated to settle down after about three to four roll pitches.

Table 6.5. Effect of roll misalignment on bulging

Misalignment (mm)	Maximum bulge (mm)	Position from upstream roll	Negative bulge (mm)	Ratio of Neg bulge to Max bulge	Max strain on solidification front (%)
0 (Roll spacing 430mm)	0.11	51.6%	0	0	0.046
1	1.05	54.2%	-0.09	0.085	0.131
2	2.08	54.2%	-0.34	0.163	0.249
3	3.12	55.8%	-0.71	0.227	0.360
5	5.26	57.5%	-1.64	0.312	0.686
10	10.65	59.2%	-4.13	0.388	1.49
15	16.03	59.2%	-6.38	0.398	2.28
∞ (One roll missing)	18.57	59.2%	-7.30	0.393	2.62
Double roll spacing 860mm	10.61	64.2%	-2.90	0.273	2.32

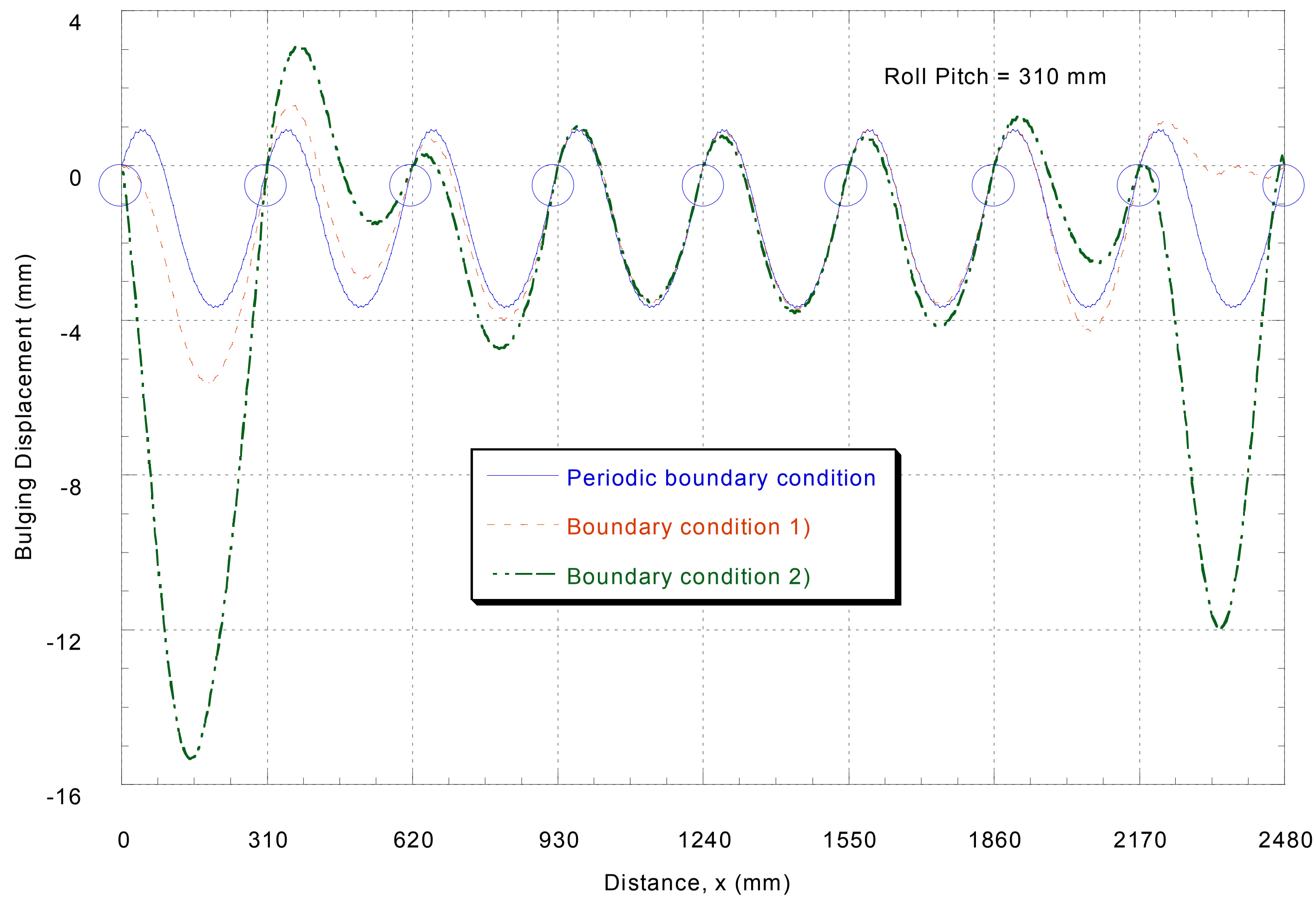

Figure 6.1. Bulging profiles for an 8-roll 310mm pitch model with different boundary conditions

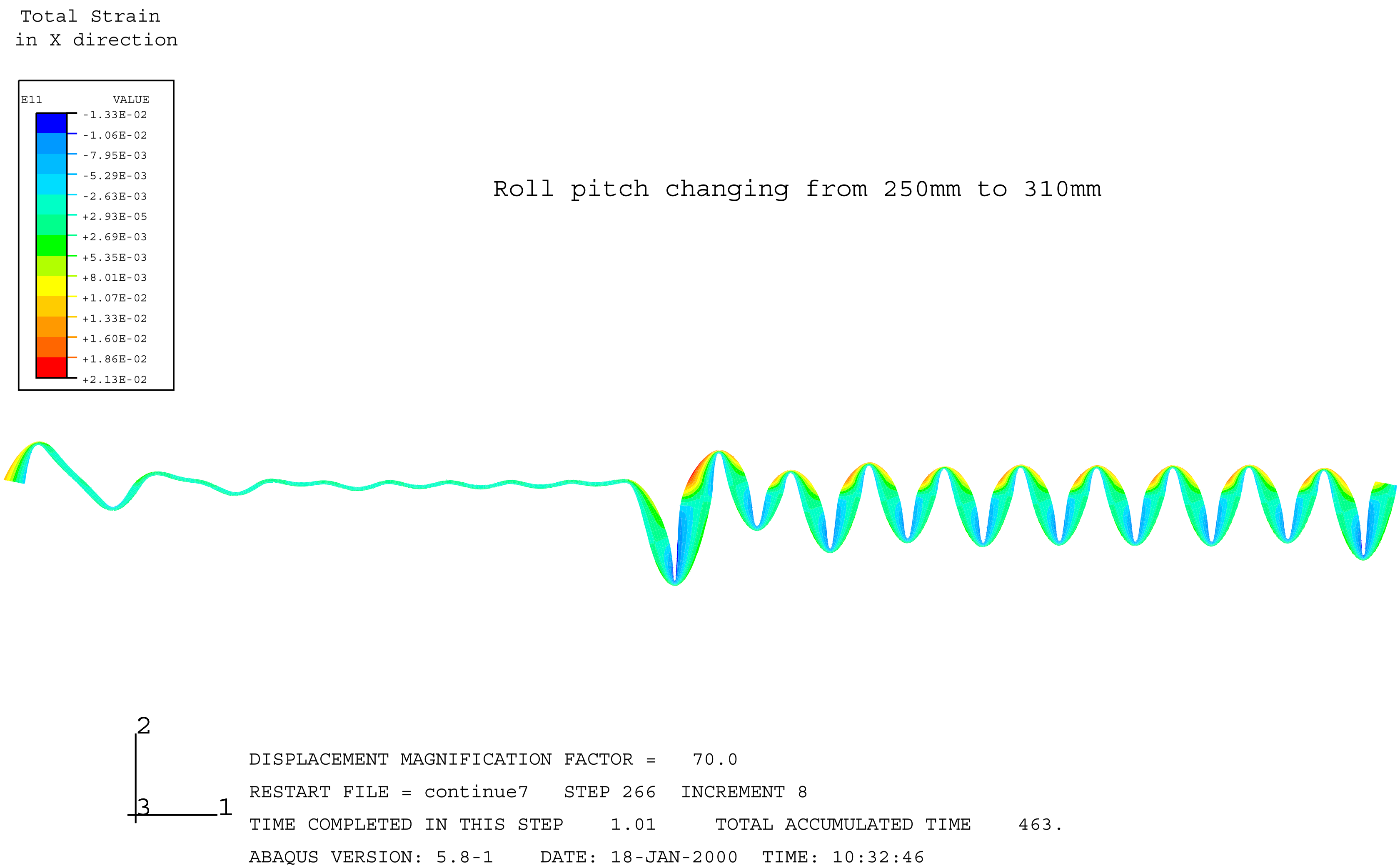

Figure 6.2. Strain contour plot for roll pitch changing from 250mm to 310mm

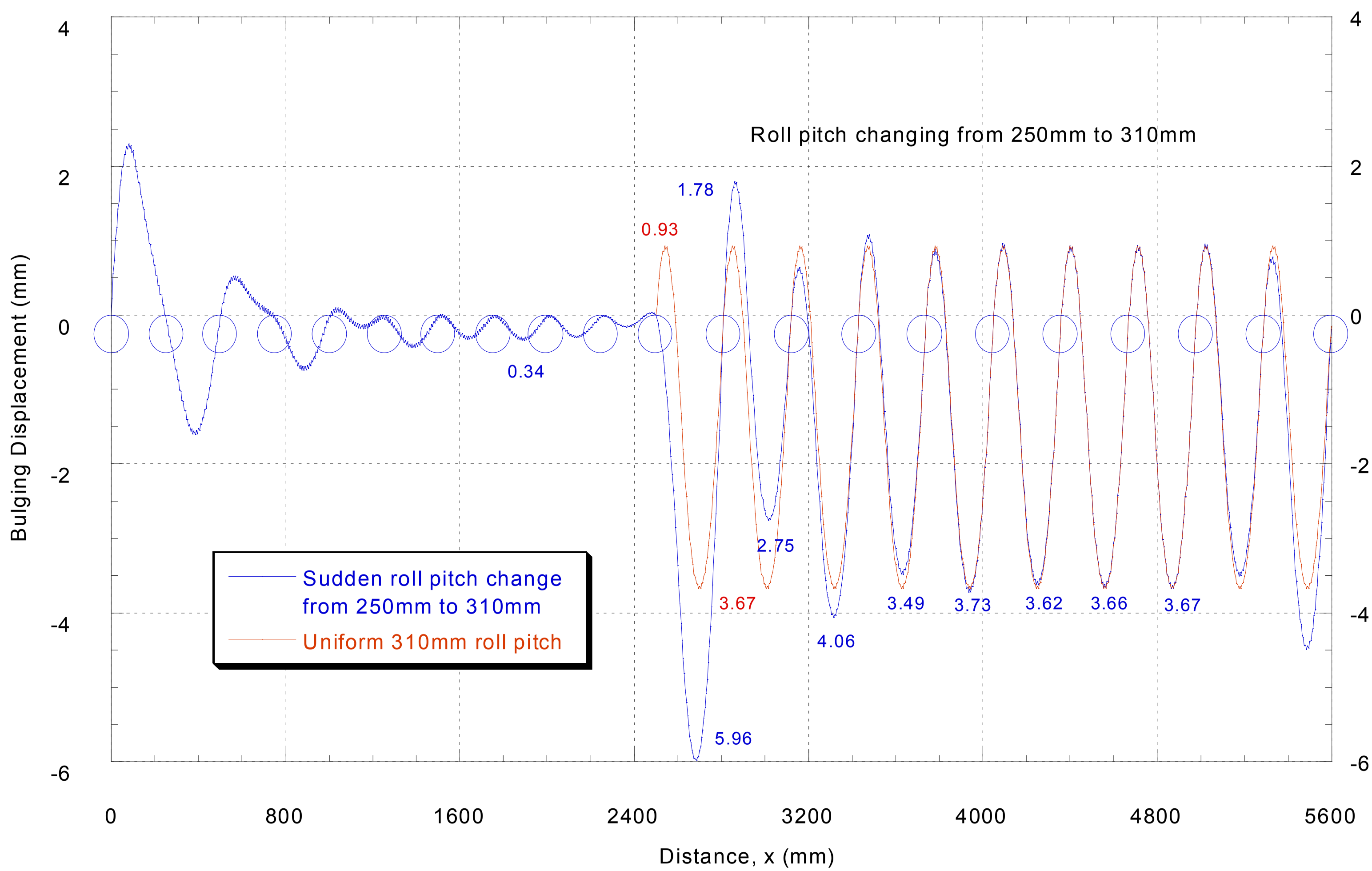

Figure 6.3. Bulging profile for roll pitch changing from 250mm to 310mm

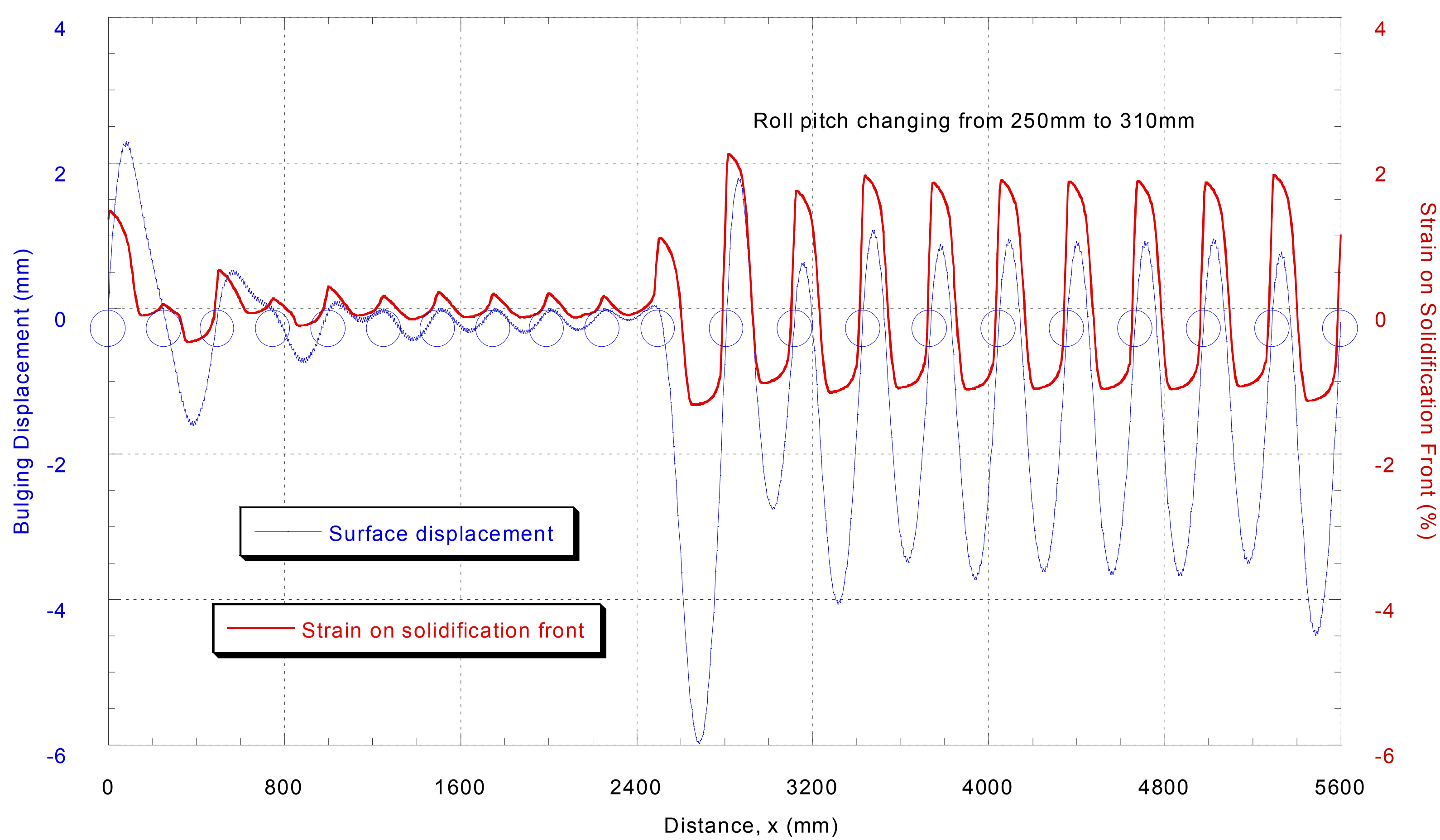

Figure 6.4. Strain on the solidification front for roll pitch changing from 250mm to 310mm

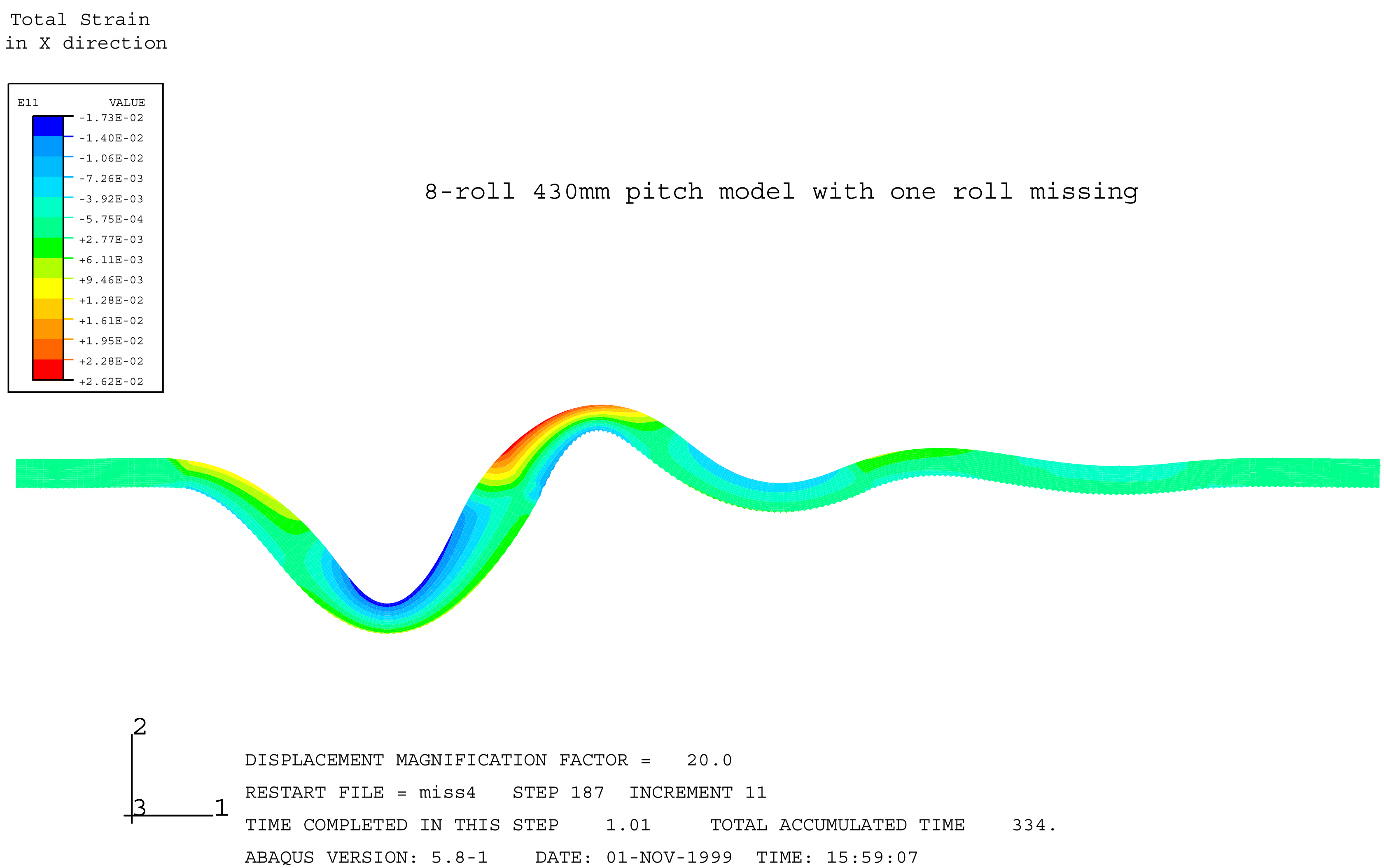

Figure 6.5. Strain contour plot for an 8-roll 430mm pitch model with one roll missing

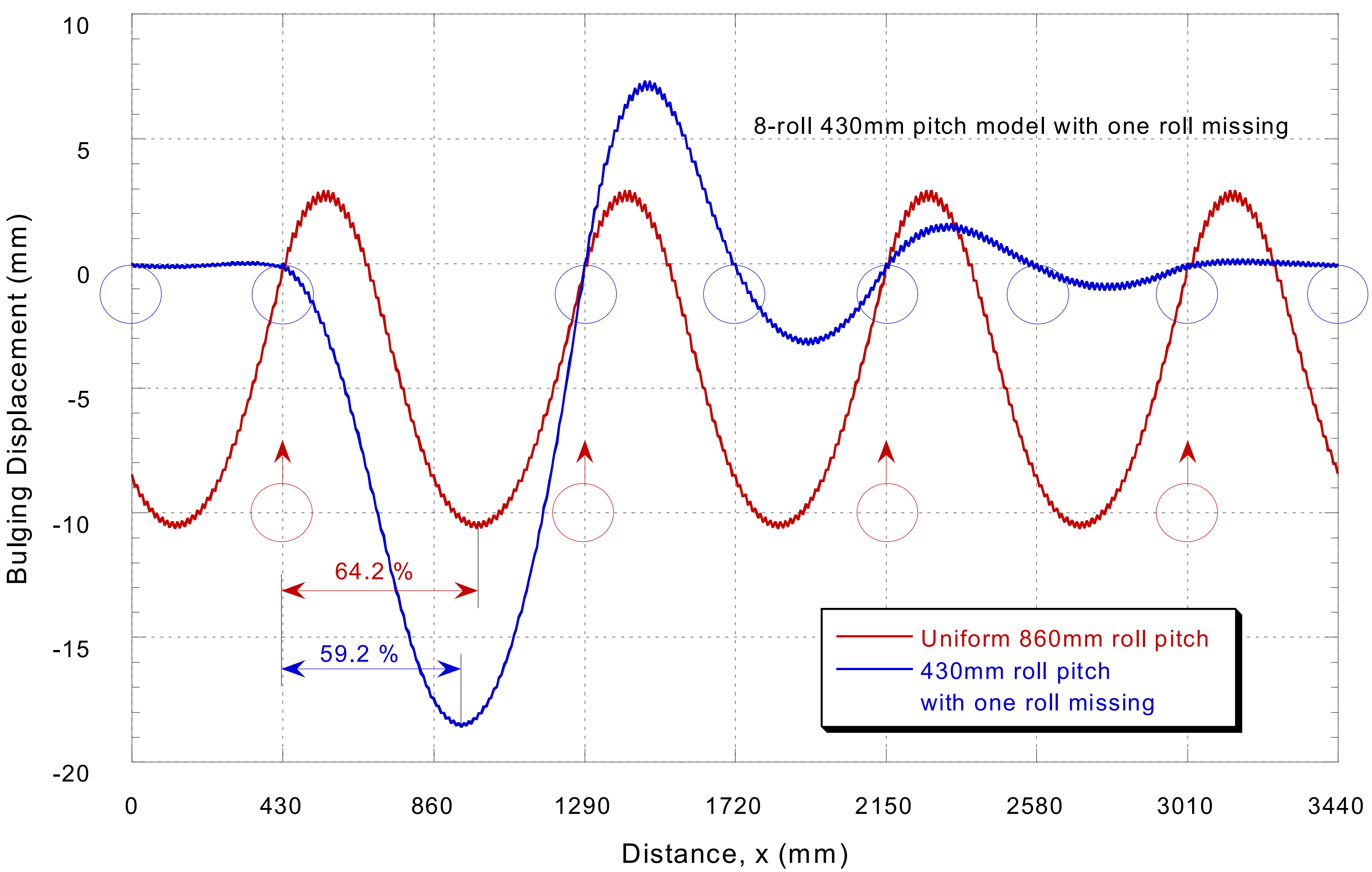

Figure 6.6. Bulging profile for an 8-roll 430mm pitch model with one roll missing

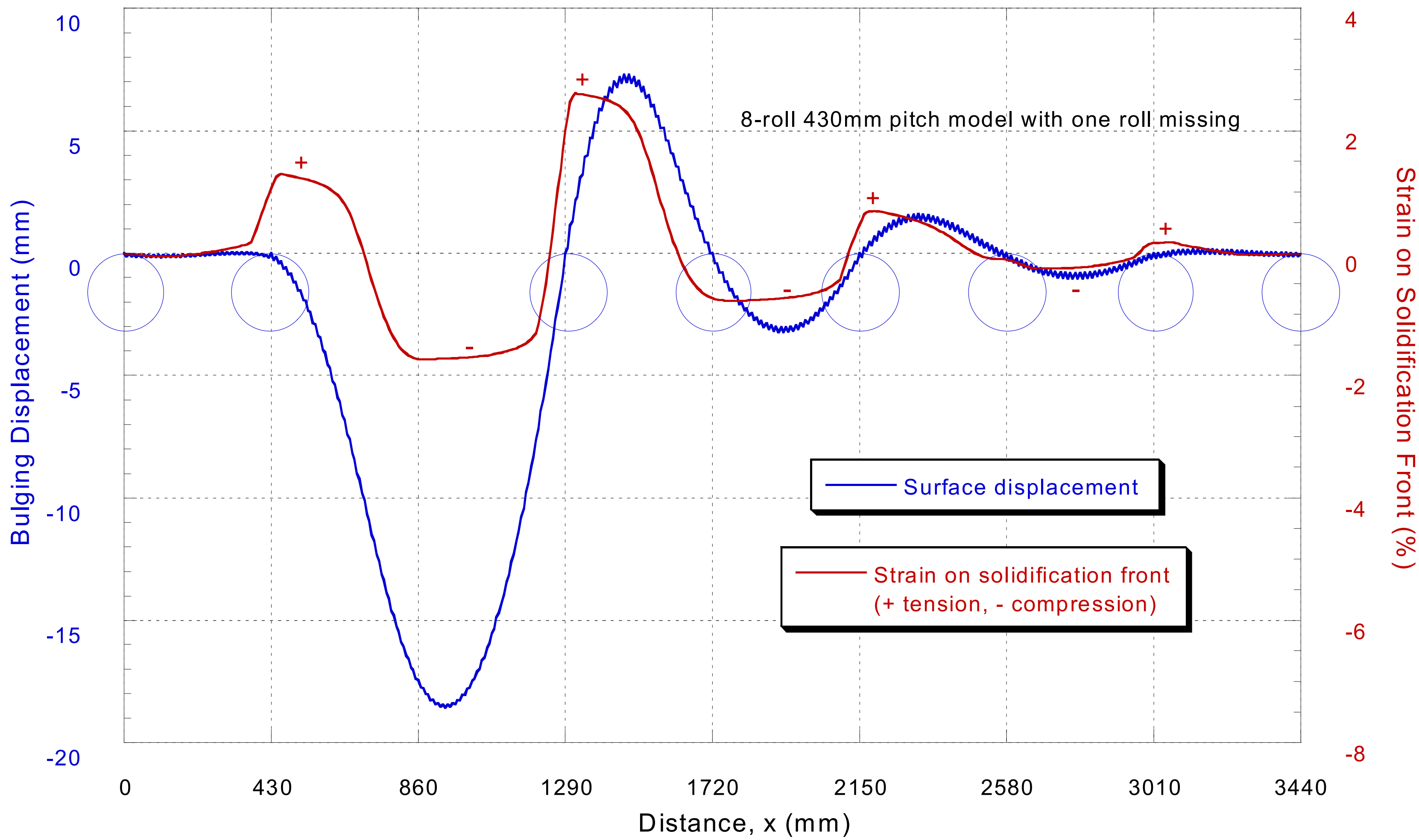

Figure 6.7. Strain on solidification front for an 8-roll 430mm pitch model with one roll missing

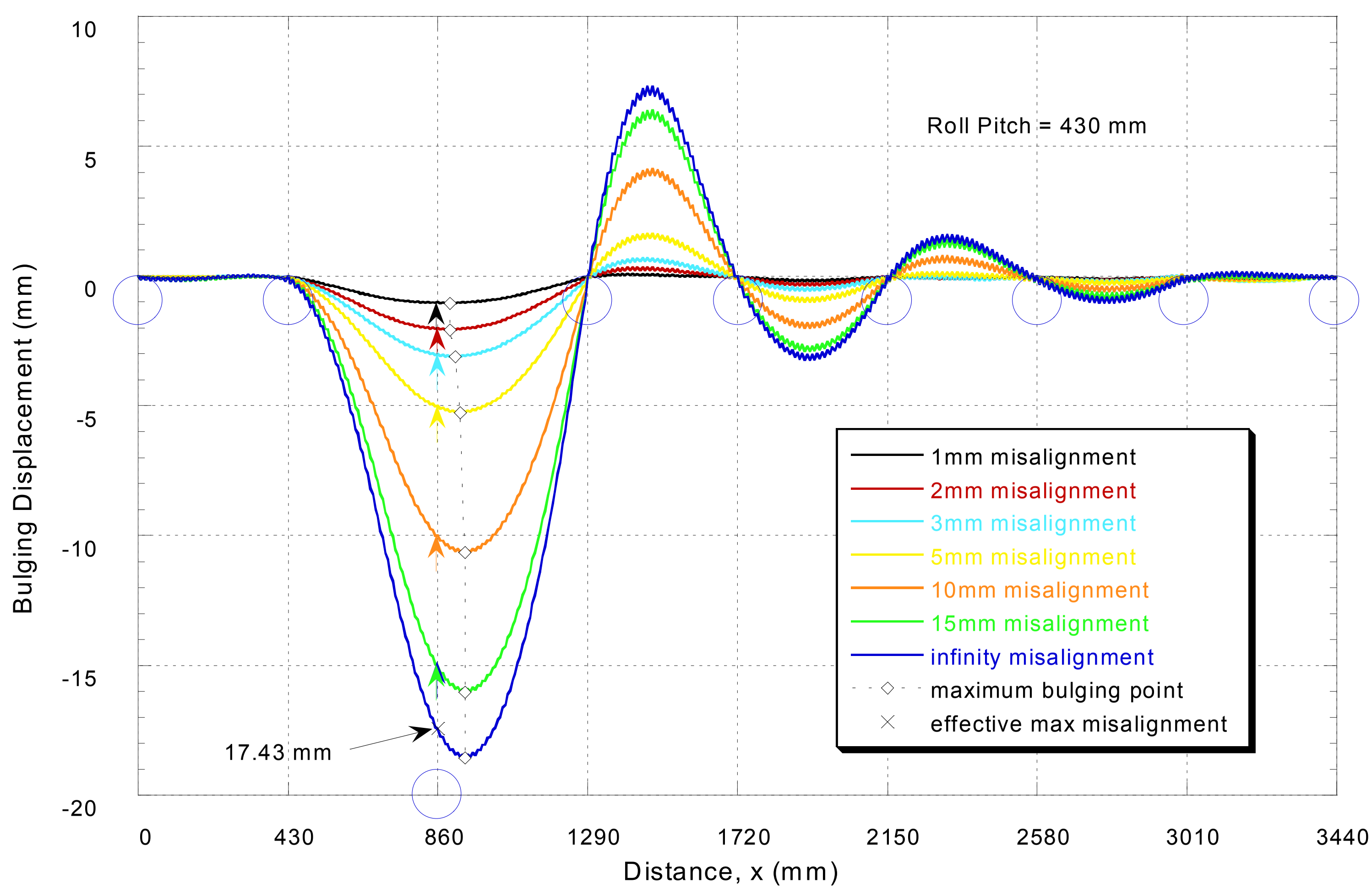

Figure 6.8. Bulging profiles for an 8-roll 430mm pitch model with different misalignments

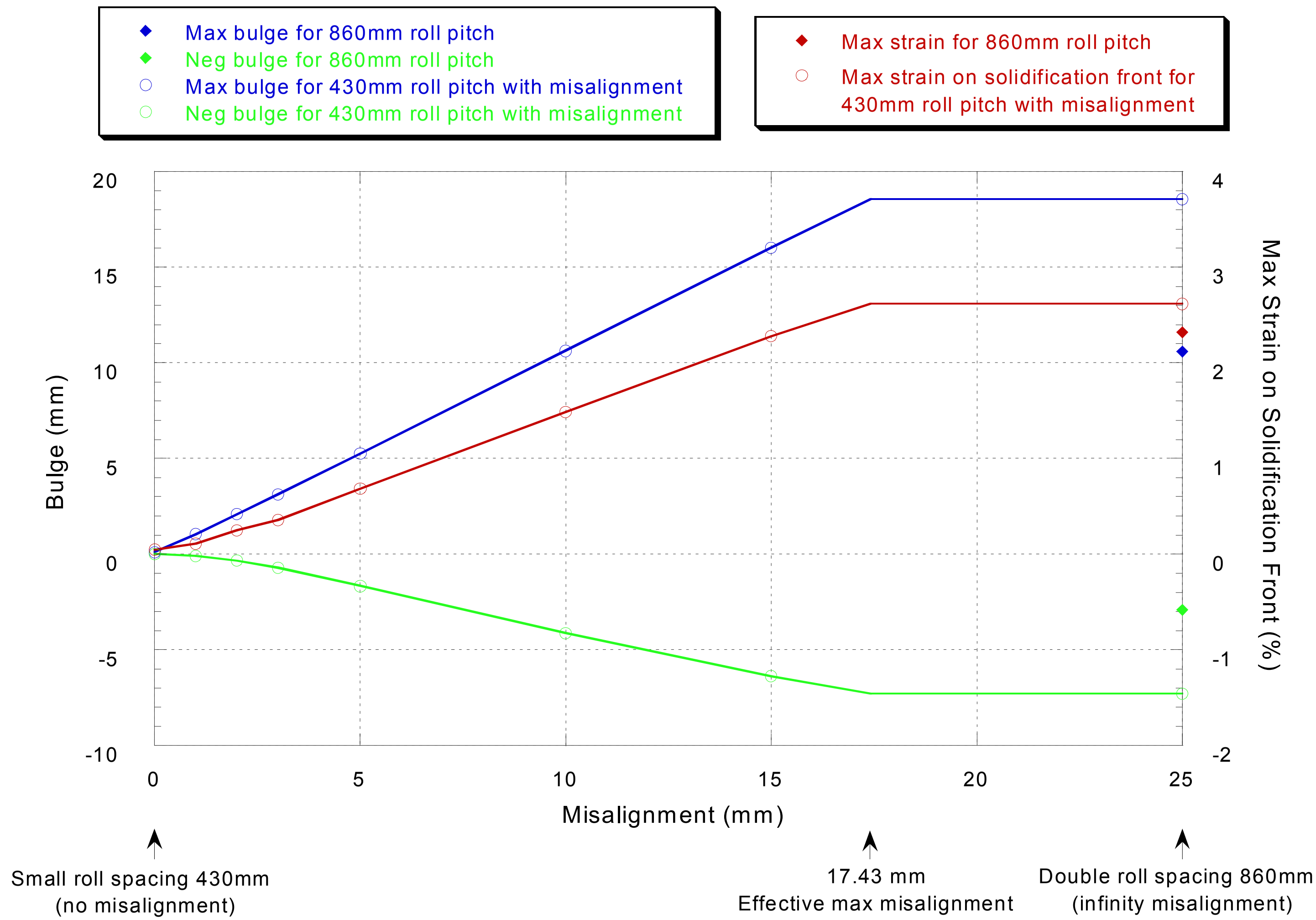

Figure 6.9. Effect of roll misalignment on bulging

7 Parametric Studies

Several casting parameters are believed to have big influences on bulging displacement. To quantify their effects on bulging, parametric studies on roll pitch and surface temperature were performed. The single roll pitch model was used with Wunnenberg conditions (see Table 2.1, except that the modeled shell thickness was 83mm instead of 79mm).

7.1 Roll Pitch Study

A parametric study with different roll pitches of 430mm, 860mm and 1290mm was performed to study the effect of roll pitch on bulging. The simulation results are compared with the Wunnenberg measurements in Table 7.1.

Table 7.1. Bulging displacement for the roll pitch study

Roll pitch	ABAQUS results	2-D shape factor	Multiplying the 2-D shape factor	Wunnenberg measurements
430 mm	0.2 mm	0.95	0.19 mm	0.4 - 1.6 mm
860 mm	6.2 mm	0.63	3.9 mm	5 - 7 mm
1290 mm	135 mm	0.34	46.3 mm	35 - 42 mm

It is clear that bulging is very sensitive to roll pitch. Increasing roll pitch leads to much larger bulging displacement. The ABAQUS model is much more sensitive to roll pitch than the measurements. It under-estimates the bulging displacement for the 430mm roll pitch and over-estimates the bulging for the 1290mm roll pitch. The slab width for the Wunnenberg measurements is 1350mm, which is close to the roll pitch of 1290mm. Due to the constraining effect of the narrow face, it may decrease bulging greatly, which would explain the disagreement for this roll pitch. After multiplying the 2-D shape factor of slab width to roll pitch ratio (Equation 2.2), the modified ABAQUS results match the measurements much better.

7.2 Surface Temperature Study

Surface temperatures of 900ºC, 1000ºC and 1100ºC were applied to the single roll pitch stress model. The results are shown in Figure 7.1 to compare with the Wunnenberg measurements.

The ABAQUS model matches the Wunnenberg measurements qualitatively: the hotter the surface temperature, the bigger the bulging displacement. The model bulging predictions also match quantitatively, but appear to be more sensitive to surface temperature than the measurements.

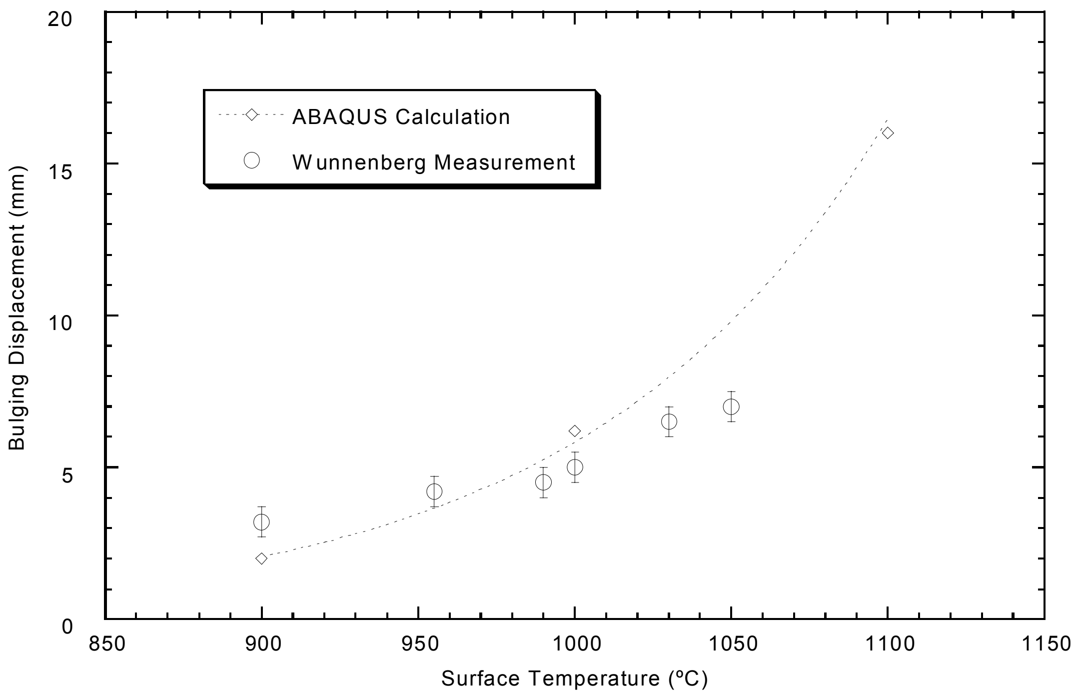

Figure 7.1. Effect of surface temperature on bulging

8 Evaluation of Empirical Bulging Prediction Equations

Three empirical bulging prediction equations were introduced in Section 2.2.3: Okamura equation (2.1), Palmares equation (2.4) and Lamant equation (2.6). These equations were applied to Wunnenberg conditions (see Table 2.1), Sumitomo conditions (see Table 2.2) and mold exit conditions (see Table 8.1).

Table 8.1. Casting conditions for the mold exit case

Slab width (W)	1143 mm
Roll pitch (L)	165 mm
Shell thickness (D)	28.3 mm
Surface Temperature (T_{surf})	1000 °C
Casting speed (V_c)	0.9144 m/min
Liquid steel density (ρ)	7000 kg/m ^{3}
Ferrostatic pressure (P)	0.1235 MPa

The calculated results using these empirical equations are compared with the simulation results of this ABAQUS model and the measurements (if available) in Table 8.2.

Table 8.2. Comparison of Different Models - Maximum Bulge (mm)

	Wunnenberg case (860mm)	Sumitomo case (310mm)	Mold exit case (165mm)
Okamura Equation	1.4985	0.4680	0.0012
Palmaers Equation	10.2025	3.5596 *	0.0332
Lamant Equation	9.0123	3.8384	0.0033
ABAQUS Model	10.61	3.67	0.02
Measurements	5~7	3.2	N/A

* Must use surface temperature 1100 °C instead of 1220 °C, so prediction is really higher.

The bulging predictions of the Okamura equation is always much too low. The Lamant equation is ok except for the mold exit case, where the prediction is too low compared to the ABAQUS model. The Palmaers equation appears to be the best. It matches the measurements and this ABAQUS model fairly well.

Recall that the exponent on roll spacing (L) for the Palmaers equation (2.4) is 5.12 and that on shell thickness (D) is -3.8. It reveals the fact that a larger roll pitch and a smaller shell thickness contribute more than other parameters to the maximum bulging amount. Greater pressure and higher surface temperature lead to a larger bulging displacement. The effect of casting speed is complicated. On one hand, increasing casting speed while maintaining constant strand shell thickness reduces creeping time, which in turn reduces bulging. On the other hand, the shell thickness decreases as casting speed increases. The combined effect will increase bulging.

9 Conclusions

Mathematical models of stress analysis and heat transfer have been developed to analyze phenomena related to the slab bulging in the continuous casting process using the commercial package ABAQUS. The thermal history of the slab has been predicted by a two-dimensional, transient, finite element, heat transfer model, which serves as input to the stress model. The stress model has been formulated for a two-dimensional longitudinal plane at the center of the wide face and is a transient, elastic-plastic, finite element analysis of the thermal stress field. Important features of the model include the incorporation of temperature history and temperature-dependent material properties, and the employment of a periodic boundary condition. A linear kinematic hardening model is used as the constitutive model based on tensile-test measurements from the literature.

The effect of surface temperature variation on bulging has been studied by incorporating the temperature history calculated by the heat transfer model into the stress model. A multiple roll pitch model has been used to predict the evolution of the bulging profile due to changes in the geometry of the support system, such as sudden roll pitch changes and roll misalignment. Parametric studies of roll pitch and surface temperature were performed on a single roll pitch model to study their effects on bulging. Three empirical bulging prediction equations have been evaluated.

The stress model has been validated by comparing the simulation results with the simple test problems and the measurements. Mechanical properties of steel at high temperature play an important role on bulging prediction. It is critical to apply appropriate material properties for accurate results.

Model predictions demonstrate that the surface temperature fluctuation caused by support rolls and water spray has a small penetration depth, so it has relatively little effect on bulging phenomena. The surface temperature variation appears to be worse for cracking problem than the case with uniform surface temperature. It produces a 6% bigger tensile stress at the cold surface, which is important for surface cracks, and a 16% larger tensile strain at the solidification front, which is responsible for internal hot tear cracks. It also increases the magnitude of bulging displacement by only 15%.

In real casters, changes in the geometry of the support system, such as sudden changes in the roll pitch between segments, roll misalignments or eccentricities, missing rolls or similar single large gaps between segments, all lead to large downstream disturbances of the bulging profile[11]. A sudden change in roll pitch may lead to a bigger bulge and tensile strain on the solidification front than those encountered for the uniform roll pitch model. It is important to avoid big jumps between segments, which directly lead to extreme extra bulging and strain in the first downstream roll pitch relative to the subsequent similar roll pitches. A faulty geometry of the support system such as roll misalignment and eccentricity will also give rise to a bulging and strain problem at the exact location of the misaligned roll. Thus, it is recommended to tightly control parameters such as roll misalignment and eccentricity during operation of the caster. The disturbances due to the changes in the geometry of the caster usually settle down after four to five roll pitches.

Parametric studies of roll pitch and surface temperature demonstrate that the bulging displacement is very sensitive to roll pitch and surface temperature. The ABAQUS stress model is more sensitive than the measurements. The bulging displacement increases greatly by increasing roll pitch and surface temperature.

Three empirical bulging prediction equations have been evaluated. The Palmaers equation (2.4) appears to be the best. It matches the measurements and this ABAQUS model fairly well.

10 Future Work

To achieve more accurate results, material properties may be improved for different steel grades. Constitutive models with time-dependent creep may be adopted to account for the effect of casting speed. Extensive parametric studies on different casting parameters are desired to obtain a bulging prediction equation and guidelines for strain at the solidification front and stress at the cold surface. A three-dimensional model should be developed to quantify the corner effect of slab width on bulging.

The bulging displacement and strain prediction model could be applied for crack formation and slab width prediction. It could also provide guidelines for caster design, such as the roll pitch design and the set up of the secondary cooling system.

Appendix A. ABAQUS Input File for Test Problem 1

```
<test1.inp>
*********************************************************************************
** ELASTO-STATIC CONTINUOUS CASTING BULGING MODEL (SINGLE 310mm ROLL PITCH)      **
** WITH 16*8 MESH (CPS8R)                                                        **
*********************************************************************************
*HEADING
ELASTO-STATIC CONTINUOUS CASTING BULGING MODEL
*RESTART,WRITE,FREQUENCY=10,OVERLAY
*PREPRINT, ECHO=NO, MODEL=NO, HISTORY=NO, CONTACT=NO
**
** DEFINE NODES
*NODE, NSET=CORNER
1001,0.,0.
1033,310.,0.
17001,0.,23.17
17033,310.,23.17
*NGEN,NSET=LEFT
1001,17001,1000
*NGEN,NSET=RIGHT
1033,17033,1000
*NFILL, NSET=ALL
LEFT, RIGHT, 32, 1
**DEFINE ELEMENTS
*ELEMENT, TYPE=CPS8R
1,1001,1003,3003,3001,1002,2003,3002,2001
*ELGEN,ELSET=BODY
1,16,2,1,7,2000,16
*ELEMENT, TYPE=CPS8R
113,15001,15003,17003,17001,15002,16003,17002,16001
*ELGEN, ELSET=BC2
113,16,2,1
*SOLID SECTION,MATERIAL=STEEL,ELSET=BODY
*SOLID SECTION,MATERIAL=STEEL,ELSET=BC2
*MATERIAL,NAME=STEEL
*DENSITY
7000.
*ELASTIC,TYPE=ISOTROPIC
10.E9,0.3
*SOLID SECTION, MATERIAL=STEEL, ELSET=BODY
.01
*SOLID SECTION, MATERIAL=STEEL, ELSET=BC2
.01
**
**SET BOUNDARY CONDITION
*BOUNDARY
LEFT,1,2
RIGHT,1,2
**
*INITIAL CONDITIONS,TYPE=STRESS
BODY,0.
BC2,0.
**********************
*STEP,INC=200
*STATIC
0.,1.01
*DLOAD
BC2,P3,.18E6
*END STEP
```

Appendix B. ABAQUS Input Files for Typical Stress Analysis

```
<utemp.inp>
*********************************************************************************
** ELASTO-STATIC CONTINUOUS CASTING BULGING MODEL (SINGLE 860mm ROLL PITCH)      **
** WITH 60*16 MESH PER ROLL PITCH (CPS8R)                                         **
** WITH USER SUBROUTINE *UTEMP                                                    **
*********************************************************************************
*HEADING
ELASTO-STATIC CONTINUOUS CASTING BULGING MODEL (SINGLE ROLL PITCH 860mm)
*RESTART,WRITE,FREQUENCY=10,OVERLAY
*PREPRINT, ECHO=NO, MODEL=NO, HISTORY=NO, CONTACT=NO
**
** DEFINE NODES
*NODE, NSET=CORNER
1001,0.,0.
1121,0.86,0.
33001,0.,0.079
33121,0.86,0.079
*NGEN,NSET=LEFT
1001,33001,1000
*NGEN,NSET=RIGHT
1121,33121,1000
*NFILL,NSET=ALL
LEFT, RIGHT, 120, 1
**DEFINE ELEMENTS
*ELEMENT, TYPE=CPS8R
1,1001,1003,3003,3001,1002,2003,3002,2001
*ELGEN,ELSET=BODY
1,60,2,1,15,2000,60
*ELEMENT, TYPE=CPS8R
901,31001,31003,33003,33001,31002,32003,33002,32001
*ELGEN, ELSET=BC2
901,60,2,1
*SOLID SECTION,MATERIAL=STEEL,ELSET=BODY
*SOLID SECTION,MATERIAL=STEEL,ELSET=BC2
*MATERIAL,NAME=STEEL
*DENSITY
7000.
*ELASTIC,TYPE=ISOTROPIC
12.00E9,0.3
**
**** TEMPERATURE USER SUBROUTINES UTEMP() ****
*USER SUBROUTINES
      SUBROUTINE UTEMP(TEMP,MSECPT,KSTEP,KINC,TIME,NODE,COORDS)
C
      INCLUDE 'ABA_PARAM.INC'
C
      DIMENSION TEMP(MSECPT), TIME(2), COORDS(3)
C
      X = COORDS(1)
      Y = COORDS(2)
      TEMP(1) = 1000 + Y/0.079*500
      RETURN
      END
********** END OF USER SUBROUTINES ***********
**SET BOUNDARY CONDITION
*BOUNDARY
LEFT,1,2
RIGHT,1,2
**
*INITIAL CONDITIONS,TYPE=STRESS
BODY,0.
BC2,0.
**********************
*STEP,INC=200
*STATIC
0.,1.01
*DLOAD
BC2,P3,2.6E5
*TEMPERATURE,USER
ALL
*NODE FILE
NT
*END STEP
```

```
<ep860.inp>
*********************************************************************************
** ELASTIC-PLASTIC CONTINUOUS CASTING BULGING MODEL (860mm)                    **
** WITH 60*16 MESH PER ROLL PITCH (CPS8R)                                      **
*********************************************************************************
*HEADING
ELASTIC-PLASTIC CONTINUOUS CASTING BULGING MODEL (4 ROLL PITCHES 860mm)
*RESTART,WRITE,FREQUENCY=10,OVERLAY
*PREPRINT, ECHO=NO, MODEL=NO, HISTORY=NO, CONTACT=NO
**
** DEFINE NODES
*NODE, NSET=CORNER
1001,0.,0.
1121,0.86,0.
33001,0.,0.079
33121,0.86,0.079
*NGEN,NSET=LEFT
1001,33001,1000
*NGEN,NSET=RIGHT
1121,33121,1000
*NFILL
LEFT, RIGHT, 120, 1
**DEFINE ELEMENTS
*ELEMENT, TYPE=CPS8R
1,1001,1003,3003,3001,1002,2003,3002,2001
*ELGEN,ELSET=BODY
1,60,2,1,15,2000,60
*ELEMENT, TYPE=CPS8R
901,31001,31003,33003,33001,31002,32003,33002,32001
*ELGEN, ELSET=BC2
901,60,2,1
*SOLID SECTION,MATERIAL=STEEL,ELSET=BODY
*SOLID SECTION,MATERIAL=STEEL,ELSET=BC2
*MATERIAL,NAME=STEEL
*DENSITY
7000.
*ELASTIC,TYPE=ISOTROPIC
** Mizukami's E(T)
32.09E9,0.3,900.
19.60E9,0.3,1000.
14.01E9,0.3,1100.
12.20E9,0.3,1200.
11.08E9,0.3,1300.
7.51E9,0.3,1400.
3.75E9,0.3,1500.
*EXPANSION,TYPE=ISO
0.1770E-4
****************Wray*****************
*PLASTIC, HARDENING=KINEMATIC
**PLASTIC,HARDENING=COMBINED, DATA TYPE=HALF CYCLE
**YIELD STRESS(MPA),PLASTIC STRAIN,TEMPERATURE
****************Wray*****************
**** 950 C, Wray data, 0.051% C, strain rate=2.4e-3
20.0E6, 0.0, 950
50.0E6,  0.05, 950
**** 1100 C, Wray data, 0.051% C, strain rate=2.9e-3
12.7E6, 0.0, 1100
27.7E6,  0.05, 1100
**** 1200 C, Wray data, 0.93% C, strain rate=2.3e-3
10.0E6, 0.0, 1200
17.5E6,  0.05, 1200
**** 1400 C
3.0E6, 0.0, 1400
13.0E6,  0.05, 1400
**** 1500 C
0.5E6, 0.0, 1500
1.0E6,  0.05, 1500
**
**SET BOUNDARY CONDITION -- COUPLED TWO ENDS
*MPC
TIE,LEFT,RIGHT
*INITIAL CONDITIONS,TYPE=STRESS
BODY,0.
BC2,0.
*INITIAL CONDITIONS,TYPE=TEMPERATURE,FILE=utemp, STEP=1, INC=1
***********************START OF APPLYING LOAD***************************
*STEP,INC=200
*STATIC
0.,1.01
*BOUNDARY
1002,1
```

```
1121,2
*DLOAD
BC2,P3,0.0103E5
*END STEP
*** STEP 5
*STEP,INC=200
*STATIC
0.,5.05
*BOUNDARY,OP=NEW
1002,1
1111,2
*DLOAD
BC2,P3,0.0206E5
*END STEP
*** STEP 10
*STEP,INC=200
*STATIC
0.,5.05
*BOUNDARY,OP=NEW
1002,1
1101,2
*DLOAD
BC2,P3,0.0309E5
*END STEP
*** STEP 15
*STEP,INC=200
*STATIC
0.,5.05
*BOUNDARY,OP=NEW
1002,1
1091,2
*DLOAD
BC2,P3,0.0412E5
*END STEP
*** STEP 20
*STEP,INC=200
*STATIC
0.,5.05
*BOUNDARY,OP=NEW
1002,1
1081,2
*DLOAD
BC2,P3,0.0515E5
*END STEP
*** STEP 25
*STEP,INC=200
*STATIC
0.,5.05
*BOUNDARY,OP=NEW
1002,1
1071,2
*DLOAD
BC2,P3,0.062E5
*END STEP
*** STEP 30
*STEP,INC=200
*STATIC
0.,5.05
*BOUNDARY,OP=NEW
1002,1
1061,2
*DLOAD
BC2,P3,0.072E5
*END STEP
*** STEP 35
*STEP,INC=200
*STATIC
0.,5.05
*BOUNDARY,OP=NEW
1002,1
1051,2
*DLOAD
BC2,P3,0.0825E5
*END STEP
*** STEP 40
*STEP,INC=200
*STATIC
0.,5.05
*BOUNDARY,OP=NEW
1002,1
1041,2
```

```
*DLOAD
BC2,P3,0.093E5
*END STEP
*** STEP 45
*STEP,INC=200
*STATIC
0.,5.05
*BOUNDARY,OP=NEW
1002,1
1031,2
*DLOAD
BC2,P3,0.103E5
*END STEP
*** STEP 50
*STEP,INC=200
*STATIC
0.,5.05
*BOUNDARY,OP=NEW
1002,1
1021,2
*DLOAD
BC2,P3,0.1135E5
*END STEP
*** STEP 55
*STEP,INC=200
*STATIC
0.,5.05
*BOUNDARY,OP=NEW
1002,1
1011,2
*DLOAD
BC2,P3,0.1235E5
*END STEP
*** STEP 60
*STEP,INC=200
*STATIC
0.,5.05
*BOUNDARY,OP=NEW
1002,1,2
1121,2
*DLOAD
BC2,P3,0.134E5
*END STEP
***************************END OF CYCLE #1*****************************
*** STEP 5
*STEP,INC=200
*STATIC
0.,5.05
*BOUNDARY,OP=NEW
1002,1
1111,2
*DLOAD
BC2,P3,0.206E5
*END STEP
*** STEP 10
*STEP,INC=200
*STATIC
0.,5.05
*BOUNDARY,OP=NEW
1002,1
1101,2
*DLOAD
BC2,P3,0.309E5
*END STEP
*** STEP 15
*STEP,INC=200
*STATIC
0.,5.05
*BOUNDARY,OP=NEW
1002,1
1091,2
*DLOAD
BC2,P3,0.412E5
*END STEP
*** STEP 20
*STEP,INC=200
*STATIC
0.,5.05
*BOUNDARY,OP=NEW
1002,1
1081,2
```

```
*DLOAD
BC2,P3,0.515E5
*END STEP
*** STEP 25
*STEP,INC=200
*STATIC
0.,5.05
*BOUNDARY,OP=NEW
1002,1
1071,2
*DLOAD
BC2,P3,0.62E5
*END STEP
*** STEP 30
*STEP,INC=200
*STATIC
0.,5.05
*BOUNDARY,OP=NEW
1002,1
1061,2
*DLOAD
BC2,P3,0.72E5
*END STEP
*** STEP 35
*STEP,INC=200
*STATIC
0.,5.05
*BOUNDARY,OP=NEW
1002,1
1051,2
*DLOAD
BC2,P3,0.825E5
*END STEP
*** STEP 40
*STEP,INC=200
*STATIC
0.,5.05
*BOUNDARY,OP=NEW
1002,1
1041,2
*DLOAD
BC2,P3,0.93E5
*END STEP
*** STEP 45
*STEP,INC=200
*STATIC
0.,5.05
*BOUNDARY,OP=NEW
1002,1
1031,2
*DLOAD
BC2,P3,1.03E5
*END STEP
*** STEP 50
*STEP,INC=200
*STATIC
0.,5.05
*BOUNDARY,OP=NEW
1002,1
1021,2
*DLOAD
BC2,P3,1.135E5
*END STEP
*** STEP 55
*STEP,INC=200
*STATIC
0.,5.05
*BOUNDARY,OP=NEW
1002,1
1011,2
*DLOAD
BC2,P3,1.235E5
*END STEP
*** STEP 60
*STEP,INC=200
*STATIC
0.,5.05
*BOUNDARY,OP=NEW
1002,1,2
1121,2
*DLOAD
```

```
BC2,P3,1.34E5
*END STEP
***************************END OF CYCLE #2*****************************
*** STEP 5
*STEP,INC=200
*STATIC
0.,5.05
*BOUNDARY,OP=NEW
1002,1
1111,2
*DLOAD
BC2,P3,1.450E5
*END STEP
*** STEP 10
*STEP,INC=200
*STATIC
0.,5.05
*BOUNDARY,OP=NEW
1002,1
1101,2
*DLOAD
BC2,P3,1.560E5
*END STEP
*** STEP 15
*STEP,INC=200
*STATIC
0.,5.05
*BOUNDARY,OP=NEW
1002,1
1091,2
*DLOAD
BC2,P3,1.675E5
*END STEP
*** STEP 20
*STEP,INC=200
*STATIC
0.,5.05
*BOUNDARY,OP=NEW
1002,1
1081,2
*DLOAD
BC2,P3,1.787E5
*END STEP
*** STEP 25
*STEP,INC=200
*STATIC
0.,5.05
*BOUNDARY,OP=NEW
1002,1
1071,2
*DLOAD
BC2,P3,1.898E5
*END STEP
*** STEP 30
*STEP,INC=200
*STATIC
0.,5.05
*BOUNDARY,OP=NEW
1002,1
1061,2
*DLOAD
BC2,P3,2.01E5
*END STEP
*** STEP 35
*STEP,INC=200
*STATIC
0.,5.05
*BOUNDARY,OP=NEW
1002,1
1051,2
*DLOAD
BC2,P3,2.120E5
*END STEP
*** STEP 40
*STEP,INC=200
*STATIC
0.,5.05
*BOUNDARY,OP=NEW
1002,1
1041,2
*DLOAD
```

```
BC2,P3,2.23E5
*END STEP
*** STEP 45
*STEP,INC=200
*STATIC
0.,5.05
*BOUNDARY,OP=NEW
1002,1
1031,2
*DLOAD
BC2,P3,2.345E5
*END STEP
*** STEP 50
*STEP,INC=200
*STATIC
0.,5.05
*BOUNDARY,OP=NEW
1002,1
1021,2
*DLOAD
BC2,P3,2.457E5
*END STEP
*** STEP 55
*STEP,INC=200
*STATIC
0.,5.05
*BOUNDARY,OP=NEW
1002,1
1011,2
*DLOAD
BC2,P3,2.568E5
*END STEP
*** STEP 60
*STEP,INC=200
*STATIC
0.,5.05
*BOUNDARY,OP=NEW
1002,1
1121,2
*DLOAD
BC2,P3,2.68E5
*END STEP
**********************END OF CYCLE #3 (END OF APPLYING LOAD)***********************
```

<c1.inp>

```
**********************************************************************************
** ELASTIC-PLASTIC CONTINUOUS CASTING BULGING MODEL (860mm)                      **
** WITH 60*16 MESH PER ROLL PITCH (CPS8R)                                        **
**********************************************************************************
*HEADING
RESTART RUN AFTER APPLYING LOAD
*RESTART,READ,WRITE,FREQUENCY=10,OVERLAY
*PREPRINT, ECHO=NO, MODEL=NO, HISTORY=NO, CONTACT=NO
*********************************START OF CYCLE***********************************
*** STEP 1
*STEP,INC=200
*STATIC
0.,1.01
*BOUNDARY,OP=NEW
1002,1
1119,2
*END STEP
*** STEP 2
*STEP,INC=200
*STATIC
0.,1.01
*BOUNDARY,OP=NEW
1002,1
1117,2
*END STEP
*** STEP 3
*STEP,INC=200
*STATIC
0.,1.01
*BOUNDARY,OP=NEW
1002,1
1115,2
*END STEP
*** STEP 4
```

```
*STEP,INC=200
*STATIC
0.,1.01
*BOUNDARY,OP=NEW
1002,1
1113,2
*END STEP
*** STEP 5
*STEP,INC=200
*STATIC
0.,1.01
*BOUNDARY,OP=NEW
1002,1
1111,2
*END STEP
*** STEP 6
*STEP,INC=200
*STATIC
0.,1.01
*BOUNDARY,OP=NEW
1002,1
1109,2
*END STEP
*** STEP 7
*STEP,INC=200
*STATIC
0.,1.01
*BOUNDARY,OP=NEW
1002,1
1107,2
*END STEP
*** STEP 8
*STEP,INC=200
*STATIC
0.,1.01
*BOUNDARY,OP=NEW
1002,1
1105,2
*END STEP
*** STEP 9
*STEP,INC=200
*STATIC
0.,1.01
*BOUNDARY,OP=NEW
1002,1
1103,2
*END STEP
*** STEP 10
*STEP,INC=200
*STATIC
0.,1.01
*BOUNDARY,OP=NEW
1002,1
1101,2
*END STEP
*** STEP 11
*STEP,INC=200
*STATIC
0.,1.01
*BOUNDARY,OP=NEW
1002,1
1099,2
*END STEP
*** STEP 12
*STEP,INC=200
*STATIC
0.,1.01
*BOUNDARY,OP=NEW
1002,1
1097,2
*END STEP
*** STEP 13
*STEP,INC=200
*STATIC
0.,1.01
*BOUNDARY,OP=NEW
1002,1
1095,2
*END STEP
*** STEP 14
*STEP,INC=200
```

```
*STATIC
0.,1.01
*BOUNDARY,OP=NEW
1002,1
1093,2
*END STEP
*** STEP 15
*STEP,INC=200
*STATIC
0.,1.01
*BOUNDARY,OP=NEW
1002,1
1091,2
*END STEP
*** STEP 16
*STEP,INC=200
*STATIC
0.,1.01
*BOUNDARY,OP=NEW
1002,1
1089,2
*END STEP
*** STEP 17
*STEP,INC=200
*STATIC
0.,1.01
*BOUNDARY,OP=NEW
1002,1
1087,2
*END STEP
*** STEP 18
*STEP,INC=200
*STATIC
0.,1.01
*BOUNDARY,OP=NEW
1002,1
1085,2
*END STEP
*** STEP 19
*STEP,INC=200
*STATIC
0.,1.01
*BOUNDARY,OP=NEW
1002,1
1083,2
*END STEP
*** STEP 20
*STEP,INC=200
*STATIC
0.,1.01
*BOUNDARY,OP=NEW
1002,1
1081,2
*END STEP
*** STEP 21
*STEP,INC=200
*STATIC
0.,1.01
*BOUNDARY,OP=NEW
1002,1
1079,2
*END STEP
*** STEP 22
*STEP,INC=200
*STATIC
0.,1.01
*BOUNDARY,OP=NEW
1002,1
1077,2
*END STEP
*** STEP 23
*STEP,INC=200
*STATIC
0.,1.01
*BOUNDARY,OP=NEW
1002,1
1075,2
*END STEP
*** STEP 24
*STEP,INC=200
*STATIC
```

```
0.,1.01
*BOUNDARY,OP=NEW
1002,1
1073,2
*END STEP
*** STEP 25
*STEP,INC=200
*STATIC
0.,1.01
*BOUNDARY,OP=NEW
1002,1
1071,2
*END STEP
*** STEP 26
*STEP,INC=200
*STATIC
0.,1.01
*BOUNDARY,OP=NEW
1002,1
1069,2
*END STEP
*** STEP 27
*STEP,INC=200
*STATIC
0.,1.01
*BOUNDARY,OP=NEW
1002,1
1067,2
*END STEP
*** STEP 28
*STEP,INC=200
*STATIC
0.,1.01
*BOUNDARY,OP=NEW
1002,1
1065,2
*END STEP
*** STEP 29
*STEP,INC=200
*STATIC
0.,1.01
*BOUNDARY,OP=NEW
1002,1
1063,2
*END STEP
*** STEP 30
*STEP,INC=200
*STATIC
0.,1.01
*BOUNDARY,OP=NEW
1002,1
1061,2
*END STEP
*** STEP 31
*STEP,INC=200
*STATIC
0.,1.01
*BOUNDARY,OP=NEW
1002,1
1059,2
*END STEP
*** STEP 32
*STEP,INC=200
*STATIC
0.,1.01
*BOUNDARY,OP=NEW
1002,1
1057,2
*END STEP
*** STEP 33
*STEP,INC=200
*STATIC
0.,1.01
*BOUNDARY,OP=NEW
1002,1
1055,2
*END STEP
*** STEP 34
*STEP,INC=200
*STATIC
0.,1.01
```

```
*BOUNDARY,OP=NEW
1002,1
1053,2
*END STEP
*** STEP 35
*STEP,INC=200
*STATIC
0.,1.01
*BOUNDARY,OP=NEW
1002,1
1051,2
*END STEP
*** STEP 36
*STEP,INC=200
*STATIC
0.,1.01
*BOUNDARY,OP=NEW
1002,1
1049,2
*END STEP
*** STEP 37
*STEP,INC=200
*STATIC
0.,1.01
*BOUNDARY,OP=NEW
1002,1
1047,2
*END STEP
*** STEP 38
*STEP,INC=200
*STATIC
0.,1.01
*BOUNDARY,OP=NEW
1002,1
1045,2
*END STEP
*** STEP 39
*STEP,INC=200
*STATIC
0.,1.01
*BOUNDARY,OP=NEW
1002,1
1043,2
*END STEP
*** STEP 40
*STEP,INC=200
*STATIC
0.,1.01
*BOUNDARY,OP=NEW
1002,1
1041,2
*END STEP
*** STEP 41
*STEP,INC=200
*STATIC
0.,1.01
*BOUNDARY,OP=NEW
1002,1
1039,2
*END STEP
*** STEP 42
*STEP,INC=200
*STATIC
0.,1.01
*BOUNDARY,OP=NEW
1002,1
1037,2
*END STEP
*** STEP 43
*STEP,INC=200
*STATIC
0.,1.01
*BOUNDARY,OP=NEW
1002,1
1035,2
*END STEP
*** STEP 44
*STEP,INC=200
*STATIC
0.,1.01
*BOUNDARY,OP=NEW
```

```
1002,1
1033,2
*END STEP
*** STEP 45
*STEP,INC=200
*STATIC
0.,1.01
*BOUNDARY,OP=NEW
1002,1
1031,2
*END STEP
*** STEP 46
*STEP,INC=200
*STATIC
0.,1.01
*BOUNDARY,OP=NEW
1002,1
1029,2
*END STEP
*** STEP 47
*STEP,INC=200
*STATIC
0.,1.01
*BOUNDARY,OP=NEW
1002,1
1027,2
*END STEP
*** STEP 48
*STEP,INC=200
*STATIC
0.,1.01
*BOUNDARY,OP=NEW
1002,1
1025,2
*END STEP
*** STEP 49
*STEP,INC=200
*STATIC
0.,1.01
*BOUNDARY,OP=NEW
1002,1
1023,2
*END STEP
*** STEP 50
*STEP,INC=200
*STATIC
0.,1.01
*BOUNDARY,OP=NEW
1002,1
1021,2
*END STEP
*** STEP 51
*STEP,INC=200
*STATIC
0.,1.01
*BOUNDARY,OP=NEW
1002,1
1019,2
*END STEP
*** STEP 52
*STEP,INC=200
*STATIC
0.,1.01
*BOUNDARY,OP=NEW
1002,1
1017,2
*END STEP
*** STEP 53
*STEP,INC=200
*STATIC
0.,1.01
*BOUNDARY,OP=NEW
1002,1
1015,2
*END STEP
*** STEP 54
*STEP,INC=200
*STATIC
0.,1.01
*BOUNDARY,OP=NEW
1002,1
```

```
1013,2
*END STEP
*** STEP 55
*STEP,INC=200
*STATIC
0.,1.01
*BOUNDARY,OP=NEW
1002,1
1011,2
*END STEP
*** STEP 56
*STEP,INC=200
*STATIC
0.,1.01
*BOUNDARY,OP=NEW
1002,1
1009,2
*END STEP
*** STEP 57
*STEP,INC=200
*STATIC
0.,1.01
*BOUNDARY,OP=NEW
1002,1
1007,2
*END STEP
*** STEP 58
*STEP,INC=200
*STATIC
0.,1.01
*BOUNDARY,OP=NEW
1002,1
1005,2
*END STEP
*** STEP 59
*STEP,INC=200
*STATIC
0.,1.01
*BOUNDARY,OP=NEW
1002,1
1003,2
*END STEP
*** STEP 60
*STEP,INC=200
*STATIC
0.,1.01
*BOUNDARY,OP=NEW
1002,1
1121,2
*END STEP
*****************************END OF CYCLE*******************************
```

<c2.inp> is same as <c1.inp>.

Appendix C. ABAQUS Input Files for Heat Transfer Analysis

```
<heat0.inp>
***************************************************************************
** THERMAL MODEL (SINGLE 860mm ROLL PITCH)                               **
** WITH 60*16 MESH PER ROLL PITCH (DC2D8)                                **
** WITH USER SUBROUTINE *FILM                                            **
***************************************************************************
*HEADING
TEMPERATURE DISTRIBUTION IN THERMAL MODEL (SINGLE ROLL PITCH 860mm)
*RESTART,WRITE,FREQUENCY=10,OVERLAY
*PREPRINT, ECHO=NO, MODEL=NO, HISTORY=NO, CONTACT=NO
**
** DEFINE NODES
*NODE, NSET=CORNER
1001,0.,0.
1121,0.86,0.
33001,0.,0.079
33121,0.86,0.079
*NGEN,NSET=LEFT
1001,33001,1000
*NGEN,NSET=RIGHT
1121,33121,1000
*NFILL,NSET=ALL
LEFT, RIGHT, 120, 1
**DEFINE ELEMENTS
*ELEMENT, TYPE=DC2D8
1,1001,1003,3003,3001,1002,2003,3002,2001
*ELGEN,ELSET=BODY
1,60,2,1,15,2000,60
*ELEMENT, TYPE=DC2D8
901,31001,31003,33003,33001,31002,32003,33002,32001
*ELGEN, ELSET=BC2
901,60,2,1
*NSET, NSET=TLINE, GENERATE
33001,33121,1
*ELSET, ELSET=BR, GENERATE
1,60,1
*SOLID SECTION,MATERIAL=STEEL,ELSET=BODY
*SOLID SECTION,MATERIAL=STEEL,ELSET=BC2
*MATERIAL,NAME=STEEL
*DENSITY
7000.
*SPECIFIC HEAT
460.0
*CONDUCTIVITY
28.5, 1000
34.0, 1500
*USER SUBROUTINES
      SUBROUTINE FILM(H,SINK,TEMP,KSTEP,KINC,TIME,NOEL, NPT,
     1 COORDS,JLTYP,FIELD,NFIELD)
C
      INCLUDE 'ABA_PARAM.INC'
C
      DIMENSION H(2),TIME(2),COORDS(3),FIELD(NFIELD)
C
      VC=0.85/60
      DT=TIME(1)
      DX=VC*DT
C
      X=COORDS(1)+DX
      IF (X.GT.0.86) THEN
        X=X-0.86
      END IF
C
      TMPLFT=0.86*3/60
      TMPRGT=0.86*57/60
      IF (X.LT.TMPLFT) THEN
       H(1)=632
      ELSEIF (X.GT.TMPRGT) THEN
       H(1)=632
      ELSEIF ((X.GE.TMPLFT).AND.(X.LE.0.301)) THEN
       H(1)=92
      ELSEIF ((X.GE.0.559).AND.(X.LE.TMPRGT)) THEN
       H(1)=92
      ELSE
       H(1)=332
```

```
      END IF
C
      SINK=130
C
      RETURN
      END
********** END OF USER SUBROUTINES ***********
**SET BOUNDARY CONDITION
*MPC
TIE,LEFT,RIGHT
**
*INITIAL CONDITIONS,TYPE=TEMPERATURE,FILE=utemp, STEP=1, INC=1
**********************
*STEP,INC=200
*HEAT TRANSFER, END=PERIOD, DELTMX=50
0.10, 60.6, 1E-5, 1, 1
*BOUNDARY
TLINE,11,11,1500
*FILM
BR,F1NU
*END STEP


<heat.inp>
***************************************************************************
** THERMAL MODEL (SINGLE 860mm ROLL PITCH)                               **
** WITH 60*16 MESH PER ROLL PITCH (DC2D8)                                **
** WITH USER SUBROUTINE *FILM                                            **
***************************************************************************
*HEADING
TEMPERATURE DISTRIBUTION IN THERMAL MODEL (SINGLE ROLL PITCH 860mm)
*RESTART,READ,WRITE,FREQUENCY=10,OVERLAY
*PREPRINT, ECHO=NO, MODEL=NO, HISTORY=NO, CONTACT=NO
*USER SUBROUTINES
      SUBROUTINE FILM(H,SINK,TEMP,KSTEP,KINC,TIME,NOEL, NPT,
     1 COORDS,JLTYP,FIELD,NFIELD)
C
      INCLUDE 'ABA_PARAM.INC'
C
      DIMENSION H(2),TIME(2),COORDS(3),FIELD(NFIELD)
C
      VC=0.85/60
      DT=TIME(2)-60.6
      DX=VC*DT
C
      X=COORDS(1)+DX
      IF (X.GT.0.86) THEN
       X=X-0.86
      END IF
C
      TMPLFT=0.86*3/60
      TMPRGT=0.86*57/60
      IF (X.LT.TMPLFT) THEN
       H(1)=632
      ELSEIF (X.GT.TMPRGT) THEN
       H(1)=632
      ELSEIF ((X.GE.TMPLFT).AND.(X.LE.0.301)) THEN
       H(1)=92
      ELSEIF ((X.GE.0.559).AND.(X.LE.TMPRGT)) THEN
       H(1)=92
      ELSE
       H(1)=332
      END IF
C
      SINK=130
C
      RETURN
      END
********** END OF USER SUBROUTINES ***********
******  STEP #2  ******
*STEP,INC=200
*HEAT TRANSFER, END=PERIOD, DELTMX=50
0.40, 1.01, 1E-5, 1, 1
*BOUNDARY
TLINE,11,11,1500
*FILM
BR,F1NU
*NODE FILE
NT
*END STEP
******  STEP #3  ******
```

```
*STEP,INC=200
*HEAT TRANSFER, END=PERIOD, DELTMX=50
0.40, 1.01, 1E-5, 1, 1
*BOUNDARY
TLINE,11,11,1500
*FILM
BR,F1NU
*NODE FILE
NT
*END STEP
******  STEP #4  ******
*STEP,INC=200
*HEAT TRANSFER, END=PERIOD, DELTMX=50
0.40, 1.01, 1E-5, 1, 1
*BOUNDARY
TLINE,11,11,1500
*FILM
BR,F1NU
*NODE FILE
NT
*END STEP
******  STEP #5  ******
*STEP,INC=200
*HEAT TRANSFER, END=PERIOD, DELTMX=50
0.40, 1.01, 1E-5, 1, 1
*BOUNDARY
TLINE,11,11,1500
*FILM
BR,F1NU
*NODE FILE
NT
*END STEP
******  STEP #6  ******
*STEP,INC=200
*HEAT TRANSFER, END=PERIOD, DELTMX=50
0.40, 1.01, 1E-5, 1, 1
*BOUNDARY
TLINE,11,11,1500
*FILM
BR,F1NU
*NODE FILE
NT
*END STEP
******  STEP #7  ******
*STEP,INC=200
*HEAT TRANSFER, END=PERIOD, DELTMX=50
0.40, 1.01, 1E-5, 1, 1
*BOUNDARY
TLINE,11,11,1500
*FILM
BR,F1NU
*NODE FILE
NT
*END STEP
******  STEP #8  ******
*STEP,INC=200
*HEAT TRANSFER, END=PERIOD, DELTMX=50
0.40, 1.01, 1E-5, 1, 1
*BOUNDARY
TLINE,11,11,1500
*FILM
BR,F1NU
*NODE FILE
NT
*END STEP
******  STEP #9  ******
*STEP,INC=200
*HEAT TRANSFER, END=PERIOD, DELTMX=50
0.40, 1.01, 1E-5, 1, 1
*BOUNDARY
TLINE,11,11,1500
*FILM
BR,F1NU
*NODE FILE
NT
*END STEP
******  STEP #10 ******
*STEP,INC=200
*HEAT TRANSFER, END=PERIOD, DELTMX=50
0.40, 1.01, 1E-5, 1, 1
*BOUNDARY
```

```
TLINE,11,11,1500
*FILM
BR,F1NU
*NODE FILE
NT
*END STEP
******  STEP #11 ******
*STEP,INC=200
*HEAT TRANSFER, END=PERIOD, DELTMX=50
0.40, 1.01, 1E-5, 1, 1
*BOUNDARY
TLINE,11,11,1500
*FILM
BR,F1NU
*NODE FILE
NT
*END STEP
******  STEP #12 ******
*STEP,INC=200
*HEAT TRANSFER, END=PERIOD, DELTMX=50
0.40, 1.01, 1E-5, 1, 1
*BOUNDARY
TLINE,11,11,1500
*FILM
BR,F1NU
*NODE FILE
NT
*END STEP
******  STEP #13 ******
*STEP,INC=200
*HEAT TRANSFER, END=PERIOD, DELTMX=50
0.40, 1.01, 1E-5, 1, 1
*BOUNDARY
TLINE,11,11,1500
*FILM
BR,F1NU
*NODE FILE
NT
*END STEP
******  STEP #14 ******
*STEP,INC=200
*HEAT TRANSFER, END=PERIOD, DELTMX=50
0.40, 1.01, 1E-5, 1, 1
*BOUNDARY
TLINE,11,11,1500
*FILM
BR,F1NU
*NODE FILE
NT
*END STEP
******  STEP #15 ******
*STEP,INC=200
*HEAT TRANSFER, END=PERIOD, DELTMX=50
0.40, 1.01, 1E-5, 1, 1
*BOUNDARY
TLINE,11,11,1500
*FILM
BR,F1NU
*NODE FILE
NT
*END STEP
******  STEP #16 ******
*STEP,INC=200
*HEAT TRANSFER, END=PERIOD, DELTMX=50
0.40, 1.01, 1E-5, 1, 1
*BOUNDARY
TLINE,11,11,1500
*FILM
BR,F1NU
*NODE FILE
NT
*END STEP
******  STEP #17 ******
*STEP,INC=200
*HEAT TRANSFER, END=PERIOD, DELTMX=50
0.40, 1.01, 1E-5, 1, 1
*BOUNDARY
TLINE,11,11,1500
*FILM
BR,F1NU
*NODE FILE
```

```
NT
*END STEP
****** STEP #18 ******
*STEP,INC=200
*HEAT TRANSFER, END=PERIOD, DELTMX=50
0.40, 1.01, 1E-5, 1, 1
*BOUNDARY
TLINE,11,11,1500
*FILM
BR,F1NU
*NODE FILE
NT
*END STEP
****** STEP #19 ******
*STEP,INC=200
*HEAT TRANSFER, END=PERIOD, DELTMX=50
0.40, 1.01, 1E-5, 1, 1
*BOUNDARY
TLINE,11,11,1500
*FILM
BR,F1NU
*NODE FILE
NT
*END STEP
****** STEP #20 ******
*STEP,INC=200
*HEAT TRANSFER, END=PERIOD, DELTMX=50
0.40, 1.01, 1E-5, 1, 1
*BOUNDARY
TLINE,11,11,1500
*FILM
BR,F1NU
*NODE FILE
NT
*END STEP
****** STEP #21 ******
*STEP,INC=200
*HEAT TRANSFER, END=PERIOD, DELTMX=50
0.40, 1.01, 1E-5, 1, 1
*BOUNDARY
TLINE,11,11,1500
*FILM
BR,F1NU
*NODE FILE
NT
*END STEP
****** STEP #22 ******
*STEP,INC=200
*HEAT TRANSFER, END=PERIOD, DELTMX=50
0.40, 1.01, 1E-5, 1, 1
*BOUNDARY
TLINE,11,11,1500
*FILM
BR,F1NU
*NODE FILE
NT
*END STEP
****** STEP #23 ******
*STEP,INC=200
*HEAT TRANSFER, END=PERIOD, DELTMX=50
0.40, 1.01, 1E-5, 1, 1
*BOUNDARY
TLINE,11,11,1500
*FILM
BR,F1NU
*NODE FILE
NT
*END STEP
****** STEP #24 ******
*STEP,INC=200
*HEAT TRANSFER, END=PERIOD, DELTMX=50
0.40, 1.01, 1E-5, 1, 1
*BOUNDARY
TLINE,11,11,1500
*FILM
BR,F1NU
*NODE FILE
NT
*END STEP
****** STEP #25 ******
*STEP,INC=200
```

```
*HEAT TRANSFER, END=PERIOD, DELTMX=50
0.40, 1.01, 1E-5, 1, 1
*BOUNDARY
TLINE,11,11,1500
*FILM
BR,F1NU
*NODE FILE
NT
*END STEP
******  STEP #26 ******
*STEP,INC=200
*HEAT TRANSFER, END=PERIOD, DELTMX=50
0.40, 1.01, 1E-5, 1, 1
*BOUNDARY
TLINE,11,11,1500
*FILM
BR,F1NU
*NODE FILE
NT
*END STEP
******  STEP #27 ******
*STEP,INC=200
*HEAT TRANSFER, END=PERIOD, DELTMX=50
0.40, 1.01, 1E-5, 1, 1
*BOUNDARY
TLINE,11,11,1500
*FILM
BR,F1NU
*NODE FILE
NT
*END STEP
******  STEP #28 ******
*STEP,INC=200
*HEAT TRANSFER, END=PERIOD, DELTMX=50
0.40, 1.01, 1E-5, 1, 1
*BOUNDARY
TLINE,11,11,1500
*FILM
BR,F1NU
*NODE FILE
NT
*END STEP
******  STEP #29 ******
*STEP,INC=200
*HEAT TRANSFER, END=PERIOD, DELTMX=50
0.40, 1.01, 1E-5, 1, 1
*BOUNDARY
TLINE,11,11,1500
*FILM
BR,F1NU
*NODE FILE
NT
*END STEP
******  STEP #30 ******
*STEP,INC=200
*HEAT TRANSFER, END=PERIOD, DELTMX=50
0.40, 1.01, 1E-5, 1, 1
*BOUNDARY
TLINE,11,11,1500
*FILM
BR,F1NU
*NODE FILE
NT
*END STEP
******  STEP #31 ******
*STEP,INC=200
*HEAT TRANSFER, END=PERIOD, DELTMX=50
0.40, 1.01, 1E-5, 1, 1
*BOUNDARY
TLINE,11,11,1500
*FILM
BR,F1NU
*NODE FILE
NT
*END STEP
******  STEP #32 ******
*STEP,INC=200
*HEAT TRANSFER, END=PERIOD, DELTMX=50
0.40, 1.01, 1E-5, 1, 1
*BOUNDARY
TLINE,11,11,1500
```

```
*FILM
BR,F1NU
*NODE FILE
NT
*END STEP
******  STEP #33 ******
*STEP,INC=200
*HEAT TRANSFER, END=PERIOD, DELTMX=50
0.40, 1.01, 1E-5, 1, 1
*BOUNDARY
TLINE,11,11,1500
*FILM
BR,F1NU
*NODE FILE
NT
*END STEP
******  STEP #34 ******
*STEP,INC=200
*HEAT TRANSFER, END=PERIOD, DELTMX=50
0.40, 1.01, 1E-5, 1, 1
*BOUNDARY
TLINE,11,11,1500
*FILM
BR,F1NU
*NODE FILE
NT
*END STEP
******  STEP #35 ******
*STEP,INC=200
*HEAT TRANSFER, END=PERIOD, DELTMX=50
0.40, 1.01, 1E-5, 1, 1
*BOUNDARY
TLINE,11,11,1500
*FILM
BR,F1NU
*NODE FILE
NT
*END STEP
******  STEP #36 ******
*STEP,INC=200
*HEAT TRANSFER, END=PERIOD, DELTMX=50
0.40, 1.01, 1E-5, 1, 1
*BOUNDARY
TLINE,11,11,1500
*FILM
BR,F1NU
*NODE FILE
NT
*END STEP
******  STEP #37 ******
*STEP,INC=200
*HEAT TRANSFER, END=PERIOD, DELTMX=50
0.40, 1.01, 1E-5, 1, 1
*BOUNDARY
TLINE,11,11,1500
*FILM
BR,F1NU
*NODE FILE
NT
*END STEP
******  STEP #38 ******
*STEP,INC=200
*HEAT TRANSFER, END=PERIOD, DELTMX=50
0.40, 1.01, 1E-5, 1, 1
*BOUNDARY
TLINE,11,11,1500
*FILM
BR,F1NU
*NODE FILE
NT
*END STEP
******  STEP #39 ******
*STEP,INC=200
*HEAT TRANSFER, END=PERIOD, DELTMX=50
0.40, 1.01, 1E-5, 1, 1
*BOUNDARY
TLINE,11,11,1500
*FILM
BR,F1NU
*NODE FILE
NT
```

```
*END STEP
******  STEP #40 ******
*STEP,INC=200
*HEAT TRANSFER, END=PERIOD, DELTMX=50
0.40, 1.01, 1E-5, 1, 1
*BOUNDARY
TLINE,11,11,1500
*FILM
BR,F1NU
*NODE FILE
NT
*END STEP
******  STEP #41 ******
*STEP,INC=200
*HEAT TRANSFER, END=PERIOD, DELTMX=50
0.40, 1.01, 1E-5, 1, 1
*BOUNDARY
TLINE,11,11,1500
*FILM
BR,F1NU
*NODE FILE
NT
*END STEP
******  STEP #42 ******
*STEP,INC=200
*HEAT TRANSFER, END=PERIOD, DELTMX=50
0.40, 1.01, 1E-5, 1, 1
*BOUNDARY
TLINE,11,11,1500
*FILM
BR,F1NU
*NODE FILE
NT
*END STEP
******  STEP #43 ******
*STEP,INC=200
*HEAT TRANSFER, END=PERIOD, DELTMX=50
0.40, 1.01, 1E-5, 1, 1
*BOUNDARY
TLINE,11,11,1500
*FILM
BR,F1NU
*NODE FILE
NT
*END STEP
******  STEP #44 ******
*STEP,INC=200
*HEAT TRANSFER, END=PERIOD, DELTMX=50
0.40, 1.01, 1E-5, 1, 1
*BOUNDARY
TLINE,11,11,1500
*FILM
BR,F1NU
*NODE FILE
NT
*END STEP
******  STEP #45 ******
*STEP,INC=200
*HEAT TRANSFER, END=PERIOD, DELTMX=50
0.40, 1.01, 1E-5, 1, 1
*BOUNDARY
TLINE,11,11,1500
*FILM
BR,F1NU
*NODE FILE
NT
*END STEP
******  STEP #46 ******
*STEP,INC=200
*HEAT TRANSFER, END=PERIOD, DELTMX=50
0.40, 1.01, 1E-5, 1, 1
*BOUNDARY
TLINE,11,11,1500
*FILM
BR,F1NU
*NODE FILE
NT
*END STEP
******  STEP #47 ******
*STEP,INC=200
*HEAT TRANSFER, END=PERIOD, DELTMX=50
```

```
0.40, 1.01, 1E-5, 1, 1
*BOUNDARY
TLINE,11,11,1500
*FILM
BR,F1NU
*NODE FILE
NT
*END STEP
******  STEP #48 ******
*STEP,INC=200
*HEAT TRANSFER, END=PERIOD, DELTMX=50
0.40, 1.01, 1E-5, 1, 1
*BOUNDARY
TLINE,11,11,1500
*FILM
BR,F1NU
*NODE FILE
NT
*END STEP
******  STEP #49 ******
*STEP,INC=200
*HEAT TRANSFER, END=PERIOD, DELTMX=50
0.40, 1.01, 1E-5, 1, 1
*BOUNDARY
TLINE,11,11,1500
*FILM
BR,F1NU
*NODE FILE
NT
*END STEP
******  STEP #50 ******
*STEP,INC=200
*HEAT TRANSFER, END=PERIOD, DELTMX=50
0.40, 1.01, 1E-5, 1, 1
*BOUNDARY
TLINE,11,11,1500
*FILM
BR,F1NU
*NODE FILE
NT
*END STEP
******  STEP #51 ******
*STEP,INC=200
*HEAT TRANSFER, END=PERIOD, DELTMX=50
0.40, 1.01, 1E-5, 1, 1
*BOUNDARY
TLINE,11,11,1500
*FILM
BR,F1NU
*NODE FILE
NT
*END STEP
******  STEP #52 ******
*STEP,INC=200
*HEAT TRANSFER, END=PERIOD, DELTMX=50
0.40, 1.01, 1E-5, 1, 1
*BOUNDARY
TLINE,11,11,1500
*FILM
BR,F1NU
*NODE FILE
NT
*END STEP
******  STEP #53 ******
*STEP,INC=200
*HEAT TRANSFER, END=PERIOD, DELTMX=50
0.40, 1.01, 1E-5, 1, 1
*BOUNDARY
TLINE,11,11,1500
*FILM
BR,F1NU
*NODE FILE
NT
*END STEP
******  STEP #54 ******
*STEP,INC=200
*HEAT TRANSFER, END=PERIOD, DELTMX=50
0.40, 1.01, 1E-5, 1, 1
*BOUNDARY
TLINE,11,11,1500
*FILM
```

```
BR,F1NU
*NODE FILE
NT
*END STEP
******  STEP #55 ******
*STEP,INC=200
*HEAT TRANSFER, END=PERIOD, DELTMX=50
0.40, 1.01, 1E-5, 1, 1
*BOUNDARY
TLINE,11,11,1500
*FILM
BR,F1NU
*NODE FILE
NT
*END STEP
******  STEP #56 ******
*STEP,INC=200
*HEAT TRANSFER, END=PERIOD, DELTMX=50
0.40, 1.01, 1E-5, 1, 1
*BOUNDARY
TLINE,11,11,1500
*FILM
BR,F1NU
*NODE FILE
NT
*END STEP
******  STEP #57 ******
*STEP,INC=200
*HEAT TRANSFER, END=PERIOD, DELTMX=50
0.40, 1.01, 1E-5, 1, 1
*BOUNDARY
TLINE,11,11,1500
*FILM
BR,F1NU
*NODE FILE
NT
*END STEP
******  STEP #58 ******
*STEP,INC=200
*HEAT TRANSFER, END=PERIOD, DELTMX=50
0.40, 1.01, 1E-5, 1, 1
*BOUNDARY
TLINE,11,11,1500
*FILM
BR,F1NU
*NODE FILE
NT
*END STEP
******  STEP #59 ******
*STEP,INC=200
*HEAT TRANSFER, END=PERIOD, DELTMX=50
0.40, 1.01, 1E-5, 1, 1
*BOUNDARY
TLINE,11,11,1500
*FILM
BR,F1NU
*NODE FILE
NT
*END STEP
******  STEP #60 ******
*STEP,INC=200
*HEAT TRANSFER, END=PERIOD, DELTMX=50
0.40, 1.01, 1E-5, 1, 1
*BOUNDARY
TLINE,11,11,1500
*FILM
BR,F1NU
*NODE FILE
NT
*END STEP
******  STEP #61 ******
*STEP,INC=200
*HEAT TRANSFER, END=PERIOD, DELTMX=50
0.40, 1.01, 1E-5, 1, 1
*BOUNDARY
TLINE,11,11,1500
*FILM
BR,F1NU
*NODE FILE
NT
*END STEP
```

Appendix D. ABAQUS Input Files for Coupled Thermal Stress Analysis

```
<heat_c1.inp>
**************************************************************************
** ELASTIC-PLASTIC CONTINUOUS CASTING BULGING MODEL (860mm)             **
** WITH 60*16 MESH PER ROLL PITCH (CPS8R)                               **
**************************************************************************
*HEADING
RESTART RUN AFTER APPLYING LOAD
*RESTART,READ,WRITE,FREQUENCY=10,OVERLAY
*PREPRINT, ECHO=NO, MODEL=NO, HISTORY=NO, CONTACT=NO
****************************START OF CYCLE*******************************
*** STEP 1
*STEP,INC=200
*STATIC
0.,1.01
*BOUNDARY,OP=NEW
1002,1
1119,2
*TEMPERATURE,FILE=heat, BSTEP=2, BINC=1
*END STEP
*** STEP 2
*STEP,INC=200
*STATIC
0.,1.01
*BOUNDARY,OP=NEW
1002,1
1117,2
*TEMPERATURE,FILE=heat, BSTEP=3, BINC=1
*END STEP
*** STEP 3
*STEP,INC=200
*STATIC
0.,1.01
*BOUNDARY,OP=NEW
1002,1
1115,2
*TEMPERATURE,FILE=heat, BSTEP=4, BINC=1
*END STEP
*** STEP 4
*STEP,INC=200
*STATIC
0.,1.01
*BOUNDARY,OP=NEW
1002,1
1113,2
*TEMPERATURE,FILE=heat, BSTEP=5, BINC=1
*END STEP
*** STEP 5
*STEP,INC=200
*STATIC
0.,1.01
*BOUNDARY,OP=NEW
1002,1
1111,2
*TEMPERATURE,FILE=heat, BSTEP=6, BINC=1
*END STEP
*** STEP 6
*STEP,INC=200
*STATIC
0.,1.01
*BOUNDARY,OP=NEW
1002,1
1109,2
*TEMPERATURE,FILE=heat, BSTEP=7, BINC=1
*END STEP
*** STEP 7
*STEP,INC=200
*STATIC
0.,1.01
*BOUNDARY,OP=NEW
1002,1
1107,2
```

```
*TEMPERATURE,FILE=heat, BSTEP=8, BINC=1
*END STEP
*** STEP 8
*STEP,INC=200
*STATIC
0.,1.01
*BOUNDARY,OP=NEW
1002,1
1105,2
*TEMPERATURE,FILE=heat, BSTEP=9, BINC=1
*END STEP
*** STEP 9
*STEP,INC=200
*STATIC
0.,1.01
*BOUNDARY,OP=NEW
1002,1
1103,2
*TEMPERATURE,FILE=heat, BSTEP=10, BINC=1
*END STEP
*** STEP 10
*STEP,INC=200
*STATIC
0.,1.01
*BOUNDARY,OP=NEW
1002,1
1101,2
*TEMPERATURE,FILE=heat, BSTEP=11, BINC=1
*END STEP
*** STEP 11
*STEP,INC=200
*STATIC
0.,1.01
*BOUNDARY,OP=NEW
1002,1
1099,2
*TEMPERATURE,FILE=heat, BSTEP=12, BINC=1
*END STEP
*** STEP 12
*STEP,INC=200
*STATIC
0.,1.01
*BOUNDARY,OP=NEW
1002,1
1097,2
*TEMPERATURE,FILE=heat, BSTEP=13, BINC=1
*END STEP
*** STEP 13
*STEP,INC=200
*STATIC
0.,1.01
*BOUNDARY,OP=NEW
1002,1
1095,2
*TEMPERATURE,FILE=heat, BSTEP=14, BINC=1
*END STEP
*** STEP 14
*STEP,INC=200
*STATIC
0.,1.01
*BOUNDARY,OP=NEW
1002,1
1093,2
*TEMPERATURE,FILE=heat, BSTEP=15, BINC=1
*END STEP
*** STEP 15
*STEP,INC=200
*STATIC
0.,1.01
*BOUNDARY,OP=NEW
1002,1
1091,2
*TEMPERATURE,FILE=heat, BSTEP=16, BINC=1
*END STEP
*** STEP 16
*STEP,INC=200
*STATIC
0.,1.01
*BOUNDARY,OP=NEW
1002,1
1089,2
```

```
*TEMPERATURE,FILE=heat, BSTEP=17, BINC=1
*END STEP
*** STEP 17
*STEP,INC=200
*STATIC
0.,1.01
*BOUNDARY,OP=NEW
1002,1
1087,2
*TEMPERATURE,FILE=heat, BSTEP=18, BINC=1
*END STEP
*** STEP 18
*STEP,INC=200
*STATIC
0.,1.01
*BOUNDARY,OP=NEW
1002,1
1085,2
*TEMPERATURE,FILE=heat, BSTEP=19, BINC=1
*END STEP
*** STEP 19
*STEP,INC=200
*STATIC
0.,1.01
*BOUNDARY,OP=NEW
1002,1
1083,2
*TEMPERATURE,FILE=heat, BSTEP=20, BINC=1
*END STEP
*** STEP 20
*STEP,INC=200
*STATIC
0.,1.01
*BOUNDARY,OP=NEW
1002,1
1081,2
*TEMPERATURE,FILE=heat, BSTEP=21, BINC=1
*END STEP
*** STEP 21
*STEP,INC=200
*STATIC
0.,1.01
*BOUNDARY,OP=NEW
1002,1
1079,2
*TEMPERATURE,FILE=heat, BSTEP=22, BINC=1
*END STEP
*** STEP 22
*STEP,INC=200
*STATIC
0.,1.01
*BOUNDARY,OP=NEW
1002,1
1077,2
*TEMPERATURE,FILE=heat, BSTEP=23, BINC=1
*END STEP
*** STEP 23
*STEP,INC=200
*STATIC
0.,1.01
*BOUNDARY,OP=NEW
1002,1
1075,2
*TEMPERATURE,FILE=heat, BSTEP=24, BINC=1
*END STEP
*** STEP 24
*STEP,INC=200
*STATIC
0.,1.01
*BOUNDARY,OP=NEW
1002,1
1073,2
*TEMPERATURE,FILE=heat, BSTEP=25, BINC=1
*END STEP
*** STEP 25
*STEP,INC=200
*STATIC
0.,1.01
*BOUNDARY,OP=NEW
1002,1
1071,2
```

```
*TEMPERATURE,FILE=heat, BSTEP=26, BINC=1
*END STEP
*** STEP 26
*STEP,INC=200
*STATIC
0.,1.01
*BOUNDARY,OP=NEW
1002,1
1069,2
*TEMPERATURE,FILE=heat, BSTEP=27, BINC=1
*END STEP
*** STEP 27
*STEP,INC=200
*STATIC
0.,1.01
*BOUNDARY,OP=NEW
1002,1
1067,2
*TEMPERATURE,FILE=heat, BSTEP=28, BINC=1
*END STEP
*** STEP 28
*STEP,INC=200
*STATIC
0.,1.01
*BOUNDARY,OP=NEW
1002,1
1065,2
*TEMPERATURE,FILE=heat, BSTEP=29, BINC=1
*END STEP
*** STEP 29
*STEP,INC=200
*STATIC
0.,1.01
*BOUNDARY,OP=NEW
1002,1
1063,2
*TEMPERATURE,FILE=heat, BSTEP=30, BINC=1
*END STEP
*** STEP 30
*STEP,INC=200
*STATIC
0.,1.01
*BOUNDARY,OP=NEW
1002,1
1061,2
*TEMPERATURE,FILE=heat, BSTEP=31, BINC=1
*END STEP
*** STEP 31
*STEP,INC=200
*STATIC
0.,1.01
*BOUNDARY,OP=NEW
1002,1
1059,2
*TEMPERATURE,FILE=heat, BSTEP=32, BINC=1
*END STEP
*** STEP 32
*STEP,INC=200
*STATIC
0.,1.01
*BOUNDARY,OP=NEW
1002,1
1057,2
*TEMPERATURE,FILE=heat, BSTEP=33, BINC=1
*END STEP
*** STEP 33
*STEP,INC=200
*STATIC
0.,1.01
*BOUNDARY,OP=NEW
1002,1
1055,2
*TEMPERATURE,FILE=heat, BSTEP=34, BINC=1
*END STEP
*** STEP 34
*STEP,INC=200
*STATIC
0.,1.01
*BOUNDARY,OP=NEW
1002,1
1053,2
```

```
*TEMPERATURE,FILE=heat, BSTEP=35, BINC=1
*END STEP
*** STEP 35
*STEP,INC=200
*STATIC
0.,1.01
*BOUNDARY,OP=NEW
1002,1
1051,2
*TEMPERATURE,FILE=heat, BSTEP=36, BINC=1
*END STEP
*** STEP 36
*STEP,INC=200
*STATIC
0.,1.01
*BOUNDARY,OP=NEW
1002,1
1049,2
*TEMPERATURE,FILE=heat, BSTEP=37, BINC=1
*END STEP
*** STEP 37
*STEP,INC=200
*STATIC
0.,1.01
*BOUNDARY,OP=NEW
1002,1
1047,2
*TEMPERATURE,FILE=heat, BSTEP=38, BINC=1
*END STEP
*** STEP 38
*STEP,INC=200
*STATIC
0.,1.01
*BOUNDARY,OP=NEW
1002,1
1045,2
*TEMPERATURE,FILE=heat, BSTEP=39, BINC=1
*END STEP
*** STEP 39
*STEP,INC=200
*STATIC
0.,1.01
*BOUNDARY,OP=NEW
1002,1
1043,2
*TEMPERATURE,FILE=heat, BSTEP=40, BINC=1
*END STEP
*** STEP 40
*STEP,INC=200
*STATIC
0.,1.01
*BOUNDARY,OP=NEW
1002,1
1041,2
*TEMPERATURE,FILE=heat, BSTEP=41, BINC=1
*END STEP
*** STEP 41
*STEP,INC=200
*STATIC
0.,1.01
*BOUNDARY,OP=NEW
1002,1
1039,2
*TEMPERATURE,FILE=heat, BSTEP=42, BINC=1
*END STEP
*** STEP 42
*STEP,INC=200
*STATIC
0.,1.01
*BOUNDARY,OP=NEW
1002,1
1037,2
*TEMPERATURE,FILE=heat, BSTEP=43, BINC=1
*END STEP
*** STEP 43
*STEP,INC=200
*STATIC
0.,1.01
*BOUNDARY,OP=NEW
1002,1
1035,2
```

```
*TEMPERATURE,FILE=heat, BSTEP=44, BINC=1
*END STEP
*** STEP 44
*STEP,INC=200
*STATIC
0.,1.01
*BOUNDARY,OP=NEW
1002,1
1033,2
*TEMPERATURE,FILE=heat, BSTEP=45, BINC=1
*END STEP
*** STEP 45
*STEP,INC=200
*STATIC
0.,1.01
*BOUNDARY,OP=NEW
1002,1
1031,2
*TEMPERATURE,FILE=heat, BSTEP=46, BINC=1
*END STEP
*** STEP 46
*STEP,INC=200
*STATIC
0.,1.01
*BOUNDARY,OP=NEW
1002,1
1029,2
*TEMPERATURE,FILE=heat, BSTEP=47, BINC=1
*END STEP
*** STEP 47
*STEP,INC=200
*STATIC
0.,1.01
*BOUNDARY,OP=NEW
1002,1
1027,2
*TEMPERATURE,FILE=heat, BSTEP=48, BINC=1
*END STEP
*** STEP 48
*STEP,INC=200
*STATIC
0.,1.01
*BOUNDARY,OP=NEW
1002,1
1025,2
*TEMPERATURE,FILE=heat, BSTEP=49, BINC=1
*END STEP
*** STEP 49
*STEP,INC=200
*STATIC
0.,1.01
*BOUNDARY,OP=NEW
1002,1
1023,2
*TEMPERATURE,FILE=heat, BSTEP=50, BINC=1
*END STEP
*** STEP 50
*STEP,INC=200
*STATIC
0.,1.01
*BOUNDARY,OP=NEW
1002,1
1021,2
*TEMPERATURE,FILE=heat, BSTEP=51, BINC=1
*END STEP
*** STEP 51
*STEP,INC=200
*STATIC
0.,1.01
*BOUNDARY,OP=NEW
1002,1
1019,2
*TEMPERATURE,FILE=heat, BSTEP=52, BINC=1
*END STEP
*** STEP 52
*STEP,INC=200
*STATIC
0.,1.01
*BOUNDARY,OP=NEW
1002,1
1017,2
```

```
*TEMPERATURE,FILE=heat, BSTEP=53, BINC=1
*END STEP
*** STEP 53
*STEP,INC=200
*STATIC
0.,1.01
*BOUNDARY,OP=NEW
1002,1
1015,2
*TEMPERATURE,FILE=heat, BSTEP=54, BINC=1
*END STEP
*** STEP 54
*STEP,INC=200
*STATIC
0.,1.01
*BOUNDARY,OP=NEW
1002,1
1013,2
*TEMPERATURE,FILE=heat, BSTEP=55, BINC=1
*END STEP
*** STEP 55
*STEP,INC=200
*STATIC
0.,1.01
*BOUNDARY,OP=NEW
1002,1
1011,2
*TEMPERATURE,FILE=heat, BSTEP=56, BINC=1
*END STEP
*** STEP 56
*STEP,INC=200
*STATIC
0.,1.01
*BOUNDARY,OP=NEW
1002,1
1009,2
*TEMPERATURE,FILE=heat, BSTEP=57, BINC=1
*END STEP
*** STEP 57
*STEP,INC=200
*STATIC
0.,1.01
*BOUNDARY,OP=NEW
1002,1
1007,2
*TEMPERATURE,FILE=heat, BSTEP=58, BINC=1
*END STEP
*** STEP 58
*STEP,INC=200
*STATIC
0.,1.01
*BOUNDARY,OP=NEW
1002,1
1005,2
*TEMPERATURE,FILE=heat, BSTEP=59, BINC=1
*END STEP
*** STEP 59
*STEP,INC=200
*STATIC
0.,1.01
*BOUNDARY,OP=NEW
1002,1
1003,2
*TEMPERATURE,FILE=heat, BSTEP=60, BINC=1
*END STEP
*** STEP 60
*STEP,INC=200
*STATIC
0.,1.01
*BOUNDARY,OP=NEW
1002,1
1121,2
*TEMPERATURE,FILE=heat, BSTEP=61, BINC=1
*END STEP
*************************END OF CYCLE***************************
```

<heat_c2.inp> is same as <heat_c1.inp>.

References

1. W.R. Irving: Continuous Casting of Steel, The Institute of Materials, 1993.

2. X. Huang and B.G. Thomas: "Modeling of Steel Grade Transition in Continuous Slab Casting Processes", Metallurgical Transactions, 1993, vol. 24B, pp. 379-393.

3. S.S. Daniel: "Roll-containment Model for Strand-cast Slabs and Blooms", Ironmaking and Steelmaking, 1982, (1), pp. 16-24.

4. K. Miyazawa and K. Schwerdtfeger: "Computation of Bulging of Continuously Cast Slabs with Simple Bending Theory", Ironmaking and Steelmaking, 1979, vol. 6 (2), pp. 68-74.

5. B. Barber, B.A. Lewis and B.M. Leckenby: "Finite-element Analysis of Strand Deformation and Strain Distribution in Solidifying Shell During Continuous Slab Casting", Ironmaking and Steelmaking, 1985, vol. 12 (4), pp. 171-175.

6. K. Wunnenberg and D. Huchingen: "Strand Bulging between Supporting Rollers during Continuous Slab Casting", Stahl und Eisen, 1978, vol. 98 (6), pp. 254-259.

7. Y. Sugitani, M. Nakamura, T. Kanazawa and J.Y. Lamant: "Measurement of Bulging Amount and Profile on the Experimental Continuous Caster", Trans. Iron Steel Inst. Jpn., 1985, vol. 25, pp. B9.

8. P. Woodberry, R. Smith and R. Davies: "Measurement of Strand Bulging", Steel Practices Conference, 1989.

9. P. Woodberry, P. Campbell and R. Davies: Measurement of Bloom Bulging, BHP-MRL Technical Note, Report No. 89/053, 1989.

10. J.Y. Lamant, M. Larrecq, J.P. Birat, J.L. Hensgen, J.D. Weber and J.C. Dhuyvetter: "Study of Slab Bulging in Continuous Caster", Continuous Casting, London, United Kingdom, 1985, pp. 37.1-37.8.

11. J. Gancarz, J.Y. Lamant, M. Larrecq and P. Rahier: "Mechanical Behaviour of the Slab During Continuous Casting", 74th Steelmaking Conference, Washington, D.C., Iron and Steel Society, Warrendale, PA, 1991.

12. T. Matsumiya, H. Kajioka and Y. Nakamura: Mathematical Analysis of Continuously Cast Slab Bulging, Nippon Steel, Chiba, Japan, Report No. 21, 1983, 347-354.

13. A. Palmaers, A. Etienne and J. Mignon: "Calculation of the Mechanical and Thermal Stresses in Continuously Cast Strands", Stahl und Eisen, 1979, vol. 99 (19), pp. 1039-1050.

14. A. Grill and K. Schwerdtfeger: "Finite-element analysis of Bulging Produced by Creep in Continuously Cast Steel Slabs", Ironmaking and Steelmaking, 1979, vol. 6 (3), pp. 131-135.

15. K. Okamura and H. Kawashima: "Calculation of Bulging Strain and its Application to Prediction of Internal Cracks in Continuously Cast Slabs", Int. Conf. Comp. Ass. Mat. Design Proc. Simul, Tokyo, ISIJ, 1993, pp. 129-134.

16. J.B. Dalin and J.L. Chenot: "Finite Element Computation of Bulging in Continuously Cast Steel with a Viscoplastic Model", International Journal for Numerical Methods in Engineering, 1988, vol. 25, pp. 147-163.

17. B. Barber and A. Perkins: "Strand Deformation in Continuous Casting", Ironmaking and Steelmaking, 1989, vol. 16 (6), pp. 406-411.

18. H. Mizukami, K. Murakami and Y. Miyashita: "Mechanical Properties of Continuously Cast Steels at High Temperatures", Nihan Kokan Corporation, Tetsu-to-Hagane (Iron and Steel), 1977, vol. 63 (146), pp. S 652, (in Japanese).

19. P.J. Wray: "Mechanical, Physical and Thermal Data for Modeling the Solidification Processing of Steels", Modelling of Casting and Welding Processes AIME Conference Proceedings, Ringe, New Hampshire, 1980, pp. 245-257.

20. D.R. Hub: "Measurement of Velocity and Attenuation of Sound in Iron up to the Melting Point", Proc. IVth Intern. Vong. Acoustics, Copenhagen, 1962, paper #551.

21. P. Kozlowski, B.G. Thomas, J. Azzi and H. Wang: "Simple Constitutive Equations for Steel at High Temperature", Metallurgical Transactions A, 1992, vol. 23A (March), pp. 903-918.

22. P.J. Wray: "Effect of Carbon Content on the Plastic Flow of Plain Carbon Steels at Elevated Temperatures", Metallurgical Transactions A, 1982, vol. 13A (January), pp. 125-134.

23. T. Suzuki, K.H. Tacke, K. Wunnenberg and K. Schwerdtfeger: "Creep Properties of Steel at Continuous Casting Temperatures", Ironmaking and Steelmaking, 1988, vol. 15 (2), pp. 90-100.

24. R.D. Cook, D.S. Malkus and M.E. Plesha: Concepts and Applications of Finite Element Analysis, 3rd ed., Wiley, New York, 1989.

25. ABAQUS: User's Manual, Hibbitt, Karlsson & Sorensen, Inc., Providence, RI, 1997.

26. T. Nozaki, J. Matsuno, K. Murata, H. Ooi and M. Kodama: "A Secondary Cooling Pattern for Preventing Surface Cracks of Continuous Casting Slab", Trans. Iron Steel Inst. Jpn., 1978, vol. 18, pp. 330-338.

27. M.T. Heath: Scientific Computing - an Introductory Survey, McGraw-Hill, 1997.

28. R.J. Roark and W.C. Young: Formulas for Stress and Strain, 5th ed., McGraw-Hill Book Company, New York, NY, 1975.

29. Y.M. Won, T.-j. Yeo, D.J. Seol and K.H. Oh: "A New Criterion for Internal Crack Formation in Continuously Cast Steel", Metallurgical and Materials Transactions, 1999, vol. 131B.